Aus dem Institut für Pharmakologie und Toxikologie

Geschäftsführender Direktor: Prof. Dr. med. Thomas Gudermann

des Fachbereichs Medizin der Philipps-Universität Marburg

und des Universitätsklinikums Gießen und Marburg, Standort Marburg

The Fibroblast Growth Factor-binding Protein (FGF-BP) and the Human Epidermal Growth Factor Receptor-2 (HER-2): Functional Studies on Two Gene Products Relevant in Ovarian Cancer

INAUGURAL–DISSERTATION

zur Erlangen des Doktorgrades der Humanbiologie

(Dr. rer. physiol.)

dem Fachbereich Medizin der Philipps-Universität Marburg

vorgelegt von

Shaker Abuharbeid

aus Gaza, Palästina

Marburg, 2005

Angenommen vom Fachbereich Humanmedizin der Philipps-Universität Marburg
am: 01.11.2005

Gedruckt mit Genehmigung des Fachbereichs

Dekan: Prof. Dr. B. Maisch
Referent: Prof. Dr. F. Czubayko
Korreferent: Prof. Dr. G. Aumüller

To my dear parents and daughters

Nour, Anwar and Rana

TABLE OF CONTENTS

1 INTRODUCTION

1.1 Basic tumor biology and biological role of oncogenes in cancer

The cell is the fundamental unit, which is capable of performing all of the processes that define life. Each of the organs in the body consists of specialized cells that carry out the organ's functions. To assure the proper performance of each organ, worn out or injured cells must be replaced and particular types of cells must proliferate in response to environmental changes. Reproduction of normal cells is a process of cell division, which is highly regulated. If anything goes wrong during this complicated process, a cell may become cancerous.

Tumor growth is often a multi-step process that starts with the loss of control of cell proliferation, which is thought to originate via the oncogenic transformation of a single cell. The cancerous cell then begins to divide rapidly, resulting in a microscopically small, spheroid tumor [1]. In order to progress to a clinically significant (macroscopic) tumor the transformed cells must be able to avoid the immune system. In some cases, the ability to cause angiogenesis (i.e. to stimulate the growth of blood vessels) is also important in progression to a clinically significant tumor. Relatively late in their existence some tumors gain the ability to escape from the site of their initial location and invade other areas of the body (metastasis). Each of these processes, i.e. oncogenic transformation, ability to escape recognition by the immune system, angiogenesis and development of metastasic potential, are associated with genetic changes.

Oncogenic transformation arises from a series of environmentally induced changes to critical genes. Genes responsible for the cancer phenotype have been termed as oncogenes or cancer-causing genes. They are derived from proto-oncogenes, cellular genes that promote normal growth and differentiation. Proto-oncogenes may become oncogenic by influences that alter their behavior *in situ*, including not only point mutations rendering a signaling molecule constitutively active, but also amplification, as seen for HER-2 in adenocarcinomas such as breast, ovary, lung, stomach and pancreatic cancer [2,3] and *N-myc* in neuroblastoma [4], and chromosomal translocations [5].

Detailed analysis of the diverse functions of the known oncogenes shows that they code for components of the signal transduction cascade, i.e. growth factors, growth factor receptors, adaptor molecules, protein kinases, G-proteins, nuclear transcription factors, as well as molecules that repair DNA, regulate the cell cycle and various check points, or mediate apoptosis, metastasis and invasion. As described by Hanahan and Weinberg [6], this catalogue of genes manifest six essential alterations in physiology that collectively dictate malignant growth, i.e. self-sufficiency in growth signals, insensitivity to growth-inhibitory signals, resistance to programmed cell death (apoptosis), limitless replicative potential, sustained angiogenesis, tissue invasion and metastasis. These six capabilities are shared in common by most and perhaps all types of human tumors.

1.2 Angiogenesis in tumor growth

Angiogenesis is the process of generating new capillary blood vessels. In the adult, the proliferation rate of endothelial cells is very low compared with many other cell types in the body. Physiological exceptions in which under tight regulation angiogenesis occurs are found in the female reproductive system and during wound healing [7]. Unregulated angiogenesis may result in different pathologies [1]. Tumor growth and metastasis are angiogenesis-dependent [8].

As the tumor mass grows, the cells will find themselves further and further away from the nearest capillary. Finally, the tumor stops growing and reaches a steady state, in which the number of proliferating cells counterbalances the number of dying cells. The restriction in size is caused by the lack of nutrients and oxygen [9]. *In situ* carcinomas may remain dormant and undetected for many years, and metastases are rarely associated with these small avascular tumors. Several months or years later, an *in situ* tumor may switch to the angiogenic phenotype, induce the formation of new capillaries, and start to invade the surrounding tissue. The "angiogenic switch" depends on a net balance of positive and negative angiogenic factors in the tumor. Thus, the angiogenic phenotype may result from the production of growth factors, including acidic fibroblast growth factor (aFGF, FGF-1), basic fibroblast growth factor-2 (bFGF, FGF-2) [10], vascular endothelial growth factor (VEGF) [11], hepatocyte growth factor (HGF) [12], epidermal growth factor (EGF), transforming growth factor-α (TGF-α) [13] and pleiotrophin (PTN) [14], by tumor cells

and/or the downregulation of negative modulators, like angiostatin [15,16], endostatin [17] and thrombospondin-1 (TSP-1) in tissues with a quiescent vasculature [18].

In both normal and pathological angiogenesis, hypoxia is the main force initiating the angiogenic process. In a tumor, the angiogenic phenotype can be triggered by hypoxia resulting from increasing distance of the growing tumor cells to the capillaries or from the inefficiency of the newly formed vessels. Also, several oncogenes such as v-*ras*, k-*ras*, v-*raf*, *src*, *fos* and v-*yes* [19-22] induce the up-regulation of angiogenic factors like VEGF and increase the production of cytokines and proteolytic enzymes [23]. Moreover, oncogene products may act directly as angiogenic factors [24].

Neovascularization of the primary tumor increases the possibility that cancer cells will enter the blood stream and spread to other organs, and is also necessary for the growth of metastases in distant organs [25]. Most of the micrometastases have a high death rate and are not vascularized until they switch to the angiogenic phenotype [1].

1.3 Fibroblast growth factors and the fibroblast growth factor-binding protein

1.3.1 Fibroblast growth factors (FGFs)

The FGF family consists of a group of structurally related polypeptide growth factors. To date, 23 different FGFs have been discovered. Defining features of this family are a strong affinity for heparin and heparan-like glycosaminoglycans (HLGAGs) [26], as well as a central core of 140 amino acids that is highly homologous between different family members. Although all FGFs are categorized by their structure, the historical nomenclature refers to the fact that the first members of FGF family, isolated from bovine pituitary extracts, stimulated fibroblast proliferation [27]. In fact, the designation "FGF" is misleading since several FGFs have a broad mitogenic spectrum. They stimulate proliferation of a variety of cells of mesodermal, ectodermal and also of endodermal origin [28,29]. The only known exception is FGF-7, which is only mitogenic for epithelial cells and not for fibroblasts or endothelial cells [30].

FGFs have been shown to interact with three different types of binding partners: heparan sulphate proteoglycans (HSPGs) [31], FGF-binding proteins (FGF-BPs) [32,33] and high affinity transmembrane FGF receptors (FGFRs) of the tyrosine kinase family which are responsible for signal transduction [34-38]. The binding of FGFs to heparin or heparan sulphate proteoglycans (HSPGs) may serve three physiologically relevant goals: first, their protection from degradation, e.g. protection of FGF-1 from proteolysis by thrombin [39] and FGF-2 from trypsin [40] or plasmin [41], secondly, the creation of a local reservoir of growth factors and thirdly, control of the release and hence of the bioactivity of FGFs. The role of FGF-BP and its binding to FGFs is discussed in detail in section 1.3.7.

Cellular responses mediated by FGFs include angiogenesis, embryonic development, cell migration, proliferation, and differentiation [42-45]. In general, formation and sprouting of new capillaries involves endothelial cell proliferation and cell migration, as well as breakdown of surrounding extracellular matrix (ECM) components. Together with vascular endothelial growth factor (VEGF), FGFs are the most important regulators of these processes. During embryonic development, FGFs play a role in organogenesis, particularly in the nervous system and the limbs [46-48]. By means of knockout studies in mice, it has been demonstrated that several FGFs including FGF-4 (Kaposi-FGF, k-FGF), FGF-8 (androgen induced factor) and FGF-10 are essential for mouse development and for lung formation. For example, FGF-4-/- [49] and FGF-8-/- [50] mutations are embryonically lethal, while FGF-10-/- mice die at birth due to insufficient lung formation [51]. On the other hand, FGF-2-/- and FGF-6-/- mice are not only viable, but are phenotypically indistinguishable from wild-type animals by gross examination [52,53]. This observation is probably due to partly substitution of FGF-2 and FGF-6 functions by other family members [54,55]. Furthermore, FGFs play a role in the final phase of wound healing and regeneration of the proximal renal tubule following chemically induced damage [56]. In different cell systems basic fibroblast growth factor (bFGF, FGF-2) participates in the regulation of apoptosis [57-59]. Moreover, in prostate cancer cells, FGF-2 has been shown to confer resistance to anticancer drugs [60].

FGFs may promote tumor growth by three different mechanisms: as angiogenic inducers, as mitogens for the tumor cells themselves, and as inhibitors of apoptosis. Since there are no documented activating mutations in FGFs themselves, the biological activities of FGFs in tumor growth are based on overexpression or increased availability of FGFs due to release of intracellular and mobilization of extracellular FGFs.

On the basis of the interplay between tumor cells and the surrounding stromal cells, overexpression of secreted FGFs may result from three possibilities: first, secretion of FGFs by tumor cells themselves without external signal as autocrine and paracrine growth factor, which has been shown to occur in the case of FGF-2 in human gliomas [61], secondly, secretion by stromal cells in response to a signal from the tumor cells, which is found for FGF-5 in pancreatic cancer [62] and thirdly, secretion of FGFs by the tumor in response to a signal from non-transformed cells, as in the case of FGF-2 in Kaposi's sarcoma [63].

Basic fibroblast growth factor (bFGF, FGF-2) is especially relevant in this thesis with regard to the fibroblast growth factor-binding protein (FGF-BP). For this reason it is described in more detail below.

Fibroblast growth factor-2 (FGF-2) was initially purified as an 15 kDa heparin-binding protein from bovine pituitary extracts [64], that was later found to represent a proteolytic product of the primary 18 kDa form [65]. FGF-2 occurs in several isoforms resulting from alternative initiations of translation: an 18 kDa isoform and four larger molecular weight isoforms (22, 22.5, 24 and 34 kDa), which are initiated at different in-frame CUG codons upstream from the conventional AUG codon (reviewed in [66]). The main structural feature of the four high molecular weight forms of FGF-2 is the presence of a nuclear localizing sequence (NLS) which directs the growth factor to the nucleus, whereas the 18 kDa FGF-2 form initiated from AUG is essentially cytosolic [67,68]. The biological significance of the different subcellular localization of the FGF-2 isoforms is still unclear.

None of the FGF-2 isoforms have a signal sequence; however, it has been demonstrated in various cell types expressing the 18 kDa FGF-2 that this growth factor can be secreted into the extracellular medium by a still unknown mechanism [69,70] and thereby can act as a paracrine or autocrine growth factor by activating specific cell surface receptors. One view of how FGF-2 is released from cells is through passive processes such as cell death, wounding, or chemical injury [71]. Haimovitz-Friedman et al. [72] reported that FGF-2 can be released into the medium after irradiation. Factors such as fibrin-split products also induce FGF-2 release [73]. A second view is that a nonclassic pathway exists for the release of proteins such as FGF-2 that lack secretion signals. It has been demonstrated that migration of an isolated single cell expressing FGF-2 can be inhibited by FGF-2-neutralizing antibodies [69]. Thus, a mechanism other than cell death can lead to FGF-2 release. Because FGF-2-

dependent cell migration was not inhibited by drugs affecting the classic secretion pathway, FGF-2 release may occur via a novel mechanism [74].

As other members of FGF family, FGF-2 binds to heparin or heparan sulphate proteoglycans (HSPGs). While the functional domain of FGF-1 for heparin-binding is dependent on residues at the carboxy terminus, probably between amino acids 122-137 [75,76], the data for binding sites of FGF-2 are contradictory. Baired et al. [77] characterized two functional heparin-binding domains in the FGF-2 molecule through the use of blocking peptides and localized these domains to amino acids 24-68 and 106-115. Another two sites of interaction have been identified [78], in which the amino acids involved were not arranged consecutively in the primary structure of the polypeptide chain, in contrast to the peptide blocking studies of Baired. Instead, the binding sites were composed of groups of basic amino acids brought together by the secondary structure of the folded polypeptide.

There are currently two different known mechanisms to explain how FGFs are released from the extracellular matrix (ECM) reservoir: the first one is based on the enzymatic cleavage of heparan sulphate proteoglycans (HSPGs) by heparanase, which has been investigated in numerous studies [79-81]. Interestingly, the expression of heparanase, which has been cloned and expressed in metastasic carcinoma cell lines independently by Vlodavsky et al. [82] and Hulett et al. [83], seems to correlate with invasive phenotype of several human breast cancer cell lines.

An alternative mechanism for the regulation of FGF release from ECM involves the fibroblast growth factor-binding protein (FGF-BP) that may act as a carrier protein for FGF-1 and FGF-2.

1.3.2 The fibroblast growth factor-binding protein (FGF-BP)

The FGF-binding protein (FGF-BP) was originally identified as a heparin-binding protein and designated HBp17 (heparin-binding protein 17 kDa) [32]. Through heparin affinity chromatography, gel filtration and reverse-phase HPLC, FGF-BP was isolated from serumfree culture medium conditioned by human epidermoid carcinoma A431 cells. The 1163 bp cDNA was cloned and the primary structure of 234 amino acids long protein was determined. In contrast to α2-macroglobulin [84], the detection of a non covalent, reversible

binding of FGF-BP to FGF-1 or FGF-2 suggested a physiological role for FGF-BP as a carrier protein. Most recently, it has been demonstrated that FGF-BP is also able to interact with FGF-7, FGF-10 and FGF-22 [85].

Furthermore, a human cDNA clone containing an open reading frame (ORF) for a protein, which has amino acid sequence similarity of 21% to FGF-BP and a homology of 41% was discovered by a gene data bank blast search. No further significant homology was found with other known proteins. Data on the protein derived from this gene, which is referred to as "killer-specific secretory protein of 37 kDa" (Ksp37), were published in a single study by Ogawa et al. [86]. They suggest that like FGF-BP, this protein could bind to proteins to regulate their activity and thereby mediate unknown functions. Consequently, in a further study this Ksp37 was also named FGF-BP2 [87] suggesting the existence of an FGF-BP family.

1.3.3 FGF-BP expression in neoplastic tissues and its regulation in skin and colon carcinogenesis

The expression pattern of FGF-BP in neoplastic cells has revealed that the expression of this protein is highly regulated and tissue-specific. A screening of different human tumor cell lines and normal human keratinocytes showed that FGF-BP mRNA was positive in most squamous cell carcinoma (SCC) cell lines derived from different origins including lung, bladder, skin, and cervix, and in normal human keratinocytes [88]. A high level of expression FGF-BP mRNA expression has also been reported in tumor tissues from patients with SCC of the head and neck [88]. Recently, *in situ* hybridization demonstrated similar results [89]. Interestingly, the highest density of microvessels was observed exclusively in FGF-BP-positive SCC, suggesting that FGF-BP may be an angiogenic factor in SCC [89]. Furthermore, high expression of FGF-BP has been demonstrated in invasive human breast cancer [90]; in some human colon cancer cell lines and tissues [91], as well as in prostate carcinoma cell lines [92].

Transfection of FGF-BP into the non-tumorigenic adrenal carcinoma cell line SW-13, which expresses constitutively high levels of FGF-2 but no FGF-BP [88], results in the release of biologically active FGF-2, formation of colonies in soft agar assay and vascularized tumors in nude mice. In further studies, the role of FGF-BP for FGF function

mainly during the early phase of tumor growth has been elucidated by means of a tetracycline-regulated expression system in SW-13 cells [93]. SW-13/tetBP cells were generated, in which the expression of FGF-BP can be regulated in xenografted tumors *in vivo* by tetracycline treatment of athymic nude mice. It was demonstrated that growth of the SW-13/tetBP xenografts is dependent on FGF-BP expression during the early stages of tumor formation and does not appear to contribute significantly to the further expansion of tumors. Furthermore, when human cervical (ME-180) and colon carcinoma (LS174T) cell lines were depleted of endogenous FGF-BP by ribozyme targeting, the release of biologically active FGF-2 from cells in culture was reduced and a decrease in the growth and angiogenesis of xenograft tumors in mice was observed, indicating that FGF-BP can serve as an angiogenic switch molecule [91]. Similarly, ribozyme-mediated reduction of FGF-BP levels decreased the proliferation of PC-3 prostate carcinoma cells *in vitro* and completely abolished the ability of highly metastatic PC-3 cells to grow s.c. tumors in athymic nude mice [92].

Due to the fact that FGF-BP is expressed in a variety of SCCs, in normal human keratinocytes, and in the mouse embryonic skin [32,88,94], the role of FGF-BP during skin carcinogenesis was further explored. Kurtz et al. [94] used a mouse model of skin carcinogenesis, which upon DMBA/TPA treatment describes a predictable multistage process of tumor formation from the clonal expansion of a normal epidermal cell into a benign sequamous papilloma that progresses into a malignant squamous cell carcinoma (reviewed by [95]), to investigate the role of FGF-BP expression during tumor progression. In DMBA/TPA-induced papillomas, levels of FGF-BP mRNA were 4-5 folds higher than in untreated skin and remained up-regulated after malignant conversion into SCC. Moreover, FGF-BP mRNA was up-regulated in cell lines derived from DMBA/TPA-induced papillomas and a cell line derived from DMBA-initiated skin and selected for resistance to Ca^{2+}-induced terminal differentiation [94].

Similarly, the role of FGF-BP in the formation of human skin SCC was examined using a human skin/SCID mouse model, where human skin (upper eyelid skin) was xenografted onto SCID mice and treated with the DMBA/TPA carcinogen protocol [96]. While upon carcinogen treatment the human skin grafts displayed no obvious macroscopic alterations, in murine skin induction of papillomas was visible within 6 weeks. Immunohistochemical analysis of the treated human skin, however, showed p53-positive keratinocytes in the epidermis, increased angiogenesis in the treated skin, enhanced proliferation of the

keratinocytes in the basal layer, and an increase of FGF-BP protein and mRNA [96]. In conclusion, these two reports demonstrate the association of mouse as well as human FGF-BP with the early neoplastic stages of skin SCC, where angiogenesis is thought to play a critical role.

Because of the high expression of FGF-BP in human colon cancer cell lines and tissues [91], the regulation of FGF-BP during colon carcinogenesis was further evaluated [97]. Up-regulation of FGF-BP expression, which coincides with a significant increase in blood vessel density, was demonstrated during early stages of human colon epithelial malignant progression. In contrast with this, in a very small portion of normal human colon biopsy samples FGF-BP expression was detectable [97].

1.3.4 FGF-BP expression in normal tissues and its regulation during embryonic development and tissue repair

In contrast to neoplastic tissues, normal human adult tissues, like brain, heart, muscle, kidney, skin, liver, spleen, larynx, tongue, lymph node, lung and breast do not appear to express FGF-BP mRNA as demonstrated by Northern blotting or *in situ* hybridization [88-90]. In the adult mouse FGF-BP mRNA was barely detectable in intestine, skin and ovaries and below detection in heart, muscle, kidney, liver, spleen, stomach, thymus and brain [94]. In contrast to the normal human tissues, high expression of FGF-BP was observed in lungs of adult mouse.

However, during embryonic development, tissue repair, wound healing, and renal diseases in children, changes in FGF-BP expression were observed. The available data of the regulation of FGF-BP during these processes is discussed below.

In immunohistochemical studies in mice, the distribution of FGF-BP protein expression was shown in a broad spectrum of tissues at various stages between day 8 and 16 of embryonic development [98]. FGF-BP is found in the digestive system, skin, hair follicles and the dental germ, in the respiratory tract, various glandular tissues, kidney, liver, and certain areas of the CNS. Immunoreactivity is detected predominantly in cells of primitive epithelia in various tissues including lung bronchi, GI tract, nasal cavity, and tongue. The comparison between different organs and tissues reveals different intensities of

immunostaining indicating heterogeneous levels of FGF-BP expression. Particularly strong staining is observed in thymus, skin, kidney, respiratory tract, GI tract, and the oral cavity. The comparison of different stages of embryonic development also reveals that in some tissues FGF-BP expression is related to the stage of differentiation. This is found in the liver, various tissues of the CNS including spinal cord and midbrain and in the heart where immunopositivity decreases with development. In contrast, the epithelia of the oral cavity show increasing FGF-BP levels during mouse embryogenesis. These data indicated that FGF-BP expression is tightly regulated during development. This study is in agreement with, but significantly extends the results of Kurtz et al. [94] on FGF-BP expression in mouse embryos.

Interestingly, the comparison of the protein levels of FGF-2 and FGF-BP during mouse embryo development reveals broad similarities as well as some marked differences in localization [98]. In general, strong FGF-2 expression overlaps with strong FGF-BP immunreactivity in the digestive tract, in skin, lung, kidney, pancreas, and various glands. This is true for skeletal and heart muscle where weak expression is seen for both molecules. In contrast to these tissues, in liver the staining patterns for FGF-2 and FGF-BP are different. While FGF-2 was relatively weak, strong FGF-BP immunopositivity was detected [98].

Recently, the effect of human FGF-BP transgene expression in chicken embryos has been explored. The expression of human FGF-BP dose-dependently induced vascular permeability, hemorrhage and embryonic lethality, which resulted from compromised microvascular structure as indicated by light and electron microscopic studies [99].

In nonmalignant diseases that include tissue repair, changes in FGF-BP expression were also observed. A strong up-regulation of FGF-BP expression was found in the kidney stroma of children with renal damage due to diverse causes that include HIV infection as well as bacterial toxins causing hemolytic uremia syndrome (HUS) [100]. In support of a role of increased FGF-BP expression during kidney repair, an enhancement of FGF-induced kidney epithelial proliferation by FGF-BP was observed [100]. Furthermore, the FGF-BP expression was found up-regulated in blood vessels of mice that succumb to premature atherogenesis [101]. In contrast to this long-term up-regulation of FGF-BP, wound healing studies in murine and human tissues showed only a transient up-regulation of FGF-BP that upon wound closure returned to baseline [96]. Recently, it was shown that FGF-BP interacts with FGF-7

and FGF-10, which have important functions for repair of injured epithelia, as well as with the recently identified FGF-22 enhancing the activities of low concentrations of these ligands [85]. The interaction of FGF-BP with FGF-7 and FGF-10 suggests that up-regulation of FGF-BP expression after epithelia injury stimulates FGF activity at the site of wound, thus enhancing the process of epithelial repair.

1.3.5 Regulation of FGF-BP expression by TPA, EGF, fetal bovine serum and retinoids

The regulation of cellular FGF-BP expression as well as the FGF-BP promoter has been extensively analyzed in the ME-180 SCC cells. Several studies have shown that FGF-BP expression is significantly up-regulated by 12-O-tetradecanoylphorbol-13-acetate (TPA), mitogens such as epidermal growth factor (EGF) and fetal bovine serum (FBS), and that it is downregulated by retinoids *in vitro* and *in vivo*.

Phorbol esters, such as TPA (12-O-tetradecanoylphorbol-13-acetate), are potent tumor promoters as pharmacological activators of the protein kinase C (PKC) pathway [102]. Recent studies demonstrated that FGF-BP is up-regulated during TPA promotion of skin cancer [94,96]. In the ME-180 cells, TPA increased FGF-BP mRNA levels in a time- and dose-dependent manner mediated via the protein kinase C signal transduction pathway [103]. The deletion or mutational analysis of the FGF-BP promoter indicated that TPA effects on FGF-BP gene transcription are tightly controlled by a complex interplay of positive elements and a novel regulatory element, which contains sequences recognized by E-box element factors [103]. The significance of these regulatory elements has also been shown by EGF-mediated FGF-BP up-regulation in ME-180 cells as well as in the breast cancer cell line MDA-MB-468 [90,104]. Although the C/EBP site in the FGF-BP promoter is a necessary element for EGF-induced FGF-BP promoter activity in both cell lines, it is noteworthy that the deletion of this site in MDA-MB-468 cells resulted in a significant increase in basal activity [90], whereas the deletion of the same site in ME-180 cells did not result in any change in the basal activity [104], suggesting a unique dual role of C/EBP site in the regulation of promoter activity specific to breast cancer cells.

Similarly, treatment of serum-starved ME-180 cells with fetal bovine serum results in a rapid increase in FGF-BP mRNA levels and in the rate of FGF-BP gene transcription [105]. Promoter analysis showed that C/EBP is the main promoter element required for the serum

response. Unlike EGF-activation of FGF-BP, transcriptional induction by serum is not significantly regulated through the AP-1 or E-box sites in the promoter [105]. These results illustrate a strict control of FGF-BP expression by various mechanisms and promoter elements, which in part depend on the stimulus.

Retinoids, a group of naturally occurring or synthetic analogues of vitamin A, are potent regulators of normal epithelial differentiation and growth and affect many neoplastic cell systems including several squamous cell carcinoma (SCC) cell lines [106-109]. Moreover, retinoids have been shown to suppress carcinogenesis in various epithelial tissues in animal model systems [110-114] and also to have clinical efficacy as chemotherapeutic agents against selected malignancies including SCCs [115-119].

FGF-BP has been found to be a target for downregulation by retinoids. Oral all-trans retinoic acid (tRA) treatment induced a significant decrease of FGF-BP protein levels in stomach, eye and lung tissues of rats as demonstrated by immunohistochemical analysis [120]. Similarly, it was demonstrated that in different squamous cell carcinoma (SCC) cell lines tRA downregulates FGF-BP mRNA in a time- and dose-dependent manner and that downregulation occurs both at the transcriptional and post-transcriptional levels [121]. Furthermore, *in vivo* tRA treatment of SCC xenografts in athymic nude mice has been shown to reduce the FGF-BP expression, correlating with inhibition of tumor angiogenesis, induction of apoptosis and a decrease in tumor growth [122]. In further studies, the relative roles of the retinoid receptor subtypes (RXR and RAR) in the transcriptional and post-transcriptional repression of FGF-BP gene expression have been investigated. It was shown that post-transcriptional degradation of FGF-BP mRNA is the predominant mechanism for reducing of FGF-BP and that RAR receptors are major regulators at this level [123].

Recently, other regulators of FGF-BP expression have been demonstrated. In prostate carcinoma PC-3 cells transfected with human full-length androgen receptor, androgen stimulation induces an increase in FGF-BP mRNA and protein, suggesting the production of FGF-BP under androgen control [124]. A subsequent study reported the up-regulation of FGF-BP by β-catenin during colon carcinogenesis [97].

1.3.6 Structural characterization of FGF-BP

Lametsch et al. [125] described the purification and characterization of FGF-BP from bovine prepartum mammary gland secretions. Inspection of the cDNA sequence predicted that the unprocessed bovine FGF-BP is 234 residues long and the amino acid sequence showed a significant similarity with that of human (60%) and mouse (53%) FGF-BP. By means of matrix assisted laser desorption ionization-time of flight-mass spectrometry (MALDI-TOF-MS), it was determined that all 10 cysteines, which are positionally conserved in human, mouse and bovine FGF-BP, participate in disulfide bonds, and the pattern was identified as Cys71-Cys88, Cys97-Cys130, Cys106-Cys142, Cys198-Cys234 and Cys214-Cys222. N- and O-glycosylation of Asn155 and Ser172, respectively, was demonstrated in bovine FGF-BP. While the bovine N-linked glycosylation site has no counterpart in the predicted amino acid sequences of human and mouse FGF-BP, the O-glycosylated residues in bovine protein are conserved in other FGF-BPs. Lametsch et al. [125] found that the purified bovine FGF-BP started at Gly32 and Ser52, respectively, whereas the human FGF-BP starts with Lys34 [32]. The enzyme responsible for cleavage of the removed peptides from unprocessed bovine FGF-BP during secretion process remains to be identified. It is noteworthy, that the C-terminus of removed peptide in bovine FGF-BP contains a dibasic sequence (Arg30-Arg31 and Lys48-X-X-Arg51), which is not found in the sequence of human FGF-BP. The presence of this sequence suggests that one or more subtilisin-like endopeptidases may be responsible for the processing [126].

While data on the FGF-binding site of FGF-BP are still lacking, data on heparin-binding sites are available. The principle heparin-binding site of human FGF-BP purified from A431-conditioned medium has been localized to residues Arg110-Phe143 characterized by the high content of basic amino acid clusters and may contribute to the binding specificity [127]. In addition to this highly basic region, there are two partial heparin-binding consensus sequences (Lys25-His32 or Lys163-Ser169), which were determined by comparison of the proposed consensus sequences of protein-heparin interactions [128,129]. It is noteworthy that the first partial heparin-binding consensus sequence (Lys25-His32) is included in the N-terminal signal sequence, which is removed from unprocessed FGF-BP during the secretion process.

1.3.7 The mechanism of FGF-BP action

The role of FGF-BP in the extracellular activation of FGF-2 is still somewhat unclear, since previous studies provide only indirect conclusions on the mechanism of action of FGF-BP or lead to partly contradictory and still incomplete results. It has been demonstrated that the transfection of FGF-BP in the non-tumorigenic FGF-BP negative human adrenal carcinoma cell line SW-13 resulted in a tumorigenic and angiogenic phenotype when these cells were injected into nude mice [88]. It was also shown that these FGF-BP transfectants form colonies in the soft agar assay and release FGF-BP into their media together with FGF-2 in a non-covalently bound form. As expected, colony formation of FGF-BP-transfected SW-13 cells can be blocked by a specific antibody against FGF-2, demonstrating that the tumorgenic potential of FGF-BP is FGF-2-dependent [88].

As an alternative approach, the effects of depletion of endogenous levels of FGF-BP on angiogenesis and tumor growth were also investigated [91]. Endogenous FGF-BP mRNA in human squamous cell carcinoma ME-180 and in human colon carcinoma LS174T cells was reduced by means of ribozyme-targeting. The reduction in FGF-BP expression resulted in decreased levels of biologically active FGF-2 released from the cells in culture. In addition, the growth and angiogenesis of xenografted ME-180 and LS174T tumors in mice was decreased in parallel to the ribozyme-mediated reduction of FGF-BP.

In further studies, it was found that FGF-BP binds to FGF-2 in a dose-dependent and specific manner and that binding is inhibited by FGF-1, heparan sulphate, and heparinoids [33]. Furthermore, in chicken chorioallantoic membrane (CAM) assays, a significant FGF-BP-dependent increase of FGF-2-mediated angiogenesis was demonstrated. Additionally, FGF-BP enhanced FGF-1- and FGF-2-dependent proliferation of NIH-3T3 fibroblasts. These results suggest a positive modulation of the biochemical and biological activity of FGF-2 by FGF-BP in multiple models. Finally, further evidence of a role of FGF-BP in the extracellular activation of FGF-2 comes from findings that FGF-BP alters the binding affinity of FGF-2 to heparin without additional cofactors, which directly proves the mechanism of FGF-2 release from the extracellular matrix [130]. Moreover, exogenously administered FGF-BP stimulates the growth of different tumor cells as well as the growth and chemotaxis of endothelial cells and, this effect is FGF-2-dependent [130].

Taken together, these data are consistent with the concept that the secreted FGF-BP can recover FGF-2 from its immobilized state on the cell surface and thus serve as an extracellular carrier molecule to its receptor (Fig. 1). As such, FGF-BP can bolster autocrine and paracrine activites of FGF-2 *in vitro* and *in vivo*.
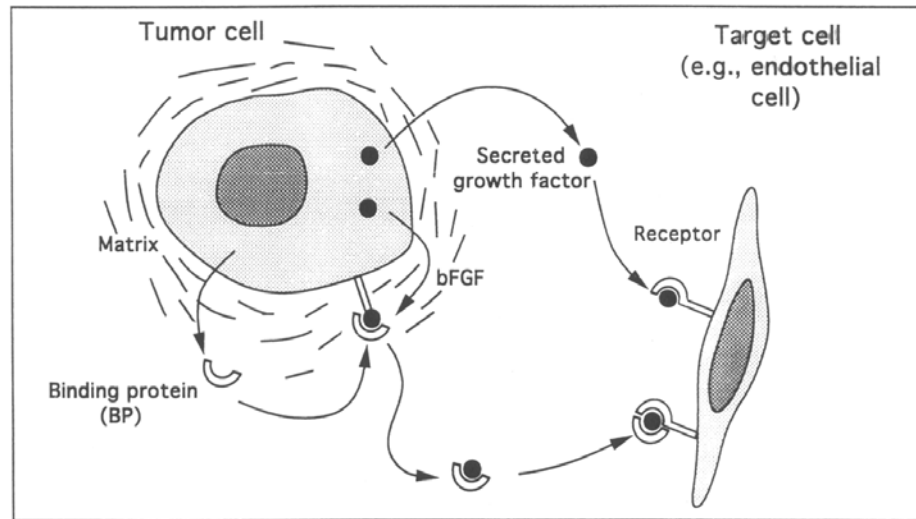
Fig. 1 **Model of mechanism of action of FGF-BP.**
In some tumors, FGF-BP expression is up-regulated and FGF-BP is secreted into extracellular environment. FGF-BP binds to immobilized FGF-2, which is stored in the extracellular matrix. FGF-2 is then released in a soluble and bioactive form, allowing it to reach its target cell receptor and exert its effects (from [132]).

On the other hand, various lines of evidence suggest that FGF-BP expression is downregulated in SSCs and has no obvious role in the release of FGF-2. By Northern and Western blotting, Sauter et al. [131] demonstrated that FGF-BP expression is decreased with progression to carcinoma. In clinical specimens, FGF-BP protein expression in normal human epithelium is relatively uniform and shows moderate to high intensity, whereas carcinomas demonstrate more focal, less intense and more heterogenous staining. Moreover, *ex vivo* transduction of FGF-BP into a transformed keratinocyte cell line (HaCaT) and tumorgenic human SSC cell lines (Det 562, FaDu) did not lead to tumor formation or increased vascularity of the tumors upon injection of the cells into SCID mice.

It was also reported that the binding of FGF-BP to FGF-1 and FGF-2 inhibits their biological activities at least in the absence of heparin and this effect is due to reduction of ligand binding [32]. Furthermore, it was shown that FGF-BP purified from conditioned medium of human epidermal carcinoma cells A431-AJC inhibits at high medium concentrations DNA synthesis and cell growth in mouse fibroblast 3T3 cells [133]. These effects are probably due to the formation of FGF-BP/FGF complexes leading to the reduction of free FGF-1 and FGF-2 concentrations and hence leading to insufficient stimulation of DNA synthesis and cell growth in these cells. When FGF-1 and FGF-2 were added back at very low concentration to medium, they reversed this inhibition by FGF-BP and cellular DNA synthesis and growth were recovered, indicating that FGF-BP interacts with both FGFs in reversible manner. The degree of specificity of FGF-BP interaction with FGF-1 and FGF-2 was shown by the fact that EGF did not reverse the inhibition of DNA synthesis and cell growth mediated by high concentrations of FGF-BP. In contrast to high concentrations of FGF-BP in conditioned medium, low concentrations induced DNA synthesis and cell growth of 3T3 cells. This biphasic action of FGF-BP on DNA synthesis in 3T3 cells suggests specific physiological roles in addition to the function as carrier protein. It is noteworthy that the biphasic action of FGF-BP was seen in normal cell lines (HUVEC: Human umbilical vein endothelial cells and 3T3: mouse fibroblast cell line), while it had no effect on human epidermal carcinoma cells A431-AJC [133].

Furthermore, FGF-BP has been postulated to exist as a dimer [134]. This and other data (Achim Aigner, unpublished data) indicated the existence of stable, covalent multimers of FGF-BP. Moreover, although the purified bovine FGF-BP from prepartum mammary gland secretion has not been shown to form multimers, discrepancies between the calculated and observed molecular weights could not be fully explained [125]. Clearly, the mechanism of FGF-BP action and the relevance of the apparent formation of the stable homo- or heterocomplexes mentioned above remain to be elucidated.

1.4 The HER-2 Receptor

The HER-2 proto-oncogene (also known as *neu*, NGL, or *c-erb*B-2) encodes a 185-kDa transmembrane glycoprotein, with extensive sequence homology to the epidermal growth factor receptor (EGF-R) [135-137]. It was originally identified as a transforming oncogene in chemically induced rat neuroglioblastomas, where a single point mutation in the

transmembrane domain of the molecule is sufficient to confer oncogenic activity [136,138]. Indeed, this and other HER-2 point mutations have only rarely been found in human cancers.

HER-2 is a member of the membrane-spanning type I receptor tyrosine kinase (RTK) family, which is also called human epidermal growth factor receptor HER or ErbB family and comprises four homologous receptors: (*a*) HER-1, also termed epidermal growth factor receptor (EGF-R) or *erb*B-1 and the first to be cloned [139]; (*b*) HER-2, *c-erb*B-2; (*c*) HER-3, *erb*B-3; and (*d*) HER-4, *erb*B-4 [140,141]. In response to growth factor ligands, members of the HER family induces a variety of cellular responses, including proliferation, differentiation, cell motility, and survival.

1.4.1 Structure of HER receptors

All HER receptors share a similar structure, comprising an extracellular ligand binding domain with four subdomains including two cysteine rich domains (I-IV), a transmembrane lipophilic segment, and an intracellular domain (Fig. 2) [142]. The intracellular portion of HER receptors consists of a tyrosine kinase domain, a juxtamembrane region, and a carboxyl tail harboring the autophosphorylation site. The highest degree of sequence homology (approximatly 80% amino acid identity) between HER-1, HER-2 and HER-4 lies in the tyrosine kinase domain, suggesting that this region is essential for the signaling function of these molecules [143]. HER-3, by contrast, contains substitutions of critical amino acids within this domain and lacks kinase activity [144,145].

The activation of HER receptors, which exist as monomers in the plasma membrane, is usually dependent on the presence of ligands [147,148] and other receptors of the HER family [149]. Ligand binding induces the homo- or heterodimerization of HER receptors. Some intriguing questions concerning the process of ligand-induced receptor dimerization have been clarified by publications describing the crystal structure of HER-1, HER-2 and HER-3 ectodomains (reviewed in [150]). As mentioned above, the extracellular region of each HER receptor consists of four domains (I-IV; Fig. 3). Determination of the structure of ligand-bound HER-1 has confirmed earlier studies (reviewed in [150]) that show the importance of domains I and III in peptide binding. Moreover, these studies also revealed that there is a direct receptor-receptor interaction promoted by the domain II dimerization arm [151,152]. In unliganded HER-3 [153] or ligand-bound inactive HER-1 [154] the

receptors assume the so-called tethered structure, in which the domain II dimerization interface is blocked by intramolecular interactions between domains II-IV.

HER-1   HER-2   HER-3   HER-4
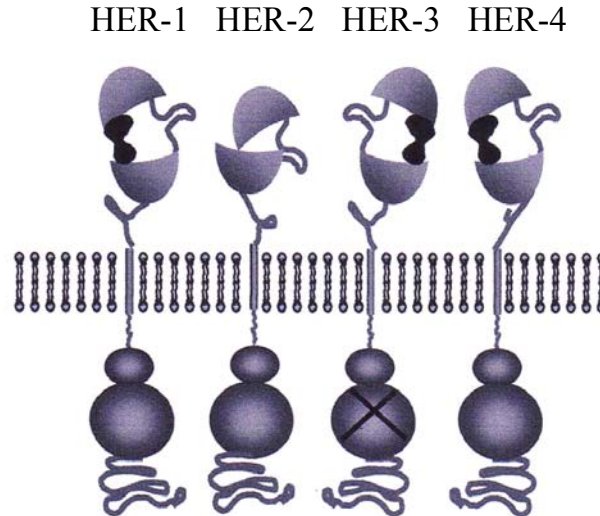
*Fig.2 **Structure of HER receptors.***
HER receptors are located at the cell membrane and have in common an extracellular ligand binding domain, a single hydrophobic transmembrane domain, and an intracellular domain. The extracellular domains comprise 2 cysteine-rich domains (represented by loops), which mediate ligand-induced dimerization. In addition, the ectodomains include 2 cysteine-free regions, each capable of binding a distinct portion of the bivalent growth factor ligand (shown as a dark structure). The highly homologous cytoplasmic regions contain a tyrosine kinase domain, a juxtamembrane region, and a carboxyl tail harboring the autophosphorylation site. HER-3 contains substitutions of critical amino acids within this domain and lacks kinase activity (from [146]).

The structure of the HER-2 extracellular region is radically different from the others. HER-2 has a fixed conformation that resembles the ligand activated state: the domain II-IV interaction is absent and the dimerization loop in domain II is exposed [155,156]. This structure is consistent with the data that indicate that HER-2 is the preferred partner for other activated HER receptors, as it is permanently poised for interaction with another ligand-bound receptor.
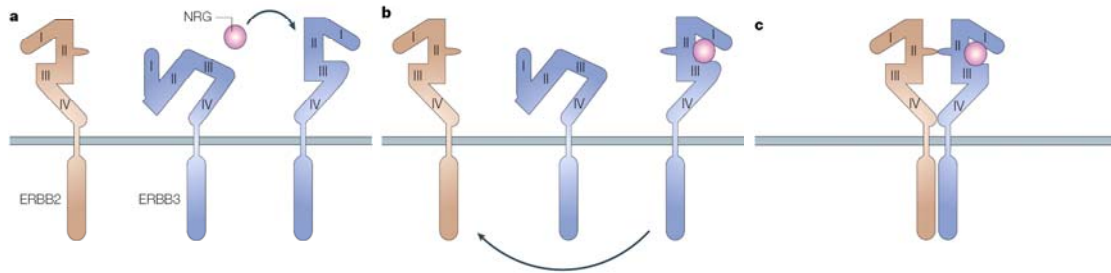
Fig.3 **Structures of HER extracellular domain.**

The extracellular region of each HER receptor consists of four domains (I-IV). It has been suggested that in the absence of ligand, HER-3 and HER-1 (not shown) assume a tethered structure. (a) Domains I and III are involved in the neuregulin (NRG) binding and, following this, the dimerization arm in domain II is exposed (b) and promotes receptor-receptor interaction (c). HER-2 has a fixed conformation that resembles the ligand-activated state of HER-1 and HER-3 (modified from [157]).

Both ligand-mediated homo- and heterodimerization of HER receptors lead to receptor transphosphorylation on tyrosine residues within the activation loop, which significantly enhances kinase activity [158,159]. Subsequent tyrosine phosphorylation on residues within the carboxyl terminal tail of the receptors enables the recruitment and activation of signaling effectors containing Src homology 2 (SH2) domains and phosphotyrosine binding (PTB) domains. Subsequently, intracellular proteins involved in the signaling pathway are phosophorylated and activated, resulting in the modulation of gene transcription [160].

1.4.2 Ligands of HER receptors

There are ten characterized human ligand genes encoding HER-specific ligands, each of which containing an EGF-like domain that confers binding specificity, allowing them to be divided into three groups (Fig. 4). The first group includes EGF, amphiregulin (AR), and transforming growth factor-α (TGF-α), which bind specifically to HER-1; the second group consists of betacellulin (BTC), heparin-binding EGF (HB-EGF), and epiregulin (EPR), which exhibit dual specificity in that they bind HER-1 and HER-4. The third group is composed of the neuregulins (NRG) and forms two subgroups based upon their capacity to bind HER-3 and HER-4 (NRG-1 and NRG-2) or only HER-4 (NRG-3 and NRG-4).

Interestingly, HER-2 is a unique member of the HER family in that it does not bind directly any of the known ligands with high affinity. Though HER-2 is thought to be an orphan receptor, it is a co-receptor for many different ligands and the preferred heterodimeric partner for other HER receptors. Neuregulins can induce the formation of HER-2/HER-3 and HER-2/HER-4 heterodimers [161,162].
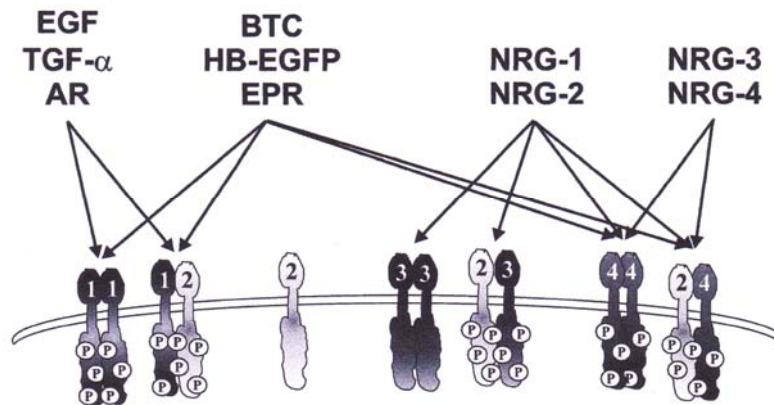
Fig.4 *The HER growth factor ligands.*

The family of the HER-specific ligands consists of ten members. They can be divided into groups depending upon binding specificity toward the HER receptors. No known direct ligand binds HER-2. Hence, it needs a heterodimerization partner to acquire signaling potential (indicated by phospho residues). Since HER-3 lacks a functional tyrosine kinase domain, HER-3/HER-3 homodimers do not signal. However, interestingly, the NRG-mediated HER-2/HER-3 heterodimers provide the most potent mitogenic signal (from [172]).

Although both ligand-mediated homo- and heterodimerization result in the activation of the HER network, heterodimers are more potent and mitogenic. Heterodimerization can provide additional phosphotyrosine residues for the recruitment of binding partners, as well as induce distinct patterns of the receptor phosphorylation and downstream signaling. In addition, the attenuation of signaling through receptor endocytosis and subsequent lysosomal degradation differs between receptor dimers [163,164]. Interestingly, heterodimers containing HER-2 have particularly high ligand binding and signaling potency as compared to heterodimers without HER-2 [165,166]. The increased potency of HER-2-containing heterodimers is attributable to several reasons, including increased ligand affinity through a decelerated rate of ligand dissociation, efficient coupling to signaling pathways, and decreased rate of receptor downregulation [165,167-169]. Furthermore, signaling through the

kinase-deficient HER-3 requires heterodimerization with a kinase-active partner. Through heterodimerization, the ligandless HER-2 and the kinase-inactive HER-3 provide the most potent mitogenic [161,170] and angiogenic signal [171].

1.4.3 HER-2-induced signaling pathways

HER signaling can not be considered as a linear pathway because of the high level of interaction that occurs between the different HER receptors. Instead, HER signaling is a very interactive system in which the ligand can lead to the formation of different homodimers or heterodimers that interact to stimulate a variety of signaling pathways. This process has been described as network signaling. The HER network play important roles in cell growth and differentiation and is implicated in signaling downstream of cellular stimuli, including cell adhesion, lymphokines, or stress signals [173].

The HER signal-transduction network consists of a stromal input layer (ligands or growth factors), a cellular information processing layer (receptors, SH2-proteins, transcription factors), and an output layer (cell growth, differentiation or migration). Receptor dimerization is important here, allowing a signaling network with an enormous potential for diversification of biological messages instead of four receptors with only four linear pathways. The coordination of the whole network, according to this model, is performed by HER-2. Furthermore, it is believed that the absence of a HER-2-specific ligand facilitates the HER-2-mediated regulation of the entire HER signaling network.

The three best characterized signaling pathways induced through HER receptors are Ras-mitogen-activated protein kinase (Ras-MAPK), Phophatidylinositol 3-kinase-protein kinase B (PI3k-PKB/Akt), and phospholipase C-protein kinase C (PLC/PKC) pathways (reviewed by [160,174,175]).

The Ras-MAPK cascade is a critical pathway for a number of signals transduced inside the cell, many of which being growth-regulating signals. Moreover, Ras genes, which encode small proteins with intrinsic GTPase activity, are the most frequently mutated oncogenes in human cancers [176], leading to the concept that this pathway is a common target for many transforming and/or carcinogenic agents. Stimulation of the Ras pathway ultimately leads to the activation of mitogen-activated protein (MAP) kinase, an enzyme with a number of

intracellular targets including nuclear transcription factors [177]. All HER ligands and receptors couple to activation of the Ras-MAPK pathway, either directly through SH2 domain-mediated recruitment of Grb-2 or indirectly through PTB domain-mediated binding of the Shc adaptor.

1.4.4 The relevance of the HER-2 network in cancer

The HER network is implicated in multiple human cancers, and deregulation of many signaling pathways induced through HER receptors can promote multiple properties of neoplastic cells, including proliferation, migration, angiogenesis, stromal invasion, and resistance to apoptosis. Hyperactivation of the HER network can occur via an autocrine secretory loop involving overproduction of ligands and receptors by the tumor cells, or paracrine growth, which is dependent on HER ligands produced by adjacent stromal cells [178]. Alternatively, aberrant growth can ensue from constitutive receptor activation [179].

The oncogenic effect of HER-2 may relate to its high basal autophosphorylation [179]. High levels of HER-2 expression may result in its constitutive homodimerization and promote transformation in tissue culture models [180,181]. In addition, ligand-independent homodimerization was observed in rats treated with carcinogen, in which a single point mutation within the transmembrane domain of the HER-2 receptor (called NeuT) results in constitutive receptor activation and the formation of neuroglioblastomas [136,137,182]. Although not naturally occuring, a comparable mutation in human HER-2 leads to increased dimerization and transforming ability [182]. Alternatively, overexpressed HER-2 may promote tumor formation as a result of spontaneous or ligand induced heterodimerization with other HER receptors [183] leading to signal potentiation. Indeed, coexpression of an additional HER receptor is required for NeuT-mediated transformation [184,185]. Furthermore, many HER-2-expressing tumors also exhibit an autocrine loop involving the expression of both HER-1 and one of its ligands, and loss of HER-2 function inhibits the proliferation of these tumor cells. Most breast, skin, lung, ovary, and gastrointestinal tract tumors express HER-3 and/or HER-4, and heteromerization of these receptors with HER-2 may be involved in some cancers, such as oral squamous cell cancer and childhood medulloblastoma [186,187].

Amplification and/or overexpression of HER-2 is relevant in human cancer, as it has been observed in 20-30 % of adenocarcinomas such as breast, ovary, lung, stomach and pancreatic cancer [2,3] and in 100 % of stage III/IV ovarian carcinoma cell lines [188]. Furthermore, HER-2 overexpression has been linked to an unfavorable prognosis and more aggressive malignant behavior of tumors in patients with breast and ovarian cancer [189]. Hence, HER-2 is a prognostic and an excellent target for novel therapeutic approaches in HER-2-overexpressing cancers.

1.4.5 Effects of HER-2 overexpression on chemotherapeutic drug sensitivity in tumor cells

The consequences of HER-2 overexpression are mainly hyperactivation of different components of the cell cycle apparatus, increased proliferation and survival rate of cells, increased metastasis (presumably through up-regulation of basement membrane degradative enzymes, such as the matrix metalloproteases (MMPs) [190]), as well as in many cases increased resistance towards cytokines, hormone therapy, certain chemotherapeutic agents [191,192] and radiation therapy [193,194] (Fig. 5).
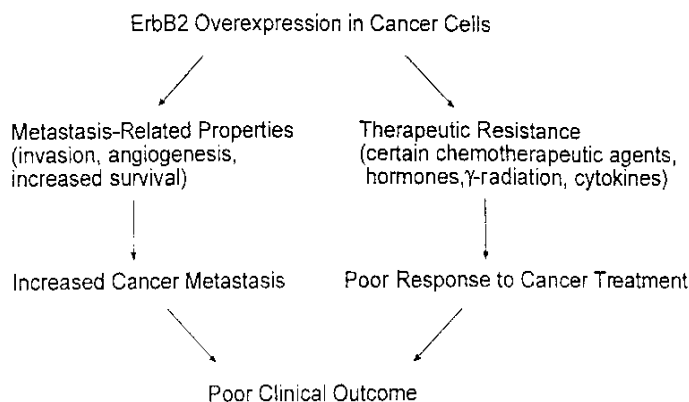
*Fig. 5 **Consequences of HER-2 overexpression in cancer cells** (according to [190]).*

The relationship between HER-2 overexpression and drug sensitivity is of considerable interest, as this may allow to better predict response to chemotherapy. Several *in vitro* studies demonstrated the association of overexpression of HER-2 receptor with chemoresistance to

several anticancer drugs in cancer cells. HER-2 overexpression can cause chemoresistance in some non-small-cell lung cancer cell lines [195]. Moreover, using a panel of established human breast cancer cell lines that express different levels of HER-2, higher levels of HER-2 expression in these cell lines were correlated with increased resistance to two chemotherapeutic drugs, paclitaxel (taxol) and docetaxel (taxotere) [196]. The analysis of molecular mechanisms underlying HER-2-mediated taxol resistance in HER-2-transfected MDA-MB-435 breast cancer cells indicated that overproduction of HER-2 up-regulates $p21^{Cip1}$, which in turn inhibits taxol-mediated activation of $p34^{Cdc2}$ kinase and thereby impedes taxol-induced apoptosis [197].

An important method for demonstrating the involvement of the HER-2 gene in drug sensitivity is the suppression of the HER-2 oncoprotein by treatment with antisense HER-2 oligonucleotides [198] or treatment with an anti-HER-2 antibody. Trastuzumab (Herceptin) is a humanized monoclonal antibody which interferes with HER-2-mediated signaling by binding to the extracellular domain of HER-2 and downregulating HER-2 receptor density. *In vitro* studies indicate that co-treatment with trastuzumab and anticancer drugs such as anthracyclines and taxanes increases drug sensitivity in an additive and synergistic manner [199-201]. Subsequent clinical studies of combination treatments with trastuzumab and doxorubicin or paclitaxel indicated an increased response rate and prolonged survival compared to treatment with either anticancer drug alone [202].

Several clinical studies confirmed the above-described relationship between HER-2 overexpression and drug sensitivity in breast tumors. A clinical study conducted in 1992 found that HER-2-overexpressing breast tumors are less responsive to adjuvant chemotherapy regimens consisting of cyclophosphamide, methotrexate and 5-fluorouracil (CMF) than are tumors that express normal amounts of HER-2 [203]. Interestingly, patients with node-positive early-stage breast tumors that overexpressed HER-2 benefitted from higher doses of chemotherapy, whereas patients with early-stage disease not exhibiting HER-2 overexpression did not [204]. Meanwhile, another study showed that the status of HER-2 expression was useful for predicting survival time only in patients receiving adjuvant therapy, further suggesting that HER-2 may be a marker of drug resistance [205]. In addition, several studies have shown that the serum level of the HER-2 protein can also predict the responsiveness of breast cancers to adjuvant treatment [206,207].

For ovarian carcinoma cells, conflicting data have been obtained. On the one hand, in the HER-2 overexpressing SKOV-3 cell subtype SKOV-3.ip1 HER-2 reduction through stable expression of adenovirus type 5 E1A protein was coincident with increased sensitivity to paclitaxel [208,209]. On the other hand, it was found that reversal of HER-2 overexpression in SKOV-3 cells led to increased rather than decreased cellular resistance towards paclitaxel [210] and, concomitantly, in another study paclitaxel-resistant SKOV-3 ovarian carcinoma cells displayed lower HER-2 levels as compared to the corresponding paclitaxel-sensitive wildtype cells [211]. Finally, Pegram et al. [192] reported that overexpression of HER-2 was not sufficient to induce intrinsic paclitaxel resistance in ovarian and breast cancer cells and concluded that HER-2 levels are not sufficient to predict changes in chemosensitivity profiles.

1.4.6 HER-2-targeting strategies

As a result of the observations to the role of HER-2 overexpression in tumor cells, HER-2 proves to be an excellent target for novel therapeutic approaches specific to HER-2-overexpressing. In the past ten years, several targeting strategies have been developed.

In the context of this thesis, different and independent HER-2 targeting strategies were employed, including treatment with the HER-2 inhibitory antibody trastuzumab (Herceptin), downregulation of HER-2 expression by ribozyme-targeting, and treatment with tyrosine kinase inhibitors. All these strategies are described in detail below.

Development of anti-HER-2 receptor antibody

The cancer-inhibitory potential of antibodies to HER-2 was realized as far back as 1984, when mice bearing tumors with an active form of rodent HER-2 were treated with specific antibodies [212]. On the basis of these observations, the exact mechanism by which anti-HER-2 antibodies inhibit cell growth has been examined. Mechanistically, the antibodies appear to act by removing HER-2 from the cell surface. It has previously been shown that the oncogenic activity of HER-2 necessitates its localization in the plasma membrane [213]. In line with blocking HER-2 action by preventing its interaction with other surface-localized HER receptors, the tumor-inhibitory potential of certain combinations of anti-HER-2 antibodies [214] correlates with the efficiency of antibody-induced downregulation of HER-2. This downregulation of cell-surface HER-2 has been observed by treating HER-2-

overexpressing tumor cells with the humanized monoclonal mouse antibody trastuzumab [215] that is known as Herceptin. In preclinical studies and Phase II and Phase III trials Herceptin has demonstrated tumor inhibitory and chemosensitizing effects for taxol and several chemotherapeutic agents [199,216-219]. Furthermore, Herceptin has been approved for the adjuvant treatment of advanced breast and ovarian cancer (for review, [220,221]).

Suppression of HER-2 expression through riboyzme targeting

Ribozymes (*ribozymes = ribonucleic acid-derived enzymes*) are one kind of catalytic RNAs with site-specific binding and cleavage activities. Hammerhead ribozymes are the best characterized ribozymes and were discovered in plant RNA viruses, which contain a single circular RNA molecule as their genetic material. These viruses replicate using a so-called 'rolling circle mechanism', in which the replication machinery constantly travels around the circular RNAs and produces a linear chain containing many copies of the RNA genome. The hammerhead ribozyme is the 'pair of scissors' in this process, snipping the linear chain into single-genome length pieces. It does this by attaching itself to the RNA genome via specific sequences at the region between its two 'hammer heads'. The minimal sequence of the hammerhead ribozyme required for catalysis comprises around 40 nucleotides folded into three stems which are connected by single-stranded regions (Fig. 6) [222,223] for review see [224]). The properties of hammerhead ribozymes, i.e. site specific mRNA binding and cleavage activity, have been applied to destruct target gene expression by artificially designed and synthesized hammerhead ribozymes [92,225-227]. Hence, Hammerhead ribozymes have long been considered a potentially useful tool for gene silencing, have demonstrated their utility in attenuating eukaryotic gene expression and have been examined in preclinical gene therapy models [228].

Ribozyme-targeting of cancer-relevant genes has attracted great attention due to the simple structure of ribozyme as well as their easy designation, site specific mRNA cleavage activity, and catalytic potential [229-234]. Furthermore, ribozyme-targeting is a very attractive and generally applicable method, which has the advantage of allowing the stable and selective reduction of an isolated gene product without interference in other cellular processes, providing a tool for the isolated functional study of the gene of interest. Ribozyme targeting of HER-2 gene expression has been recently examined by numerous studies [235-238]. In two studies, an adenovirus encoding a ribozyme targeting of HER-2 was shown to deplete HER-2 mRNA in ovarian carcinoma and in breast cancer cells. Moreover, Suzuki et

al. [235] demonstrated the repression of the tumor cell growth by ribozyme-containing adenovirus. Finally, the effects of anti-HER-2 ribozymes transfected as ribozyme-expression plasmids into ovarian carcinoma cells were investigated [236,238].
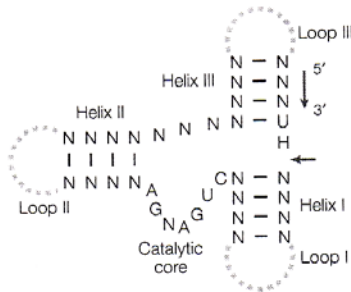
Fig.6 **Structure of a hammerhead riboyzme.**

The hammerhead motif consists of three base-paired stems connected by single-stranded regions. The arrows indicate the cleavage site on the riboyzme.

Inhibition of the tyrosine kinase activity of the HER-2 receptor through tyrosine kinase inhibitors

Tyrosine kinase inhibitors (TKIs) are small molecules that inhibit the activity of tyrosine kinases in the intracellular domain of the HER receptors, thus preventing receptor auotophosphorylation and subsequent activation [239]. They compete at the binding site for adenosine triphosphate. Gefitinib (ZD1839, Iressa), one of the most widely studied, demonstrates remarkable selectivity for HER-1 compared to other receptor tyrosine kinases. In contrast, there are some dual TKIs of HER-1 and HER-2, which are currently in clinical trials, including Lapatinib (phase III) or AEE788 (phase I) [157]. In response to ligand activation, HER-2 and HER-1 heterodimerize. This makes dual tyrosine kinase inhibition of HER-1 and HER-2 an attractive therapeutic strategy for epithelial tumors.

Early work with TKIs assessed their potential as primary chemotherapeutic chemosensitizing and radiosensitizing agents. They have been shown to inhibit the growth of cancer cell lines *in vitro*, e.g. ovarian, colon, and breast cancer cells [240] as well as *in vivo* in human tumor xenografts [241]. Furthermore, growth inhibition has been shown to be enhanced when gefitinib is combined with structurally and functionally different drugs *in vitro* and *in vivo*, such as cisplatin, paclitaxel, and topoptecan [242].

D-69491 and D-70166 represent two newly developed low molecular weight HER tyrosine kinase inhibitors (Baxter Oncology GmbH, Frankfurt/Main, Germany). The inhibitory effects of these two HER tyrosine kinase inhibitors on the HER-2 phosphorylation were first shown in HER-2 overexpressing NIH3T3 cells [243]. The cells were treated with D-69491 or D-70166 for 8 h at different concentrations the phosphorylation of HER-2 was analyzed by Western blotting. Both D-69491 and D-70166 inhibit dose-dependently HER-2 phosphorylation. While at tyrosine kinase inhibitor concentrations of 3.16 or 10 µM band intensities of non-phosphorylated HER-2 are slightly decreased, phosphorylated HER-2 is almost completely or completely (10 µM D-69491) absent indicating inhibition after 8 hours treatment.

Other HER-2-targeting strategies include:
-   Blocking of HER-2 expression through antisense oligonucleotides and antisense RNA [244,245]
-   Suppression of HER-2 expression through siRNA [246,247]
-   Downregulation of HER-2 mRNA and protein expression through Retinoic acids [248,249]
-   Transcriptional repression of HER-2 gene expression through Adenovirus type 5 E1A proteins [250-252], as well as
-   Development of anti-HER-2 intracellular single-chain antibodies, which eradicate HER-2 from the cell surface membrane by ectopic localization of the HER-2 protein to the endoplasmic reticulum [253,254]

1.5 Antineoplastic agents

1.5.1 Taxol

Taxol$^{®}$ (paclitaxel), a naturally occurring diterpenoid isolated from the bark of the Pacific yew tree (*Taxus brevifolia*), is currently considered one of the most important drugs in cancer chemotherapy. Paclitaxel has been approved by the Food and Drug Administration (FDA) for treatment of various human tumors such as advanced ovarian cancer, metastatic breast cancer and Kaposi's sarcoma [255,256]. This anticancer drug is currently undergoing clinical trials worldwide for the treatment of other cancers (e.g. lung, head and neck, prostate, and cervical

cancers) as well as in combination with other anticancer agents. Paclitaxel and docetaxel, a semisynthetic analog of paclitaxel, are the first members of a new class of microtubule-stabilizing anticancer agents.

Taxol differs from other anti-microtubule agents such as vinblastine and colchicines by causing microtubule polymerization rather than of depolymerization [257]. This stabilizing effect leads to blockade of the cell in the late G2/M phase of the cell cycle and inhibition of cell division [257]. Furthermore, it has been found that taxol stabilized the microtubule dynamics at relatively low concentrations [258]. Most of the anti-microtubule agents, including taxol, vinblastine, colchicines and estramustine, bind to β-tubulin. Taxol binding sites on β-tubulin were identified at the N-terminal 31 amino acids and at residues 217-231 of the protein [259]. These two binding sites are part of the colchicine binding site and are highly conserved among species. However, Combeu et al. [260] showed taxol binding sites on both α and β subunits of tubulin. Taxol does not bind to actin, intermediate filament proteins, or to DNA *in vivo* and *in vitro* [261].

During the last years, additional activities of taxol have been described including the effect on cell signaling and gene expression, activation of mitogen-activated protein kinases (MAPKs), Raf-1 and protein tyrosine kinases (PTK) [262-264]. Treatment of a variety of tumor cells with taxol induces apoptosis *in vivo* and *in vitro* [265], and it has been shown that the expression of apoptosis-related proteins like bcl-2, bad, bcl-x, p21-waf, and tumor necrosis factor-α (TNF-α), are regulated by taxol [266-270]. However, the exact mechanism by which taxol induces apoptosis is unkown.

1.5.2 rViscumin

Extract preparations from natural mistletoe (Viscum album) have been widely used for several decades as alternative therapy in the management of patients with malignant disease, based on presumed immunostimulatory and antineoplastic effects [271,272]. Viscumin (mistletoe lectin, ML I) is the main therapeutic principle of extracts from mistletoe [271,273]. The heterodimeric 65 kDa glycoprotein belongs to the type II ribosome-inactivating proteins (RIPs) and catalyses the selective hydrolysis of the N-glycosidic bond at the adenine-4324 in the eukaryotic 28S ribosomal RNA which inhibits the elongation step of protein biosynthesis [274]. Tumor cells often display altered, cancer-specific glycosylation patterns [275], which

seem to represent preferential binding sites for Viscumin [276] and may account for its particularly potent cytotoxic effect on cancer as compared to normal cells. *In vitro*, Viscumin is active in tissue culture in the femtomolar to the low picomolar range [277] and it induces apoptosis in several *in vitro* systems [275,277]. Furthermore, numerous studies have shown an activation and/or proliferation of cellular components of the immune system including T_H cells, granulocytes, natural killer cells and haematopoietic stem cells as well as an increased release of various inflammatory cytokines [278-280].

More recently, the ML 1 gene was sequenced and its intron-free gene was cloned [281], and in a coassociation process from the recombinant A-chain and B-chain the non-glycosylated 57 kDa Viscumin heterodimer, rViscumin, was obtained [282]. While the A-chain mediates the ribosome inactivation, the B-chain displays a carbohydrate binding activity which allows cellular uptake of the protein, and both activities of the molecule are needed for the observed cytotoxic effect of rViscumin on target cells [283]. The recombinant drug rViscumin was studied extensively in preclinical models. It was found to possess antineoplastic and immunomodulatory properties *in vitro* and *in vivo* and was tolerated well in animals [284-287]. Furthermore, the potential receptor involved in the binding of rViscumin has been identified [288,289]. In contrast to another well-known ribosome-inactivating agent, ricin, rViscumin was therefore characterized as a sialic acid-specific type II ribosome-inactivating protein. Neolacto-series gangliosides with a Neu 5Acα2-6Galβ1-4GlcNAc-terminus (CD 75s) were defined as the rViscumin receptors for the B-chain, leading to internalisation of the holoprotein [288].

rViscumin displays full cytotoxicity on tumor cells, inhibitory effects on experimental urothelial carcinogenesis, immunomodulatory effects and rRNA N-glycosidase activity *in vitro* and *in vivo* [281,282,284,290]. In animal models, rViscumin displays potent anti-tumor activity e.g. in HER-2-positive tumors like ovarian cancer [291] and urinary bladder carcinoma [290], or in sarcoma [286]. Clinical development of rViscumin as anticancer drug focuses on utilizing its immunomodulatory properties as well as its direct cytotoxicity. Clinical trials with local and systemic administration of rViscumin in cancer patients with solid tumors have been performed to monitor tolerability and biological effects [292].

1.5 Biology of ovarian cancer

Ovarian cancer is the fourth leading cause of cancer death in women and the second most commonly diagnosed gynecologic malignancy [293]. Unlike breast cancer, ovarian cancer has only few prognostic indicators of clinical outcome. The most important prognostic parameters for ovarian carcinomas are tumor stage, histologic subtype, degree of malignancy and residual tumor after surgical treatment [294].

Ovarian tumors display histological heterogeneity [295-297]. The histological classification of ovarian tumors by the World Health Organization (WHO) is based on the histogenesis of the normal ovary [295]. The histogenetic classification categorizes ovarian neoplasms with regard to their derviation from coelomic surface epithelium, germ cells, and mesenchyme (the stroma and the sex cord). Each category includes a number of subtypes. Combinations of different subtypes, either intimately intermixed or side-by-side within a single tumor, are found with some frequency. Tumors that combine two or more subtypes are designated as mixed.

Molecular genetic analyses have indicated that either activation of oncogenes or inactivation of tumor suppressor genes is involved in the tumorgenic mechanisms of various human tumors [298]. There are many oncogenes and tumor suppressor genes that have been hypothesized to be involved in the pathogenesis and progression of ovarian cancers. For example, mutations in both *BRCA-1* [299] and *BRCA-2* [300] increase susceptibility to ovarian cancer. *BRCA-1* mutations occur in about 5% of patients younger than 70 years with ovarian cancer. The estimated risk of ovarian cancer in women bearing *BRCA-1* and *BRCA-2* is 16% by age of 70 years [300]. Approximately 30% of ovarian adenocarcinomas express high levels of HER-2 oncogene, which correlates with a poor prognosis. Mutations in the host tumor suppressor gene p53 are found in 50% of ovarian carcinomas [301].

2 OBJECTIVES AND STRUCTURE OF THIS THESIS

The aim of this thesis was to study two gene products in ovarian cancer: the fibroblast growth factor-binding protein (FGF-BP) and the human epidermal growth factor receptor-2 (HER-2). In contrast to HER-2, the expression status of FGF-BP in ovarian carcinomas had not been examined so far and its mechanisms of action were poorly understood. Therefore, the following points were studied:

1. Examination of the expression of FGF-BP in normal ovaries and ovarian carcinomas by immunohistochemical analysis of tissue microarrays.
2. Analysis of mechanisms of FGF-BP action using the following strategy:
   a) Generation of full length FGF-BP-CFP and FGF-2-YFP constructs as well as C- and N-terminal FGF-BP truncations.
   b) Analysis of the subcellular localization of the fusion proteins by confocal microscopy.
   c) Analysis of the subcellular colocalization and interaction of FGF-BP constructs with FGF-2 by confocal microscopy.
   d) Analysis of the biological functions of full length FGF-BP.
   e) Analysis of the biological significance of the interaction of various FGF-BP truncated mutants with FGF-2 in soft agar assays.
   f) Analysis of the cellular uptake of exogenous FGF-BP and its dependence on the interaction with FGF-2.

Previously, conflicting data were obtained regarding the role of HER-2 overexpression in the chemoresistance towards anticancer drugs particularly in ovarian carcinomas and in ovarian carcinoma cell lines. Therefore, the following aspects were studied in this thesis:

1. Downregulation or inhibition of the HER-2 activity in human SKOV-3 cells by different strategies.
2. Analysis of the effects of HER-2 downregulation or inhibition on the cellular sensitivity towards
   a) Paclitaxel and other established cytotoxic agents (doxorubicin and cisplatin).
   b) The novel anticancer drug rViscumin.
3. Analysis of the underlying cellular mechanisms of these effects.

3 MATERIALS AND METHODS

3.1 Materials

3.1.1 Reagents

Standard chemicals and reagents were purchased from SIGMA, Merck and ROTH.

Name	Supplier
Agarose, Electrophoreses Grade	PEQLAB
Ammonium peroxodisulfate APS	Merck
Ampicilline (aminobenzylpenicilline)	ROTH
Bacto-Agar	Becton
Bromphenol blue	ROTH
BSA	ROTH
Cell Proliferation Reagent WST-1	Roche
3,3'-Diaminobenzidine tetrahydochloride DAB	SIGMA
Diethylpyrocarbonate DEPC	SIGMA
DNA ladder (1 kb)	Fermentas
Ethidium bromide	ROTH
Fluorescent mounting medium	DAKO
Harris hematoxylin solution	SIGMA
Human FGF-2	Natu Tec
JetPEI	Polyplus
2-Mercaptoethanol	SIGMA
Milk powder	SIGMA
NaI^{125}	Amersham Pharmacia
Ni-NTA sepharose	QIAGEN
Normal goat serum	Vector
Normal horse serum	Vector
N,N,N',N',-Tetramethylethylendiamine TEMED	SIGMA
peqGOLD TriFast^{TM}	PEQLAB
Prestained protein ladder, 10-180 kDa	Fermentas
RotiPhorese® Gel 40	ROTH
Salmon sperm DNA	SIGMA
Tryptone	Becton
Tween 20	SIGMA
Yeast Extract	Becton

3.1.2 Chemotherapeutic agents and phoshotyrosine kinase inhibitors

Name	Supplier
Paclitaxel	Pharmacy, Philipps-University Medical Center, Marburg
Doxorubicin	Pharmacy, Philipps-University Medical Center, Marburg
Cisplatin	Pharmacy, Philipps-University Medical Center, Marburg
rViscumin	VISCUM, Bergisch-Gladbach
D-69491	Baxter, Frankfurt/Main
D-70166	Baxter, Frankfurt/Main

3.1.3 Kits and enzymes

Name	Supplier
QIAprep Mini-prep Kit	QIAGEN
LumiGLO HRP Western blot kit	Cell Signaling
NUCLEOBOND Midi-prep Kit	Macherey-Nagel
10mM dNTP Mix	Fermentas
Rediprime™ II random prime labeling system	Amersham Pharmacia
Restriction enzymes: EcoRI, XhoI, NotI, HindIII, and XbaI	Fermentas
Ribonuclease Inhibitor	Fermentas
Taq Polymerase	Fermentas
T4 DNA Ligase supplied with 10x Ligation Buffer	Fermentas
Transcriptor Reverse Transcriptase supplied with 10x Reaction Buffer	Roche

3.1.4 Antibodies

Name	Supplier
Alexa Fluor 488-conjugated goat anti-rabbit	Molecular Probes
Anti-β-actin, mouse monoclonal	SIGMA
Anti-bcl-2, mouse monoclonal	DAKO
Anti-caspase-7, rabbit polyclonal	Cell Signaling
Anti-caspase-3, rabbit polyclonal	PharMingen International
Anti-ERGIC, mouse monoclonal	H.-P. Hauri, Basel
Anti-FGF2, rabbit polyclonal	Sigma
Anti-FGF-BP, mouse monoclonal	R&D
Anti-GFP, rabbit polyclonal	Clontech
Anti-p38, rabbit polyclonal	Cell Signaling
Anti-p42/44, rabbit polyclonal	Cell Signaling
Anti-SAPK/JNK, rabbit polyclonal	Cell Signaling

Anti-phospho p38, rabbit polyclonal   Cell Signaling
Anti-phospho p42/p44, rabbit polyclonal   Cell Signaling
Anti-phospho SAPK/JNK, rabbit polyclonal   Cell Signaling
Biotinylated horse anti-mouse IgG   Vector
Horseradish peroxidase-conjugated donkey anti-mouse antibodies   Amersham Pharmacia
Horseradish peroxidase-conjugated donkey anti-rabbit antibodies   Amersham Pharmacia
Texas Red-conjugated horse anti-mouse   Vector

3.1.5 Oligonucleotides and primers

All oligonucleotides and primers were purchased from MWG BIOTECH, Germany.

Name	Sequence
FGF-BP_1_f	5'-GGGAATTCATGAAGATCTGTAGCCTCAC-3'
FGF-BP_1_r	5'-CCGCTCGAGGCATGACGTGTCCTGCAC-3'
BP-N215_1_f	5'- GGGAATTCATGAAGATCTGTAGCCTCAC-3'
BP-N215_1_r	5'-CCGCTCGAGTCCACAGAACTCCAGGGC-3'
BP-N150_1_f	5'-GGGAATTCATGAAGATCTGTAGCCTCAC-3'
BP-N150_1_r	5'-CCGCTCGAGTAGCTTAAGACTGGATTCTG-3'
BP-N99_1_f	5'-GGGAATTCATGAAGATCTGTAGCCTCAC-3'
BP-N99_1_r	5'-CCGCTCGAGATTGCCAGCAAAGACACA-3'
BP-C91_1_f	5'-AAGGAAAAAAGCGGCCGCCGAATTTTCCTGTGTCTTTGC-3'
BP-C91_1_r	5'-CCGCTCGAGGCATGACGTGTCCTGCAC-3'
BP-C146_1_f	5'-AAGGAAAAAAGCGGCCGCCTCCAGTCTTAAGCTAGTCAG-3'
BP-C146_1_r	5'-CCGCTCGAGGCATGACGTGTCCTGCAC-3'
FGF-BP_2_f	5'-CCCAAGCTTATGAAGATCTGTAGCCTCAC-3'
FGF-BP_2_r	5'-GCTCTAGATTAGCATGACGTGTCCTGCAC-3'
BP-N215_2_f	5'-CCCAAGCTTATGAAGATCTGTAGCCTCAC-3'
BP-N215_2_r	5'-GCTCTAGTATATCCACAGAACTCCAGGGC-3'
BP-N150_2_f	5'-CCCAAGCTTATGAAGATCTGTAGCCTCAC-3'
BP-N150_2_r	5'-GCTCTAGATTATAGCTTAAGACTGGATTCTG-3'
BP-N99_2_f	5'-CCCAAGCTTATGAAGATCTGTAGCCTCAC-3'
BP-N99_2_r	5'-GCTCTAGATTAATTGCCAGCAAAGACACAG-3'
BP-C91_2_f	5'-CCCAAGCTTATGAAGATCTGTAGCCTCAC-3'
BP-C91_2_r	5'-GCTCTAGATTAGCATGACGTGTCCTGCAC-3'
BP-C146_2_f	5'-CCCAAGCTTATGAAGATCTGTAGCCTCAC-3'
BP-C146_2_r	5'-GCTCTAGATTAGCATGACGTGTCCTGCAC-3'
FGF-2_1_f	5'-CCCAAGCTTGGCGGACAGAAGAGCG-3'
FGF-2_1_r	5'-GGAATTCCGAGCTCTTAGCAGACATTGG-3'
FGF-2_2_f	5'-CCCAAGCTTGGCGGACAGAAGAGCG-3'
FGF-2_2_r	5'-GCTCTAGATCAGCTCTTAGCAGACATTGG-3'
RT-FGFr1_f	5'-CAAGGTCCGTTATGCCACCTG-3'
RT-FGFr1_r	5'-CATCACTGCCGGCCTCTCTTC-3'
FGFr1_South	5'-CTGCGTCCTCAAAGGAGAC-3'
BP_South_1	5'-GGAATTCATGAAAGTGGTCTCAGAACAAAA-3'
BP_South_2	5'-GGAATTCATGTCCAGTCTTAAGCTAGTCAG -3'

3.1.6 Bacterial cells and Vectors

Name	Supplier
Escherichia coli DH5α	Gibco BRL
pRc/CMV expression plasmid	Invitrogen
Derivative pcDNA 3.1-based plasmid containing CFP	W. Chubanov (Department of Pharmacology and Toxicology, Philipps-University, Marburg)
Derivative pcDNA 3.1-based plasmid containing YFP	W. Chubanov (Department of Pharmacology and Toxicology, Philipps-University, Marburg)

3.1.7 Tissue culture media and reagents

Name	Supplier
Iscove's Modified Eagle's Medium (IMDM) supplemented with glutamine	PAA
SF 900 II supplemented with glutamine	Life Technologies
Fetal calf serum (FCS)	PAA
Trypsin/EDTA	PAA
Phosphate buffered saline (PBS)	PAA
Geniticin® (G418 Sulphate)	CALBIOCHEM

3.1.8 Cell lines

Cell line	Type	Source
COS7	Simian fibroblasts cells	American type culture collection (ATCC)
SW-3	Adrenal carcinoma cell line	American type culture collection (ATCC)
SKOV-3	Ovarian carcinoma cell line	American type culture collection (ATCC)
HepG2	Hepatoblastoma cell line	American type culture collection (ATCC)
SF-9	Insect cells	American type culture collection (ATCC)

3.1.9 Equipment, devices and working materials

Name	Supplier
Adjustable air-displacement pipettes Pipetman®	Gilson
Autoclave Varioklav®	H+P Labortechnik
Biomax MS films	Kodak
Centricon-10 vials	Amicon
Centrifuge Biofuge	Heraeus
Centrifuge Megafuge 1.0 R	Heraeus
Centrifuge Sorvall RC 5B	Du Pont
CO_2-incubator Hera Cell	Heraeus
Confocal laser scanning inverted microscope LSM 510 META	Carl Zeiss
Digital Camera Digital Science DC 120 Zoom	Kodak
Dounce homogenizer	B.Braun
ELISA reader	BIO-TEK
Exposition chamber Hypercassette™	Amersham Pharmacia
Hyperfilm ECL	Amersham Pharmacia
Incubatior Function Line	Heraeus
Laminar flow hood Hera Safe	Heraeus
Light microscope Wilovert A	Hund
Magnetmixer Variomag®	H+P Labortechnik
Microspin column (gel filtration)	BIO-RAD
Nitrocellulose membrane	Schleicher & Schuell
Nylon membrane (HyBond N)	Amersham Pharmacia
PCR machine T3 Thermal cycler	Biometra
pH-meter	Radiometer
Poly-Prep® Chromatography columns	BIO-RAD
Orbital Shaker	Forma Scientific
Refrigerator -86C Freezer	Forma Scientific
Rotor SS-34	Sorvall
γ-Sintillation counter	Packard
Ultracentrifuge L7-55	Beckman
UV-Bank UV Transilluminator 2000	Bio-Rad
Vortex Genie 2	Scientific Industries
XCell II Blot Module	NOVEX

3.1.10 Standard solutions, buffers and bacterial growth media

Cell culture freezing medium

DMSO	5% (w/v)
FCS	20% (v/v)
IMDM	Ad 100% (v/v)

10x PBS (Phosphate-buffered saline)

NaCl	1.5 M
Na_2HPO_4	52 mM
KH_2PO_4	17 mM

PBS-T

NaCl	150 mM
Na_2HPO_4	5.2 mM
KH_2PO_4	1.7 mM
Tween 20	0.05% (v/v)

10xTBS-T

Tris-HCl	1 M
NaCl	1.5 M
Tween 20	0.5% (v/v)

Denaturating lysis buffer

SDS	4 % (v/v)
2-Mercaptoethanol	40 % (v/v)
Glycerol	20 % (v/v)
Bromphenol blue	0.01 % (w/v)

10x SDS electrophoresis buffer

Tris-HCl	2.9 % (w/v)
Glycine	14.4 % (w/v)
SDS	1 % (w/v)

10x Electrophoresis transfer buffer

Tris-HCl	2.9 % (w/v)
Glycine	14.4 % (w/v)
pH adjusted to 8.5	

10x Western blot electrophoresis transfer buffer

Tris-HCl	2.9 % (w/v)
Glycine	14.4 % (w/v)
pH adjusted to 8.5	

Stacking gel (4%)

RotiPhorese® Gel 40 (38 % Acrylamid, 2 % Bisacrylamid)	10 % (v/v)
1 M Tris-HCl pH 6,8	12.5 % (v/v)
10% SDS	1 % (v/v)
ddH_2O	Add 100% (v/v)

For 4 ml stacking gel (4%):

10 % (w/v) APS	40 µl
TEMED	4 µl

Separating gel (12%)

RotiPhorese® Gel 40 (38 % Acrylamid, 2 % Bisacrylamid)	30 % (v/v)
1 M Tris-HCl pH 8,9	37.5 % (v/v)
10% SDS	1 % (v/v)
ddH$_2$0	Add 100% (v/v)

For 12.5 ml separating gel (12%):

10 % (w/v) APS	62.5 µl
TEMED	6.25 µl

Western blot stripping buffer

2-Mercaptoethanol	100 mM
Tris-HCl pH 6.7	2.5 mM
SDS	2% (w/v)

Coomassie blue staining solution

Coomassie blue	0.125% (w/v)
Ethanol	25% (v/v)
Glacial acetic acid	10% (v/v)

Destaining solution

Glacial acetic acid	10% (v/v)
Ethanol	20% (v/v)

Drying solution

Glycerol	7% (v/v)
Methanol	55% (v/v)

Lysis buffer

Guanidinehydrochloride	6 M
Sodium phosphate	0.1 M
Tris-HCl	0.01 M
pH adjusted to 8.0	

Elution buffer (Ni-NTA affinity chromatography)

Urea	8 M
Sodium phosphate	0.1 M
Tris-HCl	0.01 M
pH adjusted to 8.0	

10x TAE (Tris/acetate/EDTA) electrophoresis buffer

Tris-HCl	2 M
Glacial acetic acid	1 M
EDTA (pH 8.0)	0.05 M

10 x DNA loading buffer

Glycerol	50% (v/v)
EDTA	0.1 M
SDS	0.1% (w/v)
Bromophenol blue	0.05% (w/v)
Xylene cyanol FF	0.05% (w/v)

Southern blot denaturation solution

NaCl	1.0 M
NaOH	0.5 M

Southern blot neutralization solution

NaCl	1.5 M
Tris-HCl	0.5 M (pH 7.2)
EDTA	1 mM

20× SSC

NaCl	3.0 M
Sodium citrat	0.3 M

50x Denhardt's reagent

Ficoll 400	1% (w/v)
Polyvinylpyrrolidone	1% (w/v)
Bovine serum albumin (BSA)	1% (w/v)

Southern prehybridization solution

SSC	5x
Denhardt	5x
SDS	0.5%
Add 100µl denaturated salmon sperm (10 mg/ml)/10 ml solution	

Hydridization membrane washing solution

SSC	2x
SDS	0.1% (w/v)

SOB medium

Tryptone	2 % (w/v)
Yeast extract	0.5 % (w/v)
NaCl	10 mM
KCl	2.5 mM
$MgCl_2$	10 mM
$MgSO_4$	10 mM

Medium was prepared and autoclaved without magnesium. Filter sterilized stock solutions of 1 M $MgCl_2$ and 1 M $MgSO_4$ were added directly before use.

Transformation buffer

PIPES	10 mM
Yeast extract	15 mM
$CaCl_2$	10 mM
KCl	250 mM
$MnCl_2$	55 mM

The buffer was made without manganese, pH was adjusted to 6.7 and then $MnCl_2$ was added.

LB Medium

Tryptone	1 % (w/v)
Yeast extract	0.5 % (w/v)
NaCl	1 % (w/v)

pH adjusted to 7.5

LB Plates with ampicilline

LB medium	
Bacto-Agar	1.5 % (w/v)
Ampicilline	100 μg/ml

3.2 Methods

3.2.1 Cell culture methods

3.2.1.1 Handling of COS-7, SW-13, HepG2, SKOV-3 and SF-9 cells

Handling and propagation of all cell lines was performed under sterile conditions. All solutions were stored at 4^oC and pre-warmed to 37^oC in a water-bath before using. Cell culture media and FCS used for all cell lines were filter-sterilized. COS-7, SW-13, HepG2 and SKOV-3 cells were grown under standard conditions (37^oC, 5% CO_2) in Iscove's Modified Eagle's Medium (IMDM) supplemented with glutamine and 10% heat-inactivated fetal bovine serum (FCS) unless indicated otherwise. Spodoptera frugiperda (SF-9) cells were grown in SF 900 II medium supplemented with L-glutamine and 10% FCS in a 27^oC non-humidified incubator.

3.2.1.2 Thawing of cultured cell lines

The cell line aliquots were stored in 1 ml freezing medium at -80^oC or in liquid nitrogen. To grow up a cell line, the freeze down was thawed quickly in a 37^oC water-bath then transferred into a 75 cm2 cell culture flask containing 10 ml medium. After 4 h incubation under standard conditions (5% CO2, 37^oC for COS-7, HepG2, SW-13 and SKOV-3 cells, 27^oC for SF-9 cells) the medium was changed and the cells were further cultivated.

3.2.1.3 Maintenance of cells in culture

All cell lines were grown in a 37^oC or 27^oC incubator and split in certain ratios depending on the stage of confluency and the proliferation rate of each cell line. SF-9 cells were detached through gentle tapping and split in several flasks containing fresh medium. The amount of medium added to the flask was dependent on its size. For 75 cm2 flasks, 10 ml medium were added. The medium was changed every three days. To split COS-7, SW-13 and SKOV-3 cells, the medium was completely aspirated from the flask and the cells were washed briefly with 5-10 ml of PBS to remove traces of FCS. After removing the PBS, 2 ml trypsin was added to the flasks and the flasks were then incubated at 37^oC. The cells were

detached after about 1-2 min with occasional gentle tapping. The trypsin was then immediately inactivated by adding 8 ml of serum-containing medium to each flask. This suspension was transferred into a 15 ml tube and centrifuged at 1,000 x g for 5 min. The supernatant was aspirated and the cell pellet was resuspended in medium and split into 3 to 5 new flasks.

3.2.1.4 Preparation of freeze-stocks of cultured cell lines

To freeze cells for long term storage, cells were harvested (at least one 75 cm2 flask of 80 % confluent cells) and centrifuged at 1,000 x g for 5 minutes. The media was then aspirated and cells were resuspended in 1 ml of cell culture freezing medium. The resuspended cell solution was transferred to Cryo-tubes and placed at -80°C in an isopropanol-containing cell freezing container, which guarantees a slow freezing process. After 24 hours, the tubes were transferred to a storage box at -80°C or in liquid nitrogen.

3.2.1.5 Transient and stable transfection of COS-7 and SW-13 cells

Transfections were performed using JetPEI as tranfection reagents. Prior to transfection, cells were grown to 80% confluency in 6-well plates in 2 ml/well IMDM medium containing 10 % FCS. For one well 3 µg DNA and 12 µl jetPEI (N/P ratio 10) were separately dissolved in 100 µl 150 mM NaCl then mixed together. After incubation at room temperature for 1 h, the DNA/jetPEI complexes were added to the cells. The medium was changed after 5 h. Analysis of transient expression was performed 48 h after transfections, or selection for stable integrants started at the same time point by addition of 500 µg/ml (SW-13) or 1000 µg/ml (COS-7) G418 for 3-4 weeks.

3.2.1.6 Growth assays

3.2.1.6.1 WST-1 proliferation assay

Experiments to study anchorage-dependent proliferation of SKOV-3 wildtype and different clonal derivative cell lines were carried out in a humidified incubator under standard conditions. SKOV-3 wildtype cells and stable ribozyme-transfected clonal cell lines were plated in quadruplicates into 96 well plates at 200 cells/well and cultivated for at least

24 h prior to addition of paclitaxel, doxorubicin, cisplatin or HER-2 inhibitors D-69491 or D-70166 at the concentrations indicated in the figures. In double-treatment experiments, cells were kept on D-69491 or D-70166 for 24 h before paclitaxel was added. Experiments were performed with cells grown in IMDM medium supplemented with 10% FCS unless indicated otherwise or, upon addition of D-69491 or D-70166, in IMDM / 2% FCS. For growth assays, culture media were changed every 24 h; treatment with paclitaxel, doxorubicin or cisplatin was performed for 3 - 5 days. Cell numbers were assessed using a colorimetric assay, which is based on the cleavage of the tetrazolium salt WST-1 by mitochondrial dehydrogenases in viable cells, according to the manufacturer's protocol. The WST-1 reagent was added to a final dilution 1:10, and after 1 h incubation, the plate was measured with the ELISA reader at 450 nm. For comparison of the cell lines, the highest absorbance was defined as 100 % and all other values were normalized accordingly. For determination of IC_{50} values, curve fitting was performed using SigmaPlot.

3.2.1.6.2 Soft agar assay

To study of anchorage-independent growth of COS-7 and SW-13 cells, soft agar assay was performed.SW-13 and COS-7 cells, transfected with the empty vector were used as a control. Melted, pre-sterilized Bacto-agar (1.2 g in 50 ml dd H_2O) was mixed with 150 ml IMEM containing 10% FCS, 5 ml 10x IMEM, and kept at 42-44°C. From this 0.6% agar, a 1 ml bottom layer was poured in 35-mm dishes and allowed to solidify at room temperature. The cells were cultured, grown in IMEM medium supplemented with 10% FCS and harvested as previously described and suspended in a concentration of about 10,000–20,000 cells in 0.5 ml culture medium. This cell suspension was mixed with an equal volume of culture medium and 1.5 ml of the agar stock solution. This suspension (0.36% agar) was layered onto the bottom layer (0.8 ml/dish), and allowed to solidify. The dishes were then incubated at 37°C for 14–28 days. Colonies more than 50 μm in diameter were counted independently by two blinded investigators. Experiments were carried out in triplicate sets of 35-mm dishes.

To study the effects of recombinant FGF-2 and FGF-BP on the proliferation of COS-7 in soft agar assay, FGF-2 and FGF-BP were diluted in PBS and were filter-sterilized and directly applied onto the solidified top agar.

3.2.2 Biochemical and immunochemical methods

3.2.2.1 Immunohistochemistry

Immunohistochemistry (IHC) studies were performed using a standard streptavidin biotin-peroxidase complex method. Tissue sections were pretreated 5 min in a microwave oven and then deparaffinized in xylene and rehydrated in graded alcohols. After washing with PBST, tissue sections were treated in 10 mM citrate buffer, pH 6.0, at 90°C for 15 minutes, for antigen retrieval. The slides were then washed with PBST and endogenous peroxidase activity was blocked with 0.3% hydrogen peroxide for 30 minutes at 4°C. After washing again, nonspecific binding was blocked with 10% normal horse serum in PBST, 2% BSA for 1 h. The tissue sections were then incubated with a monoclonal anti-FGF-BP antibody (1:100 in PBST, 2% BSA) at 4°C overnight in humidified chamber. Subsequently, the slides were washed with PBST and incubated sequentially with biotinylated anti-mouse antibodies at a concentration of 1:150 in PBST, 2% BSA for 1 h at RT and with a streptavidin-peroxidase conjugate for 1 h at 37°C and 3,3'-diaminobenzidine as a chromogene substrate. The tissue sections were counterstained using hematoxylin and then mounted.

Tissue microarrays (TMAs) were obtained from G. Sauter (University Hospital Eppendorf) and stained as described above except for a shorter incubation time in the DAB staining solution.

3.2.2.2 Immunofluorescence

80,000 cells were grown on glass slides for at least 24 h under standard conditions prior to the experiment. Transient transfections were performed as described above with 1-3 μg DNA. The medium was aspirated and slides were washed three times with PBS and fixed in 3% paraformaldehyde in PBS for 10 min at RT. Cells were washed twice with PBS prior to incubation in 10 mM ammonium chloride for 30 min to quench paraformaldehyde-mediated autofluorescence, washed in PBS and permeabilized with 0.1% Triton-X100 in PBS for 7 min at RT. After washing with PBST, cells were blocked with 1% BSA in PBST for 30 min, and with 2.5% normal goat serum or normal horse serum in PBST for 5 min at RT. Cells were washed again in PBST, and the slides were incubated with rabbit polyclonal anti-FGF2 (1:1000), mouse monoclonal anti-FGF-BP (1:100) or mouse monoclonal anti-ERGIC (kindly

provided by H.-P. Hauri, Basel; 1:1000) antibodies diluted in PBST containing 1% BSA for 1 h at RT. After washing again, slides were incubated with the appropriate secondary antibody (Texas Red-labeled horse anti-mouse, 1:100 in 2.5% horse serum/PBST, or Alexa Fluor 488 labeled goat anti-rabbit, 1:100 in 2.5% goat serum/PBST) for 30 min at RT. After extensive washing, slides were mounted and analyzed by confocal microscopy.

To analyze the cellular uptake of exogenous FGF-BP in COS-7 cells, 3 µg recombinant FGF-BP was diluted in 300 µl medium and added to the cells at 48 h post transfection. After 1 h incubation of the cells under standard conditions ($37^{o}C$, 5% CO_2), medium was aspirated and cells were washed and fixed using the same procedures.

3.2.2.3 Purification of recombinant FGF-BP

Recombinant FGF-BP with N-terminal and C-terminal His_6 tags was expressed as described previously [130] as non-secreted protein in SF-9 insect cells using the BAC-TO-BAC baculovirus expression system (Life Technologies, Bethesda MD). In the context of this thesis, the recombinant FGF-BP was purified and used to study the cellular uptake of exogenous recombinant FGF-BP in COS-7 and SW-13 cells as well as the effects of recombinant FGF-BP on proliferation of COS-7 cells in soft agar.

SF-9 cells were infected with recombinant baculoviruses and harvested 4-6 days after infection through tapping and centrifugation at 1000 x g for 5 min. The supernatants were used for further infection cycles of newly cultivated SF-9 cells. The pellets were either used directly to purify FGF-BP or stored at $-20^{o}C$. Purification of recombinant FGF-BP was performed under denaturing conditions. SF-9 cell pellets were resuspended in 15 ml lysis buffer and incubated at $4^{o}C$ for 20 min prior to sonication (5 bursts, 10 sec each), treatment with a Dounce homogenizer and centrifugation at 10,000 x g for 15 min. The supernatant was loaded onto 0.5 ml Ni-NTA sepharose equilibrated with lysis buffer, and the loaded resin was washed with 5 ml lysis buffer and with 5 ml washing buffer at pH 8.0, 6.3 and 5.9, respectively. Elution was performed with 0.5 ml of the same buffer at pH 4.0, the eluate was concentrated in Centricon-10 vials and stored at $4^{o}C$.

3.2.2.4 SDS-polyacrylamide gel electrophoresis (SDS-PAGE) and Western blotting

Sodium dodecyl sulfate-polyacrylamide gel electrophoresis (SDS-PAGE) is used to separate complex protein mixtures by their molecular size. The standard Laemmli method [302] is applied for discontinuous gel electrophoresis under denaturing conditions in the presence of SDS. Western blotting (immunoblotting) is applied to identify specific proteins (antigens) recognized by polyclonal or monoclonal antibodies. After separation by SDS-PAGE, the proteins are electrically transferred onto nitrocellulose membranes. The transferred proteins are bound to the surface of the membrane providing access for immunodetection reagents. All remaining binding sites are blocked by immersing the membrane in a solution containing either a protein or a detergent-based blocking agent. After probing with the primary antibody, the membrane is washed and the antigen is identified by detection with a secondary horseradish peroxidase-conjugated anti-IgG antibodies. Visualization of the antigen/antibody complex is performed by enhanced chemiluminescence using sensitive light-films. Experimental details for the antibodies used are listed in Table 1.

To analyze the expression of FGF-BP-CFP fusion protein in COS-7 cells by Western blotting, 100,000 cells were grown in 6-wells for at least 24 h under standard conditions. Transient transfections were performed as described above with 3 μg DNA. At 48 h post transfection, cells were lysed by addition of 200 μl denaturing lysis buffer and boiled for 5 min. After centrifugation at 13,000 rpm for 5 min, 20 μl supernatant was separated by SDS-PAGE (200V, 35 min). Proteins were transferred onto nitrocellulose membranes for 45 min at 25 V. Membranes were blocked for 1 h in TBST containing 5% BSA or milk, washed and probed at 4°C overnight with dilutions of antibodies listed in table 1. The blots were then washed in TBST and incubated with a 1:2000 dilution of donkey anti-rabbit or anti-mouse secondary antibody coupled to horseradish peroxidase for 1 h at RT. After additional washing in TBST bound antibody was visualized using the enhanced chemiluminescence reagents system from Amersham.

To examine the expression of recombinant FGF-BP in SF-9 cells, 25μl of eluate was mixed with 8μl denaturing lysis buffer and denatured at 100°C for 5 min. Western blotting was performed as described above.

For analysis of apoptosis-relevant proteins or of the phosphorylation of downstream signal transduction proteins, SKOV-3 wildtype and RzB-8 cells were grown in 6-wells over at least

48 h. At 40–50 % confluency, cells were treated with paclitaxel or rViscumin in normal media for 24 h or as indicated in the texts and in the figures. After removal of the media, cells were immediately lysed by addition of 200 µl denaturing lysis buffer, scraped, sonicated and boiled for 5 min. After centrifugation, 20µl supernatant was subjected to SDS-PAGE and Western blotting using appropriate antibodies as described above. To control for the amounts of detected proteins, blots were stripped in stripping buffer for 2 h at 65°C and reprobed with antibodies recognizing the unphosphorylated proteins or β-actin. Films were scanned using the Kodak Electrophoresis and Documentation System 120 which quantifies intensities of bands in arbitrary units.

Table 1: Antibodies, appropriate working dilutions and blocking solutions

Antibody	Blocking solution	1st antibody dilution buffer	Washing buffer system
Anti-GFP	5% milk/TBST	5% milk/TBST 1:100	TBST
Anti-FGF-BP	3% BSA/TBST	3%BSA/TBST 1:100	TBST
Anti-phospho p38	5% milk/TBST	5% milk/TBST 1:1000	TBST
Anti-p38	5% milk/TBST	5 % BSA/TBST 1:1000	TBST
Anti-phospho p42/p44	5% milk/TBST	5% milk/TBST 1:1000	TBST
Anti-p42/44	5% milk/TBST	5 % BSA/TBST 1:1000	TBST
Anti-phospho SAPK/JNK	5% milk/TBST	5% milk/TBST 1:1000	TBST
Anti-SAPK/JNK	5% milk/TBST	5 % BSA/TBST 1:1000	TBST
Anti-caspase-7	5% milk/TBST	5% milk/TBST 1:1000	TBST
Anti-caspase-3	5% milk/TBST	5% milk/TBST 1:1000	TBST
Anti-bcl-2	5% milk/TBST	5% milk/TBST 1:400	TBST
Anti-β-actin	5% milk/TBST	5% milk/TBST 1:400	TBST

3.2.2.5 Dot blotting

0.2 µg FGF-2 or BSA were dotted onto a nitrocellulose membrane. The membrane was incubated in 5% dry milk solution in TBST for 1 h to block non-specific protein binding, washed 3×5 min in TBST and incubated with FGF-BP solution (0.2 µg/ml in TBST) at 4°C overnight. After washing with TBST, the membrane was incubated with incubated with the dilution of anti-FGF-BP antibody (1:100 in 3% BSA/TBST) for 2 h at RT. The membrane was then washed in TBST and incubated with a 1:2000 dilution of donkey anti-mouse secondary antibody coupled to horseradish peroxidase for 1 h at RT. After additional washing in TBST, bound antibody was visualized as described above in Western blotting procedures.

3.2.2.6 Protein staining with Coomassie brillant blue

To stain with Coomassie immediately after completion of electrophoresis, gels were soaked in Coomasie blue solution for 30-60 min with shaking. Gels were destained with the destaining solution until bands became visible, then soaked in drying solution for 30 min and put in a drying frame between two pieces of cellophane for preservation.

3.2.2.7 [^{125}I]-labeling of FGF-BP and rViscumin

[^{125}I]-labeling of FGF-BP and rViscumin was performed using N-chloro-p-toluenesulfonamide (Chloramin T). 10 µg recombinant FGF-BP or 100 µg rViscumin was diluted in 80 µl 200 mM Na-phosphate buffer (pH 8.2) prior to addition of 500 µCi ^{125}I iodine and 40 µl Chloramin T (1 mg/ml). After 5 min incubation at room temperature, 12 µl 200 mM DTT was added and labeled FGF-BP or rViscumin were purified by gel filtration.

3.2.2.8 Analysis of cellular uptake of [^{125}I]-FGF-BP in COS-7 and SW-13 cells through subcellular fractionation

100,000 cells were grown in 6-wells for at least 24 h under standard conditions. COS-7 cells were transiently transfected as described above with 3 µg DNA (pRC/CMV empty vector or FGF-2 expression vector). At 48 h post transfection, 30µl [^{125}I]-FGF-BP (5,000 cpm)/well was added to the cells. After 1 h incubation under standard conditions (5% CO_2,

37°C), the medium were aspirated and cells were washed three times with PBS. The cells were then fractionated by differential centrifugation. 1 ml of 0.25 M sucrose/well was added to the cells and the cells were carefully scraped and homogenized. The resulting homogenate was transferred into tubes and centrifuged at 600 x g for 10 min at 4°C to yield the nuclear (NUC) fraction. The pellet was washed three times with PBS and measured in a γ-scintillation counter. The supernatant was first measured in a γ-scintillation counter and then centrifuged at 100,000 x g for 2 h at 4°C to obtain mitochondrial and microsomal (MIT and MIC) fractions. The resulting pellet was washed once with PBS and measured in a γ-scintillation counter.

3.2.2.9 Analysis of cellular rViscumin binding/uptake

For rViscumin binding/uptake studies, 2 µg [^{125}I]-rViscumin (550,000 cpm) in 300 µl medium was added to 20,000 cells/well prior to incubation at 37°C/5% CO_2 for the time points indicated. Supernatants were aspirated, cells were washed three times with PBS and lysed in 200 µl 1 % SDS. Lysates were measured in a γ-scintillation counter or 25 µl was subjected to non-reducing SDS-PAGE and the gel was autoradiographed overnight using Biomax MS films. Films were scanned using the Kodak Electrophoresis and Documentation System 120 which quantitates intensities of bands in arbitrary units. In all experiments, wells without cells were treated in the same way and served as negative control for nonspecific binding to the plastic which was generally low and subtracted from the lysates.

3.2.3 Molecular biological methods

3.2.3.1 Polymerase chain reaction (PCR)

The fragments were amplified in a 100 µl total reaction volume using primers and template DNAs as listed in table 2. The mixtures were prepared on ice by addition of the reagents in the following order:

Master-Mix 1	
DNA (template)	~0,5 µg
10 mM dATP	2 µl
10 mM dTTP	2 µl
10 mM dCTP	2 µl
10 mM dGTP	2 µl
10 pmol/µl forward primer	3 µl
10 pmol/µl reverse primer	3 µl
dd H_2O	35,5 µl

Master-Mix 2	
10x reaction buffer with 50 mM $MgCl_2$	10 µl
dd H_2O	39 µl
Taq polymerase	1 µl

To start the PCR, master mix 1 and 2 were combined, and PCR vial was immediately transferred into the thermocycler and PCR was performed under the following conditions:

$$3 \text{ min } 94^{o}C$$

$$30 \text{ sec } 94^{o}C$$
$$30 \text{ sec } 54^{o}C \quad (35 \text{ cycles})$$
$$90 \text{ sec } 72^{o}C$$

$$6 \text{ min } 72^{o}C$$

PCR products were analysed on a 1% agarose gel and visualized by ethidium bromide intercalation under UV light.

Table 2: Constructs, primers and templates

Generation of the FGF-BP-CFP constructs			
Constructs	**Forward primer**	**Reverse primer**	**DNA (Template)**
FGF-BP-CFP full length (1- 234)	FGF-BP_1_f	FGF-BP_1_r	Full length FGF-BP
BP-N-215-CFP (1-215)	BP-N215_1_f	BP-N215_1_r	Full length FGF-BP
BP-N-150-CFP (1-150)	BP-N150_1_f	BP-N150_1_r	Full length FGF-BP
BP-N-99-CFP (1-99)	BP-N99_1_f	BP-N99_1_r	Full length FGF-BP
BP-C-91-CFP (91-234)	BP-C91_1_f	BP-C91_1_r	Full length FGF-BP
BP-C-146-CFP (146-234)	BP-C146_1_f	BP-C146_1_r	Full length FGF-BP

Generation of FGF-BP deletion mutants			
FGF-BP full length	FGF-BP_2_f	FGF-BP_2_r	Full length FGF-BP
BP-N-215 (1-215)	BP-N215_2_f	BP-N215_2_r	Full length FGF-BP
BP-N-150 (1-150)	BP-N150_2_f	BP-N150_2_r	Full length FGF-BP
BP-N-99 (1-99)	BP-N99_2_f	BP-N99_2_r	Full length FGF-BP
BP-C-91 (91-234)	BP-C91_2_f	BP-C91_2_r	BP-C-91-CFP
BP-C-146(146-234)	BP-C146_2_f	BP-C146_2_r	BP-C-146-CFP

Generation of FGF-2-YFP construct			
FGF-2-YFP (18 kDa)	FGF-2_1_f	FGF-2_1_r	pET15b FGF2

Generation of FGF-2 (18 kDa)			
FGF-2 (18 kDa)	FGF-2_2_f	FGF-2_2_r	pET15b FGF2

3.2.3.2 Electrophoretic separation of DNA fragments in agarose gels

For the analysis and purification of DNA fragments of different sizes horizontal agarose gel electrophoresis was performed. For preparation of the gel, the appropriate amount of agarose dissolved in 200 ml 1x TAE buffer was boiled in the microwave oven and after cooling down to 60°C, ethidium bromide was added to reach an end concentration of 0.5 µg/ml. Agarose solution was poured into a gel chamber and combs with appropriate pocket size were inserted. After solidification, the gel was transferred into an electrophoresis chamber filled with 1x TAE buffer. The samples were mixed with the appropriate volume of

DNA loading buffer and pipetted into gel pockets. The electrophoresis was performed at 90 V. DNA fragments were visualized by ethidium bromide intercalation under UV light.

3.2.3.3 Phenol-chloroform extraction of DNA

The extraction of DNA with a mixture of phenol/chloroform/isoamylalcohol (25:24:1) and chlorophorm/isoamylalcohol (24:1) is a standard method for the removal of proteins from nucleic acid preparations. The purification was performed as follows:

An equal volume of phenol mixture was added to the DNA solution, mixed well and centrifuged for 5 min at 13,000 rpm. The upper DNA containing phase was carefully pipetted into a new vial. In order to remove the rest of phenol, it was mixed with the same volume of chlorophorm/isoamylalcohol mixture. After mixing and centrifugation at 13,000 rpm for 5 min the upper phase was again pipetted in a new vial.

Precipitation of DNA was performed by adding 2-2.5 volumes ethanol and 1/10 volume 3 M potassium acetate pH 5.0 to the extracted DNA solution. Samples were incubated for 5 min at RT. After centrifugation at 13,000 rpm for 10 min at 4°C, the DNA pellet was washed with 70% ethanol and the precipitate was dried in the air at RT. The dried pellet was dissolved in sterile water. Purity and concentration of DNA was determined by measuring the absorbance at 260 and 280 nm against water.

3.2.3.4 Linearization of the expression vectors and restriction digest of PCR products

For cloning of the FGF-BP-CFP fusion proteins, plasmids and PCR products were digested using restriction endonucleases listed in the table 3 The restriction was carried out in a total volume of 20 µl, containing the plasmid DNA or PCR products, and 5-10 U of every restriction endonuclease. To start the reaction, the components were mixed with the restriction endonucleases being added last and the reaction was incubated at 37°C for 1 hour to allow the enzymes to work at optimal conditions. Then, 1µl of the sample was loaded on a DNA gel for electrophoresis. Samples were run on the gel with a 1 kb DNA marker at 90 V for 30 min. The gel was checked under an UV light for a correct, complete digest.

Table 3: Restriction endnucleases used to digest plasmids and PCR products

FGF-BP-CFP fusion proteins	
PCR products/Vector	**Restriction endonucleases**
FGF-BP-CFP	EcoRI and XhoI
BP-N-215-CFP	EcoRI and XhoI
BP-N-150-CFP	EcoRI and XhoI
BP-N-99-CFP	EcoRI and XhoI
BP-C-91-CFP	NotI and XhoI
BP-C-146-CFP	NotI and XhoI
A derivative pcDNA 3.1-based plasmid containing CFP	EcoRI and XhoI
A derivative pcDNA 3.1-based plasmid containing CFP and the N-terminal signal peptide of FGF-BP	NotI and XhoI

FGF-BP deletion mutants	
PCR products/Vector	**Restriction endonucleases**
FGF-BP	HindIII and XbaI
BP-N-215	HindIII and XbaI
BP-N-150	HindIII and XbaI
BP-N-99	HindIII and XbaI
BP-C-91	HindIII and XbaI
BP-C-146	HindIII and XbaI
pRC/CMV expression plasmid	HindIII and XbaI

FGF-2-YFP fusion protein	
PCR products/Vector	**Restriction endonucleases**
FGF-2-YFP	HindIII / EcoRI
A derivative pcDNA 3.1-based plasmid containing YFP	HindIII / EcoRI

FGF-2 without fusion protein	
PCR products/Vector	**Restriction endonucleases**
FGF-2	HindIII / XbaI
pRC/CMV expression plasmid	HindIII / XbaI

3.2.3.5 Dephosphorylation of digested DNA

After the digestion with restriction enzymes, the vector was dephosphorylated by Shrimp alkaline phosphatase (SAP) to remove the phosphate group at 5'-end and thus to prevent self ligation of the vector. 2 Units SAP were mixed with 4µl 10x SAP buffer and 35µl sterile water. The mixture was added to the 20µl sample after digestion and incubated 10 min at 37ºC. Then, to inactivate SAP, the sample was incubated at 65ºC for 5 min.

3.2.3.6 DNA isolation from agarose gel

For isolation of DNA fragments from agarose gels, the DNA was separated by gel electrophoresis in 0.7% agarose gels at 90 V and visualized by ethidium bromide staining under UV light. The appropriate DNA bands were excised under UV light and transferred into an eppendorf vial with a very small opening created with a scalpel. The vial was inserted in another larger tube and centrifuged at 13,000 rpm, until sufficient liquid was collected in the larger tube (1-5 min)

3.2.3.7 Ligation

The typical ligation reaction was carried out in a total volume of 10 µl containing vector and insert DNA (molar ratio vector : insert was approx. 1:5), 1/10 volume of 10x T4 ligase buffer and 3 U of T4 Ligase. The ligation was performed at room temperature for 4 h or at 16°C overnight.

3.2.3.8 Preparation of chemically competent Escherichia coli cells

To prepare chemically competent E.coli cells, the DH5α strain was used. Cells were plated on an LB-agar plate and incubated overnight at 37°C. Next day, a single colony of approximately 2 mm in diameter was transferred into 250 ml SOB medium and the flask was incubated at 18°C with 180 rpm shaking for 2-3 days until the as cell density of ~0.6 OD_{600nm} was reached. The flask was kept on ice for 10 min and then, to harvest the cells, a centrifugation at 2500 x g and 4°C for 10 min was performed. The pelleted cells were resuspended in 80 ml ice-cold transformation buffer and incubated for another 10 min on ice. A second centrifugation was carried out as described above. The pellet was then resuspended in 18.6 ml ice-cold transformation buffer and 1.4 ml DMSO was added slowly with gentle stirring to the final concentration of 7% (v/v). After 10 min incubation on ice, cells were aliquotted in eppendorf vials, frozen immediately in liquid nitrogen and stored at -80°C for storage.

3.2.3.9 Transformation of chemically competent Escherichia coli cells

An eppendorf vial containing 100 µl frozen chemically competent E.coli in transformation buffer was thawed on ice, 1 µl of a typical ligation reaction or 50 ng plasmid DNA (up to 10 µl) was added and the vial was kept on ice for other 30 min. After "heat shock" at 42°C for 90 seconds, the vial was placed on ice for 2 min and then 300 µl LB medium were added. The cells were incubated at 37°C with shaking for 1 h and then spread on an LB-agar plate containing 100 µg/ml ampicilline prior to incubation at 37°C overnight. The next day, positive colonies were analyzed and propagated.

3.2.3.10 Bacterial culture

E.coli cells were cultivated in LB liquid medium at 37ºC with shaking with 240 rpm. For selection and cultivation of transformed cells, 100 µg/ml ampicilline was added to the medium. To start a new culture, cells from glycerol stocks were used.

3.2.3.11 Preparation of the glycerol stocks

Exponentially growing cultures from E.coli cells were mixed with 0.25 volumes of 80% sterilized glycerol and immediately kept at -80ºC.

3.2.3.12 Colony lift and Southern blotting

3.2.3.12.1 Bacterial colony transfer

This methodology was chosen to define a clone of interest via hybridization experiments. The agar plates containing the subclone colonies were placed next to an open flame to minimize aerosol contamination. A nylon membrane was then carefully placed onto the agar surface and slightly pressed by using a sterile glass spatula. It is important to mark the orientation on the membrane itself and on the plate.

The membranes were then transferred into a Petri dish containing Whatman paper, covered with a small volume of denaturation solution, for 8 min. Two neutralization steps (8 min each) followed in Petri dishes containing Whatman paper soaked in neutralization

solution. In the last step, the membrane was briefly submersed into a 2x SSC solution to remove the cell debris. The damp membrane was then crosslinked through either UV light for 2 min or heat exposure at 80°C for 2 h.

3.2.3.12.2 Southern blotting

Southern blotting was used to analyze DNA from agarose gel. The transfer was performed as described in Sambrook/Fritsch/Maniatis laboratory manual.

Upon completion of electrophoresis, a gel picture was taken with a ruler to facilitate the size determination of hybridization signals afterwards. Before transfer, the upper corner of the gel was cut for orientation. The gel was flipped and placed on one layer of soaked Whatman paper on a glass plate. The Whatman paper reaches into a container filled with 20x SSC solution. A gel size nylon transfer membrane was put onto the gel and covered with two fitting and 20x SSC-soaked Whatman papers. A stack of fitting paper towels was put on top. Adding weights helps to evenly distribute pressure to the gel. The transfer was performed overnight.

3.2.3.12.3 Radioactive Labeling of Nucleic Acids

Radioactive nucleotides were used to perform Random Primed Labeling or to label oligonucleotides

Random Primed Labeling for colony lift

Random Primed Labeling was performed by incorporation of radioactive nucleotides using the Rediprime[TM] II kit provided by Amersham Pharmacia Biotech. In this kit, the concentration of dCTP is 20-fold lower the concentration of the other nucleotides to ensure the incorporation of radioactive α-[32]P dCTP into the newly synthesized DNA.

60 ng double stranded DNA were mixed with sterile H_2O up to a final volume of 45 µl and then denatured for 5 min at 95°C. The denatured DNA was then transferred into the reaction vial provided in the kit. 5 µl α-[32]P dCTP was added and the solution was mixed, by pipetting it up and down about 10 times, followed by incubation at 37°C for 30 min. To remove remaining free nucleotides, the mix was loaded onto a prepared gel permeation

chromatography column (Microspin columns). Finally, the specific activity of the probe was measured in a scintillation counter.

Labeling of oligonucleotides

In order to detect complementary DNA sequence (FGF-BP deletion mutants and FGFR1), e.g. on a blot, radioactively labeled oligonucleotides were used as probes.

The labeling reaction was performed in a volume of 20 µl containing 1 µl PNKinase (PN=polynucleotide), 2 µl 10x PNKinase buffer, 20 pmole oligonucleotide and 50 µCi γ-^{32}P ATP. The enzyme was added last and the sample was incubated for 30 min at 37°C.

3.2.3.12.4 Hybridization with labeled DNA

The membrane containing the crosslinked DNA was carefully rolled and inserted into a hybridization tube, the surface with the nucleic acids facing inwards. Approximately 10 ml prehybridization solution was added and the tube was incubated in a hybridization oven for at least two hours at 42°C. After the prehybridization, the radioactive probe was added and the membrane was incubated overnight under the same temperature conditions.

3.2.3.12.5 Washing of membranes

Both membranes were washed in the same way. First the radioactive hybridization solution was transferred into a tube and stored for possible further use at -20°C. Then, the membranes were washed twice with ~15 ml 2x SSC/0.1% SDS for 15 min at 42°C. After discarding the washing solution, autoradiography of radioactive membranes was performed.

3.2.3.12.6 Autoradiography of radioactive membranes

The membranes were taken out of their hybridization tubes and sealed into plastic foil. After checking the activity, the sealed membranes were put into a KODAK film cassette and exposed to Biomax MS films at -80°C for a time depending on the activity of the probe. In these studies exposure times ranged from 20 min to 2 days.

3.2.3.13 DNA Plasmid Purification

DNA plasmids were purified for purposes of analytical restriction digests, sequencing, cloning and generation of probes. The plasmid purification was achieved by using Qiagen QIAprep Mini-prep Kit for plasmid screening of transformed bacterial colonies and NUCLEOBOND Midi-prep Kit for purification of larger amounts of DNA for sequencing and generation of probes.

3.2.3.13.1 Qiagen Mini-prep DNA plasmid isolation

5 ml LB medium containing 100 µg/ml ampicilline was inoculated with bacterial cells and incubated overnight at $37^{o}C$. The cultured cells were centrifuged at 3,000 x g for 10 min in order to form a bacterial cell pellet. The medium was aspirated and the pellet was resuspended in 250 µl buffer P1, containing RNase A, and transferred into a fresh tube. For alkaline cell lysis 250 µl buffer P2 was added and mixed with the solution by gently inverting the tube. The lysis reaction, which solubilizes the phospholipids and proteins of the cell membrane and denatures the chromosomal and plasmid DNA, was allowed to proceed for 5 min. Then, 350 µl buffer N3 was added for neutralization purposes. To avoid any localized precipitation, the solution was mixed immediately after the addition of buffer. The sample was centrifuged at 3,000 x g for 15 min with the cell debris and SDS precipitate forming a pellet. The supernatant, containing the plasmid DNA was then transferred to a QIAprep spin column and centrifuged at 3000 x g for 1 min. The silica-gel membrane ensures a selective absorption of plasmid DNA in high salt buffer. To wash the column salt contaminants, 750 µl buffer PE were added and the column was centrifuged for 1 min at 3000 x g. To elute plasmid DNA, the column was placed on a clean microfuge tube and 50µl H_2O were added in the center of the column. After waiting for 3 min the column was centrifuged at 3000g for 1 min. Due to the low salt concentration of the H_2O, the plasmid DNA was eluted from the column and collected. The DNA yield was defined by spectrophotometry.

3.2.3.13.2 NUCLEOBOND Midi-prep DNA plasmid isolation

The plasmid DNA purification principle using the NUCLEOBOND Midi-prep kit is similar to the process of the Qiagen Mini-prep. Bacterial cells were incubated in 250 ml LB

medium, containing 100 µg/ml ampicilline overnight at 37°C. To harvest the bacterial cells, the culture was centrifuged at 5,000 x g for 15 minutes. All traces of supernatant were removed and the bacterial cell pellet was resuspended in 4 ml buffer S1 containing RNase. The suspension was transferred into a fresh tube and 4 ml of buffer S2 was added. The solution was mixed and incubated at RT for 5 min. Next, 4 ml buffer S3 was added and immediately mixed with the solution. The sample was incubated on ice for 5 min and then centrifuged at 12,000 x g for 30 min at 4°C. Meanwhile, AX 100 columns were equilibrated by applying 2.4 ml buffer N2 onto the column and allowing it to elute by gravity flow. The supernatant from the centrifugation was immediately removed, applied to the equilibrated column and allowed to enter a resign by gravity flow. Subsequently, the column was washed twice with 5 ml buffer N3. Addition of 5 ml buffer N5 onto the column eluted the plasmid DNA. The DNA then was precipitated by adding 3.6 ml isopropanol. The sample was mixed and subsequently centrifuged at 15,000 x g for 30 min at 4°C. The supernatant was decanted and the DNA pellet was washed with 70% ethanol and centrifuged at 15,000 x g for 10 min. The supernatant was aspirated and the pellet was air-dried for 5-10 min. The plasmid DNA was dissolved in 50-100 µl H_2O and the concentration was determined.

3.2.3.14 DNA Sequencing

DNA sequencing was done by commercial sequencing (MWG Biotech, Ebersberg).

3.2.3.15 Preparation of total RNA from SW-13 and COS-7 cells

RNAs from SW-13 and COS-7 cells were prepared by using peqGOLD TriFast^{TM} reagent as described by the manufacturer (PEQLAB, Erlangen). After growth of cells in a culture flask to 80% confluency, the culture medium was discarded, and the cells were resuspended in 2 ml ice-cold peqGOLD TriFast^{TM} and incubated at RT for 5 min. Afterwards, 200 µl chloroform/ml peqGOLD TriFast^{TM} reagent was added, vials were vigorously mixed and centrifuged at 13,000 rpm for 10 min at 4°C. The organic phase including the protein-containing interphase was discarded. Total RNA was precipitated by adding 0.5 ml 2-propanol to the aqueous phase. After centrifugation at high speed for 30 min at 4°C, the pellet was washed twice with 70% ethanol. The dried pellet was resuspended in 30 µl DEPC-treated ddH_2O.

Diethylpyrocarbonate (DEPC) treatment of water

   200 µl of DEPC was added to 100 ml of ddH$_2$O, stirred vigorously to emulsify DEPC in the solution and finally autoclaved.

3.2.3.16 RT-PCR

   RT-PCR was performed with 2 µg denatured RNA using recombinant Transcriptor Reverse Transcriptase as described by the manufacturer (Roche, Mannheim, Germany). The cDNA product (2 µl) was amplified in a 50 µl final volume containing 5 µl 10x PCR buffer without Mg^{2+}, 3 µl 25 mM MgCl$_2$, 0.2 mM dNTPs, 10 pmol of each primer listed in table 4 and 0.5 µl Taq polymerase for 35 cycles under the following conditions:

$$3 \text{ min } 94^{\circ}C$$

$$
\begin{array}{l}
30 \text{ sec } 94^{\circ}C \\
30 \text{ sec } 52^{\circ}C \quad (35 \text{ cycles}) \\
90 \text{ sec } 72^{\circ}C
\end{array}
$$

$$6 \text{ min } 72^{\circ}C$$

PCR products were loaded on a 1.3 % agarose gel and visualized by ethidium bromide staining.

Table 4: Primers for cDNA amplification

FGF-BP deletion mutants		
Construct (cDNA)	**Forward primer**	**Reverse primer**
FGF-BP	FGF-BP_2_f	FGF-BP_2_r
BP-N-215	BP-N215_2_f	BP-N215_2_r
BP-N-150	BP-N150_2_f	BP-N150_2_r
BP-N-99	BP-N99_2_f	BP-N99_2_r
BP-C-91	FGF-BP_2_f	FGF-BP_2_r
BP-C-146	FGF-BP_2_f	FGF-BP_2_r

FGFR1		
FGFR1	RT-FGFr1_f	RT-FGFr1_r

3.2.4 Confocal laser-scanning microscopy

Confocal imaging of COS-7 and SW-13 cells was performed with a confocal laser scanning inverted microscope LSM 510 META (Carl Zeiss GmbH, Germany). To analyze the cells by confocal microscopy, 80,000 cells were grown on glass slides for at least 24 h under standard conditions prior to the experiment. Transient transfections were performed as described above using 1-3 µg DNA. After 48 h, the medium was aspirated and slides were washed with PBS. The cells were either fixed as described above or analyzed directly by confocal microscopy using a Plan-Apochromat 63x/1.4 Oil lens. For detection of different fluorescent dyes used in this study, the appropriate microscope settings was used as indicated in table 5.

Table 5: Microscopy configuration

Fluorescent dyes	Laser lines used for excitation	Filters used for detection of the emmision
Microscopy configuration for detection of a single fluorescent dye		
CFP	458 nm line of Argon laser	475 nm long pass filter
YFP	514 nm line of Argon laser	530 nm long pass filter
Alexa Flour	488 nm line of Argon laser	505 nm long pass filter
Texas red	543 nm line of HeNe laser	560 nm long pass filter

Microscopy configuration for parallel detection of CFP/YFP		
CFP	458 nm line of Argon laser	BP 475–525 nm band pass filter
YFP	514 nm line of Argon laser	BP 530–600 nm band pass filter

Microscopy configuration for parallel detection of CFP/Texas red		
CFP	458 nm line of Argon laser	BP 475–525 nm band pass filter
Texas red	543 nm line of HeNe laser	560 nm long pass filter

Microscopy configuration for parallel detection of YFP/Texas red		
YFP	514 nm line of Argon laser	BP 530–600 nm band pass filter
Texas red	543 nm line of HeNe laser	560 nm long pass filter

The confocal aperture was adjusted to give optical sections < 0.8 µm.

4 RESULTS

4.1 The fibroblast growth factor-binding protein (FGF-BP) in ovarian carcinomas

4.1.1 Characterization of the monoclonal anti-human FGF-BP antibody

The specificity and sensitivity of the FGF-BP antibody used in the immunohistochemical studies is very important in order to produce reliable results regarding the expression of FGF-BP in nonmalignant and malignant ovarian tissues. First, this monoclonal antibody was characterized by Western blotting (Fig. 7 a). Recombinant FGF-BP with N-terminal and C-terminal His$_6$ tags was expressed as non-secreted protein in SF-9 insect cells using the BAC-TO-BAC baculovirus expression system [130], and partially purified under denaturating conditions. Western blotting analysis using the monoclonal anti-human FGF-BP antibody revealed a single band of FGF-BP (~30 kDa) and showed very low background (Fig. 7 a).

To further analyze the usefulness of the anti-FGF-BP antibody in immunohistochemistry, stainings of prostate carcinoma sections with already established FGF-BP overexpression were performed. As negative control, the primary antibody was replaced by the dilution buffer (2% BSA in TBST, Fig. 7 b). In contrast to negative controls, which showed no immunopositivity, strong brown color was observed in the cytosol of glandular epithelial cells of prostate carcinoma tissues, confirming the specificity and sensitivity of the anti-human FGF-BP antibody (Fig. 7 b).
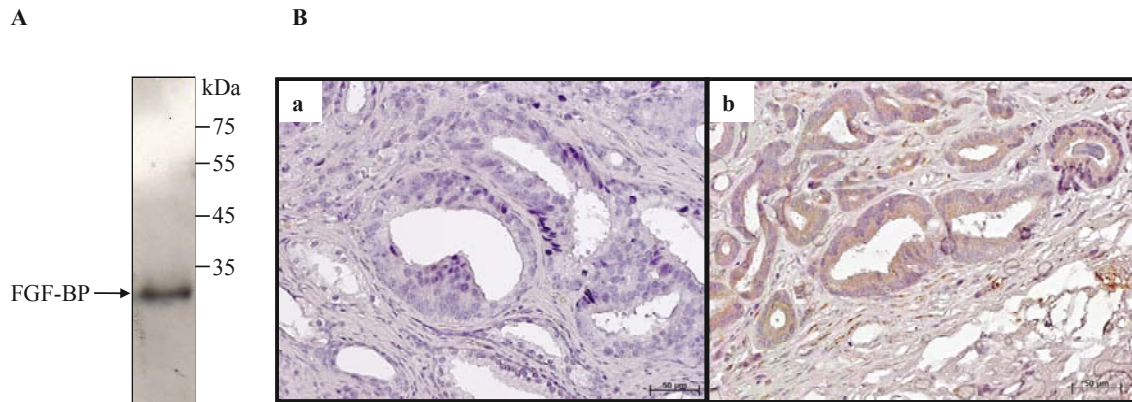
A   B

*Fig. 7 **Determination of specificity and sensitivity of the monoclonal anti-human FGF-BP antibody by Western blotting and immunohistochemistry.***

A) Identification of a single band of recombinant FGF-BP by Western blotting using the monoclonal anti-human FGF-BP antibody. B) Immunohistochemical analysis of prostate carcinomas tissues using anti-FGF-BP antibody. While negative controls (a) showed no brown signals, FGF-BP specific staining was strong in the cytoplasm of glandular epithelial cells of prostate carcinoma (b), confirming previous data on the expression of FGF-BP in prostate carcinomas [303]. These results demonstrate the sensitivity and specificity of the monoclonal anti-human FGF-BP antibody.

4.1.2 FGF-BP overexpression in human ovarian carcinoma

Immunohistochemistry was used in the context of this thesis to examine the expression status of FGF-BP in 28 normal ovaries and 123 ovarian carcinomas by tissue microarrays. Informative tissue microarray (TMA) results were observed in 26 of 28 normal ovarian tissues and in 106 of 114 ovarian carcinomas. The lost samples were considered as non-informative samples and not included in the current data compilation.

In the evaluation of FGF-BP IHC staining in different ovarian tissue samples, expression of FGF-BP in nonmalignant and malignant tissues was observed primarily as cytoplasmic immunopositivity (Fig. 8 e and f). Because the IHC conditions for all tissues in the TMA sections were identical, semiquantitative scoring criteria for IHC evaluation were used in which the staining intensities were evaluated from 0 to 4 (negative = 0, weak = 1, moderate = 2, strong = 3, and very strong = 4). IHC results were recorded independently by two blinded investigators.

The expression pattern of FGF-BP in epithelial cells from different ovarian tissues was heterogeneous, with different staining intensities. Because the FGF-BP expression in all normal ovarian tissues was negative (0) or weak (1) (Fig. 8 a and b), staining intensities 0-2 were interpreted as normal expression of FGF-BP, whereas values 3-4 were interpreted as overexpression of this protein (Fig. 8 c and d). Using this rating, overexpression of FGF-BP was detected in 43 of 106 informative ovarian carcinomas (40%) (Table 6). In contrast, the normal ovarian tissues did not show overexpression of FGF-BP.

Table 6: The expression of FGF-BP in normal ovaries and in ovarian carcinomas

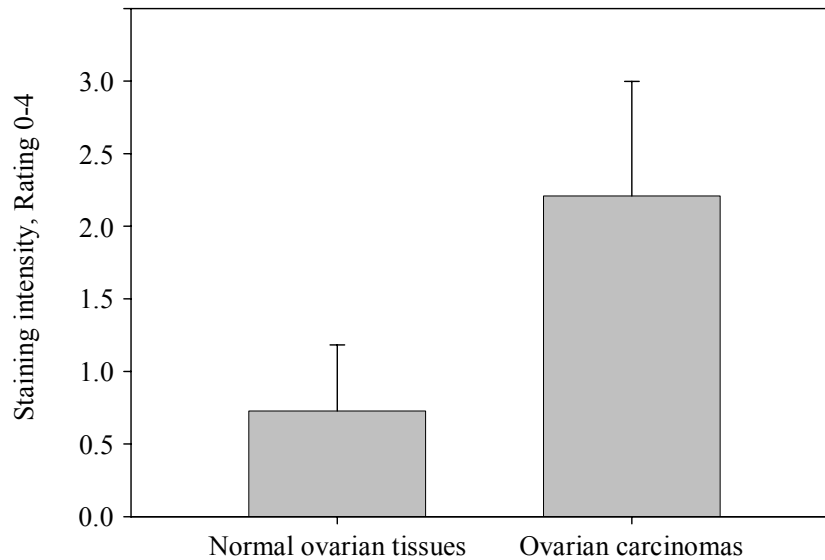| Tissue type	No. of samples with informative results	FGF-BP: No. of tissue samples (%)	
		Normal expression	Overexpression
Normal ovary	26	26 (100%)	0 (0%)
Ovarian carcinomas	106	63 (60%)	43 (40%)

A
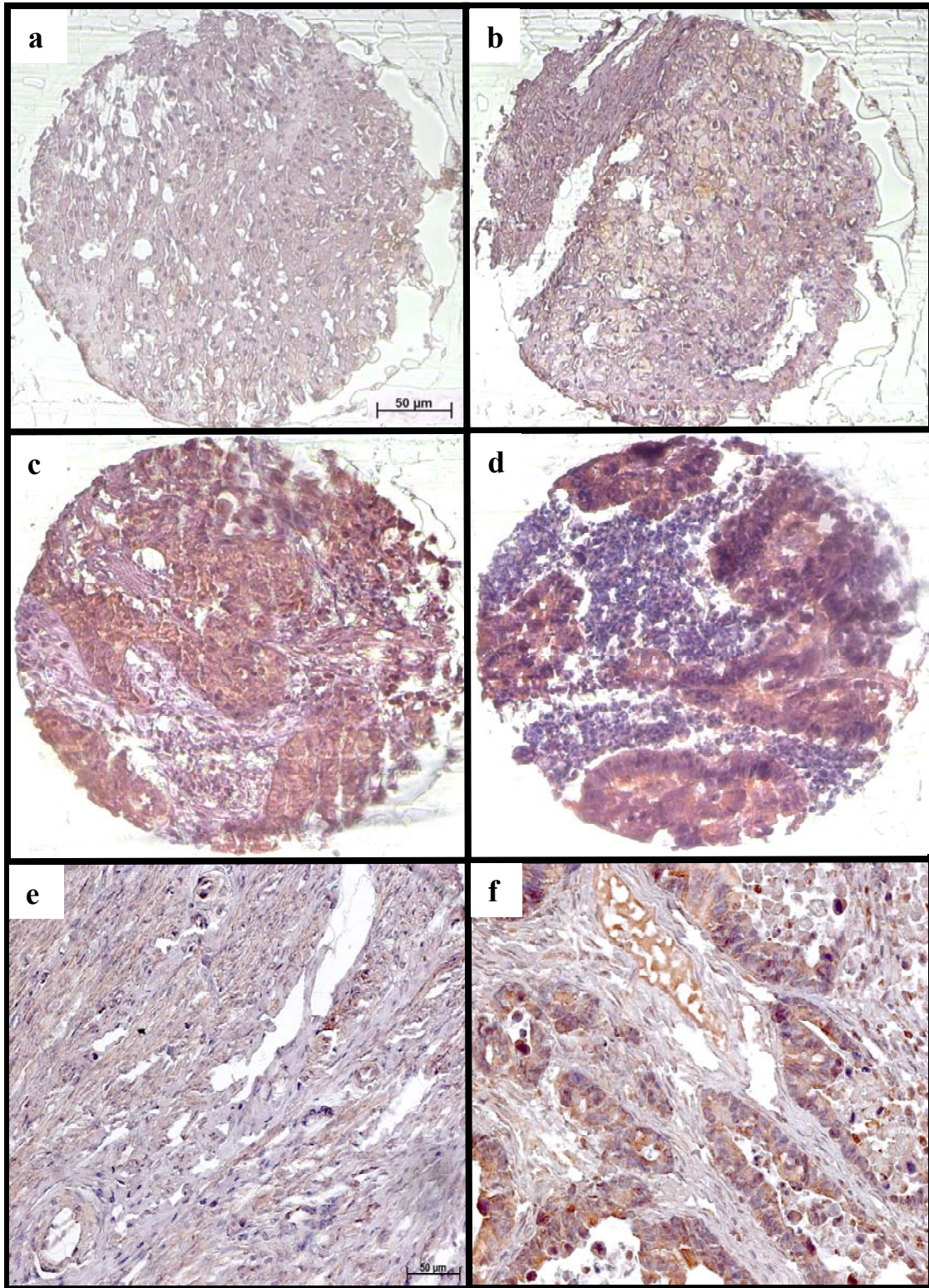
B

*Fig. 8 **Expression of FGF-BP in ovarian tissues.***

A) The expression pattern of FGF-BP in different ovarian tissues was heterogeneous, with different staining intensities. a and b represent the staining intensity of normal ovarian tissues, which was 0 (a) or 1 (b). In contrast, in ovarian carcinomas the FGF-BP IHC staining ranged from 1-4 and 40% of samples showed staining intensity 3 (c) or 4 (d). Positive expression of FGF-BP in nonmalignant (e) and malignant tissues (f) was observed primarily as a cytoplasmic pattern. B) Graphic presentation of the mean of staining intensities of normal and malignant ovarian tissues (Mean +/- SD). In ovarian carcinomas, the mean of staining intensities was ~3 fold higher compared to normal ovarian tissues. IHC results were obtained independently by two blinded investigators.

4.2 Mechanism of FGF-BP action

4.2.1 Subcellular distribution of FGF-BP in COS-7 and SKOV-3 cells

To gain insight into the cellular functions of FGF-BP, an expression vector for full length FGF-BP-CFP was constructed by fusing CFP to the C-terminus of FGF-BP (Fig. 9 a). For the analysis of the subcellular localization of this FGF-BP-CFP fusion protein in COS-7 and SKOV-3 cells by confocal microscopy, cells were grown on coverslips 24 h under standard conditions prior to the transient transfection with the FGF-BP-CFP expression vector. At 48

h post transfection, the medium was aspirated and substituted by phosphate buffered saline (PBS), and the cells were analyzed by confocal microscopy without fixation. Detection of the fluorescence of CFP showed that FGF-BP-CFP was diffusely localized in the cytoplasm in both cell lines. Interestingly, strong fluorescence in the Golgi region as well as in vesicular elements concentrated in the Golgi area was seen (Fig. 9 c).
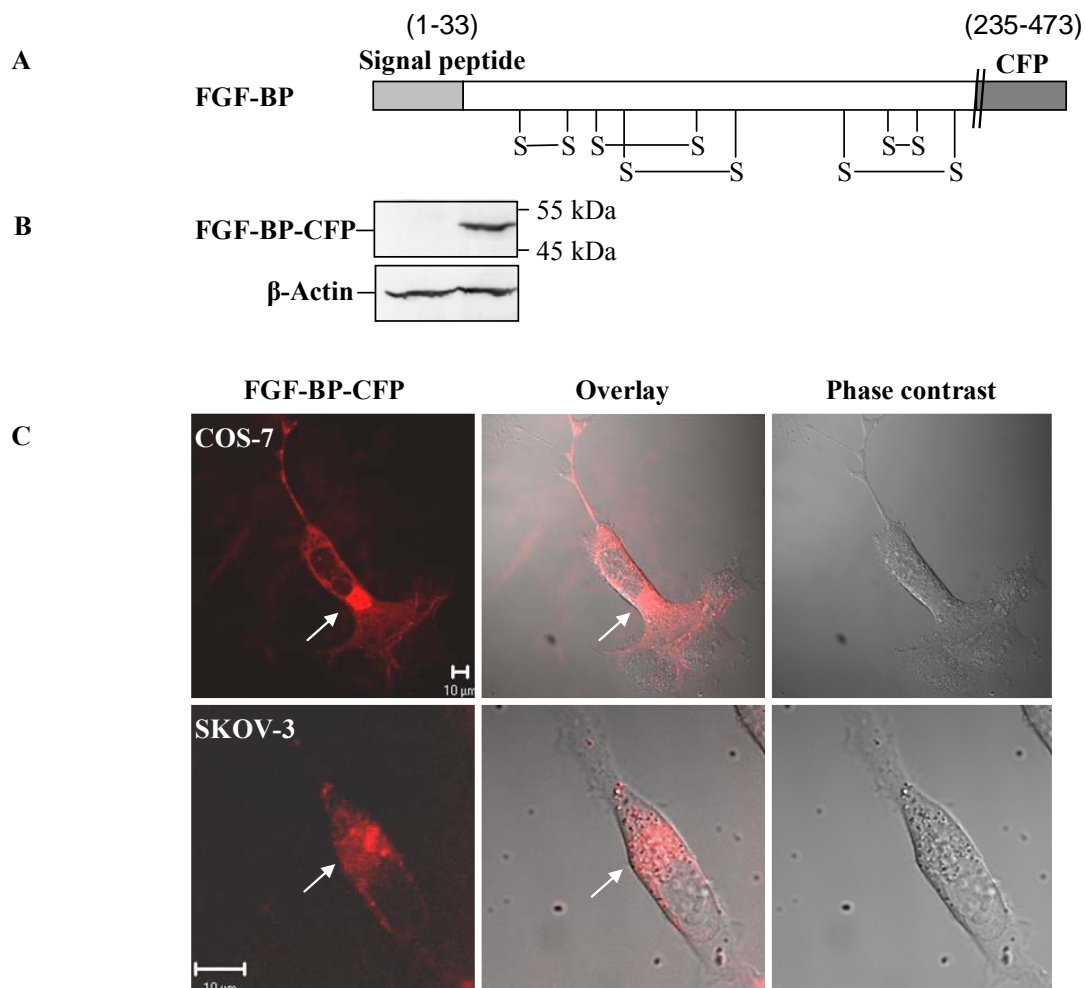
*Fig. 9 **Subcellular localization of FGF-BP-CFP in COS-7 and SKOV-3 cells.***

A) Schematic diagram of CFP-tagged full length FGF-BP. FGF-BP-CFP was constructed by fusing CFP to the C-terminus of full length FGF-BP. Numbers listed above refer to amino acids. COS-7 cells were transiently transfected with FGF-CFP expression vector. After 48 h, the cells were either lysed and subjected to SDS-PAGE and Western blot using anti-GFP antibodies (B) or analyzed by confocal microscopy (C). Western blot analysis demonstrated the expression of FGF-BP-CFP in transfected COS-7 cells (~52 kDa). Confocal microscopy analysis showed the cytoplasmic localization of FGF-BP-CFP, with strong fluoresence in Golgi area in both cell lines COS-7 and SKOV-3 (C).

4.2.2 FGF-BP colocalization with ERGIC in COS-7 cells

FGF-BP is a secretory protein since it contains a classical N-terminal signal peptide. The newly synthesized secretory proteins undergo folding and post-translational modification reactions before becoming competent to be transported out of the endoplasmic reticulum (ER) [304-306]. Transport along this pathway occurs via an intermediate compartment called ER-Golgi intermediate compartment (ERGIC). The observed fluorescence pattern of FGF-BP-CFP in Golgi area suggested the presence of FGF-BP in the ERGIC. Therefore, the colocalization of FGF-BP-CFP with the ERGIC-specific protein was analyzed in COS-7 cells. COS-7 cells were transiently transfected with FGF-BP-CFP expression vector and fixed at 48 h post transfection. By means of indirect immunoflouresence, the ERGIC marker
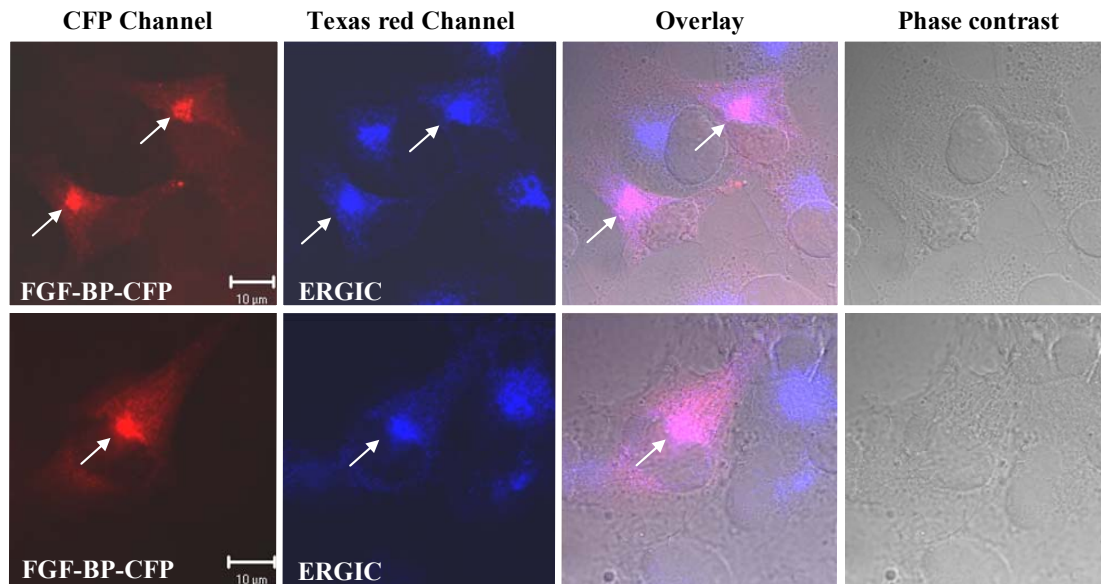
Fig. 10 Colocalization of FGF-BP-CFP with ERGIC-53 in COS-7 cells.

By indirect immunofluorescence, ERGIC was detected using mouse monoclonal anti-ERGIC antibodies in FGF-BP-CFP-expressing COS-7 cells. Texas red conjugated anti-mouse antibodies were used to visualize the primary antibody. The fluorescence of CFP (red) and Texas red (blue) was detected using the appropriate microscope configuration for parallel detection of CFP and Texas red. Confocal images of COS-7 cells expressing FGF-BP-CFP revealed colocalization of FGF-BP-CFP with ERGIC-53. The arrows indicate the colocalization of both proteins in the same cells. Note that there are FGF-BP-negative cells since COS-7 cells were transiently transfected with FGF-BP-CFP expression vector.

protein ERGIC-53 was detected using mouse monoclonal anti-ERGIC and Texas Red-conjugated anti-mouse antibodies. Double labeling of cells for FGF-BP and ERGIC-53 showed colocalization of both proteins (Fig. 10).

4.2.3 Translocation of FGF-BP into the nucleus upon Coexpression of FGF-BP with FGF-2

FGF-2 is considered the best characterized binding partner for FGF-BP. To study the effects of the interaction of FGF-2 with FGF-BP on the subcellular distribution of both proteins in COS-7 cells, changes in their subcellular localization upon coexpression were examined. These experiments were carried out using the 18 kDa isoform of FGF-2.

In the first set of experiments, an expression vector for FGF-2-YFP was constructed by fusing YFP to the C-terminus of FGF-2. COS-7 cells were transiently transfected with the FGF-2-YFP expression vector and the fluorescence of YFP was detected after 48 h by confocal microscopy. Confocal images revealed a primarily nuclear localization of FGF-2 in COS-7 cells (Fig. 11 a). Fluorescence in the cytoplasm could be observed to some extent (Fig. 11 a).

Next, COS-7 cells were transiently cotransfected with FGF-BP-CFP and FGF-2 expression vectors and analyzed by confocal laser scanning microscopy at 48 h post transfection. While cytoplasmic localization of FGF-BP as well as localization to ERGIC were observed in cells transfected only with the FGF-BP-CFP construct (Fig. 11 b), confocal microscopy revealed a nuclear localization of FGF-BP-CFP upon coexpression with non labeled FGF-2 (Fig. 11 c), indicating translocation of FGF-BP into the nucleus.
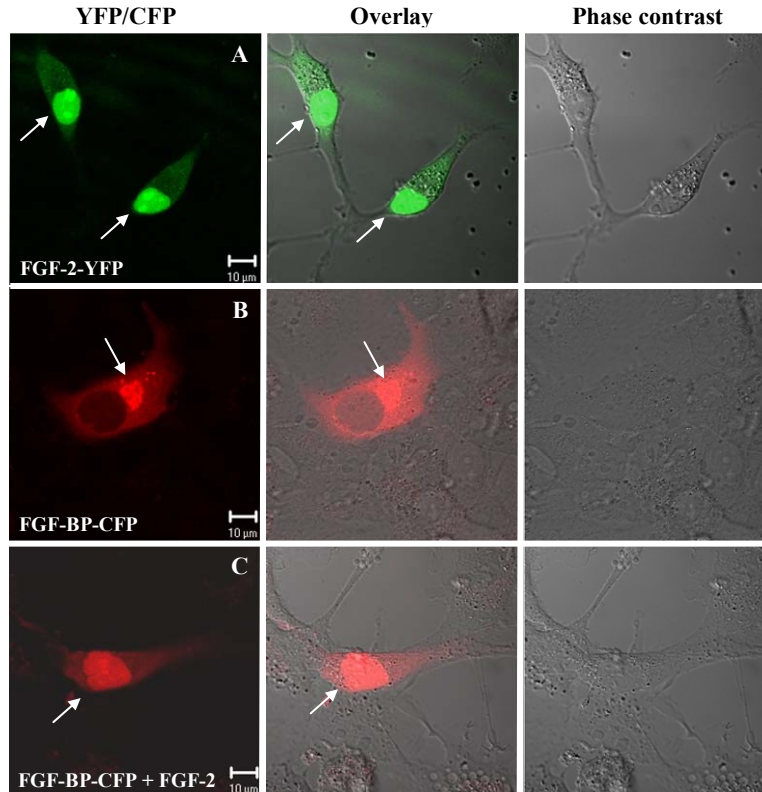
Fig. 11 **Upon coexpression with nuclear FGF-2, cytoplasmic FGF-BP is localized in nucleus in COS-7 cells.**

A) Nuclear localization of FGF-2-YFP fusion protein (green) in COS-7 cells was detected by confocal microscopy analysis. Very strong YFP fluorescence was detectable in the nucleoli. YFP fluorescence in the cytoplasm was very weak compared to nucleus. B) Confocal images of COS-7 cells transfected only with FGF-BP-CFP construct revealed cytoplasmic localization of FGF-BP (red) in COS-7 cells. C) Coexpression of FGF-BP-CFP (red) with non labeled FGF-2 translocates FGF-BP into the nucleus in COS-7 cells. Localization of FGF-BP to ERGIC was not seen upon coexpression with FGF-2.

4.2.4 Colocalization of FGF-BP with FGF-2 in the nucleus

The previous findings regarding the translocation of FGF-BP into the nucleus upon coexpression with FGF-2 indicated that FGF-BP probably interacts with FGF-2 in the nucleus. To examine the subcellular colocalization of FGF-2 and FGF-BP, COS-7 cells were transiently cotransfected with both constructs of fusion proteins (FGF-BP-CFP and FGF-2-YFP) and analyzed by confocal laser scanning microscopy.

In this analysis the adjustment and setting of microscopy configuration is very important in order to ensure complete separation of fluorescence of CFP and YFP during the simultaneous recording of both proteins. The microscopy configuration in the first set of images (Fig. 12 a) showed a complete separation of CFP and YFP fluorescence as seen by comparison of two cells which were either transfected with FGF-BP-CFP or with FGF-2-YFP expression vectors. Furthermore, different subcellular localization of FGF-BP (cytoplasmic) and FGF-2 (nuclear) was seen in these cells. These settings of configuration were chosen as standard for all images taken for parallel detection of CFP and YFP in the experiments in this thesis.

As expected from the previous data of translocation of FGF-BP into the nucleus upon coexpression of FGF-2, colocalization of both proteins in the nucleus was demonstrated in cells coexpressing both fusion proteins (Fig. 12 b).
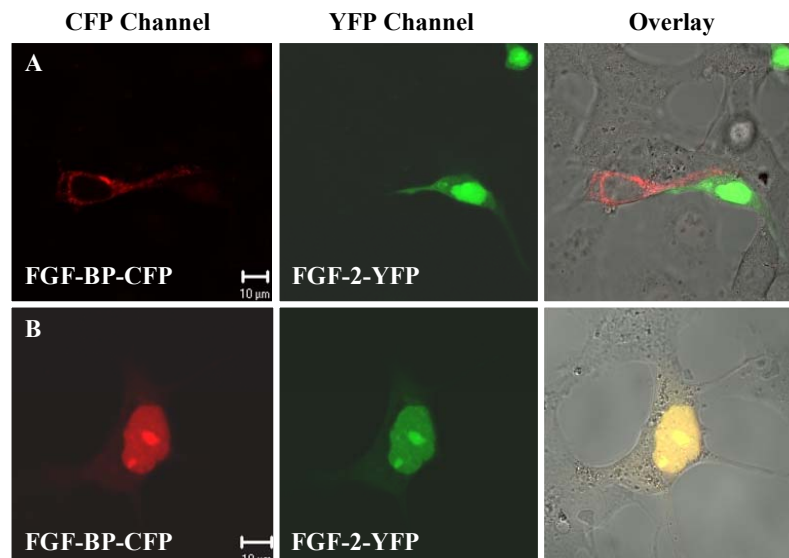
Fig. 12 FGF-BP colocalizes with FGF-2 in the nucleus.
COS-7 cells were transienly cotransfected with FGF-BP-CFP and FGF-2-YFP expression vectors. At 48 h post transfection, medium was aspirated and substituted by phosphate buffered saline (PBS) and the cells were analyzed by confocal microscopy without fixation. A) Control for the microscopy configuration for parallel detection of CFP (red) and YFP (green) fusion proteins. Complete separation of CFP and YFP fluorescence was achieved. B) Colocalization of FGF-BP (red) and FGF-2 (green) was seen in cells coexpressing FGF-BP-CFP and FGF-2-YFP. Colocalization is indicated by the yellow color resulting from the overlay of red and green.

4.2.5 Subcellular distribution of FGF-BP and FGF-2 in SW-13 cells

The non-tumorigenic adrenal carcinoma cell line SW-13 expresses constitutively high levels of FGF-2 but no FGF-BP [88]. Due to these properties of SW-13 cells, several studies have been performed using this cell line to analyze the role of FGF-BP in the activation of FGF-2. In the context of this thesis, SW-13 cells were chosen to study the subcellular localization of FGF-BP as well as the effects of interaction of FGF-2 with FGF-BP on cell proliferation.

SW-13 cells were transiently transfected with the FGF-BP-CFP construct and were analyzed by confocal microscopy after 48 h. In contrast to COS-7 cells, FGF-BP was localized primarily in the nucleus of SW-13 cells (Fig. 13 a). Furthermore, localization of FGF-BP to ERGIC was not seen.

To address the question if the subcellular localization of endogenous FGF-2 is similar to the subcellular distribution of FGF-BP-CFP, immunofluorescence was performed to detect the endogenous FGF-2 in SW-13 cells. SW-13 cells were grown on coverslips for 24 h prior to fixation. Endogenous FGF-2 was detected using anti-FGF-2 antibodies and Alexa Fluor 488-conjugated anti-rabbit antibodies. A mainly nuclear localization of endogenous FGF-2 was observed with some additional cytoplasmic staining (Fig. 13 b). These results indicate that both proteins are colocalized in the nucleus.

A) FGF-BP-CFP   **CFP Channel**   **Overlay**   **Phase contrast**

B) FGF-2 (Immunofluorescence)   **Alexa Fluor Channel**   **Overlay**   **Phase contrast**
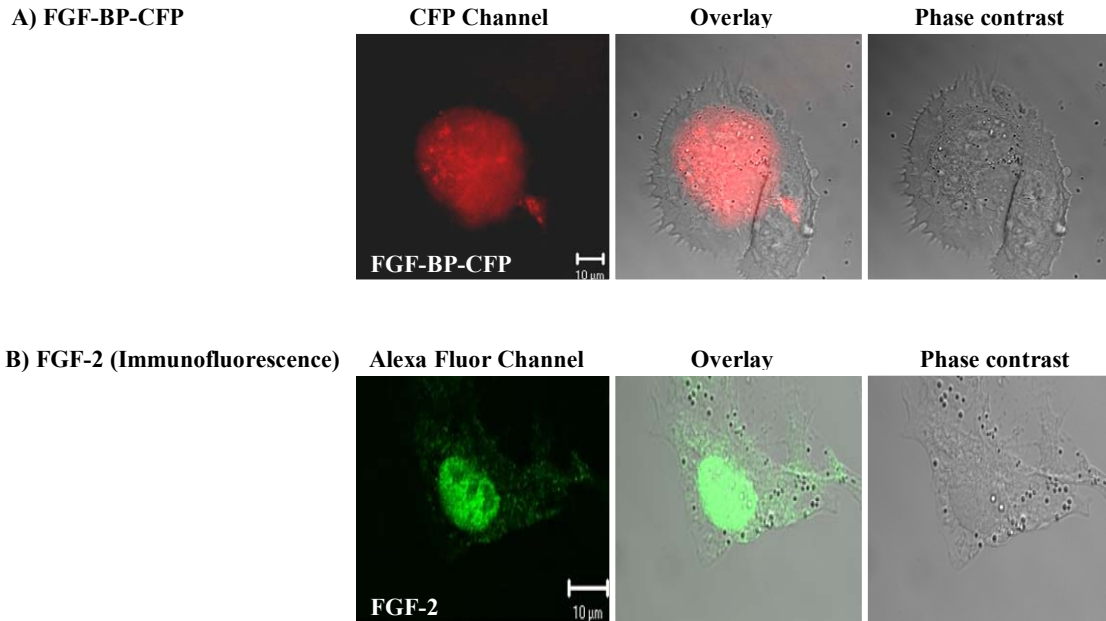
*Fig. 13 **Subcellular localization of FGF-BP and FGF-2 in SW-13 cells.***
A) SW-13 cells were transfected with the FGF-BP-CFP expression vector. At 48 h post transfection, cells were analyzed by confocal microscopy without fixation. Confocal images revealed a nuclear localization of FGF-BP-CFP (red) in SW-13 cells. B) Endogenous FGF-2 (green) localizes primarily to the nucleus in SW-13 cells as detected by immunofluorescence.

4.2.6 Generation of C- and N-terminal truncations of FGF-BP

The data regarding the colocalization of FGF-BP and FGF-2 as well as the translocation of FGF-BP into the nucleus of COS-7 cells upon coexpression with FGF-2 led to the question of which segment(s) of FGF-BP are responsible for the interaction with FGF-2 and nuclear translocation. This analysis was performed through the generation of C- or N-terminally truncated FGF-BP constructs as CFP-tagged proteins. This included the targeted disruption of certain disulfide bonds in the full length FGF-BP. The N-terminal signal sequence for secretion, however, was attached to all N-terminally truncated FGF-BP constructs (Fig. 14).
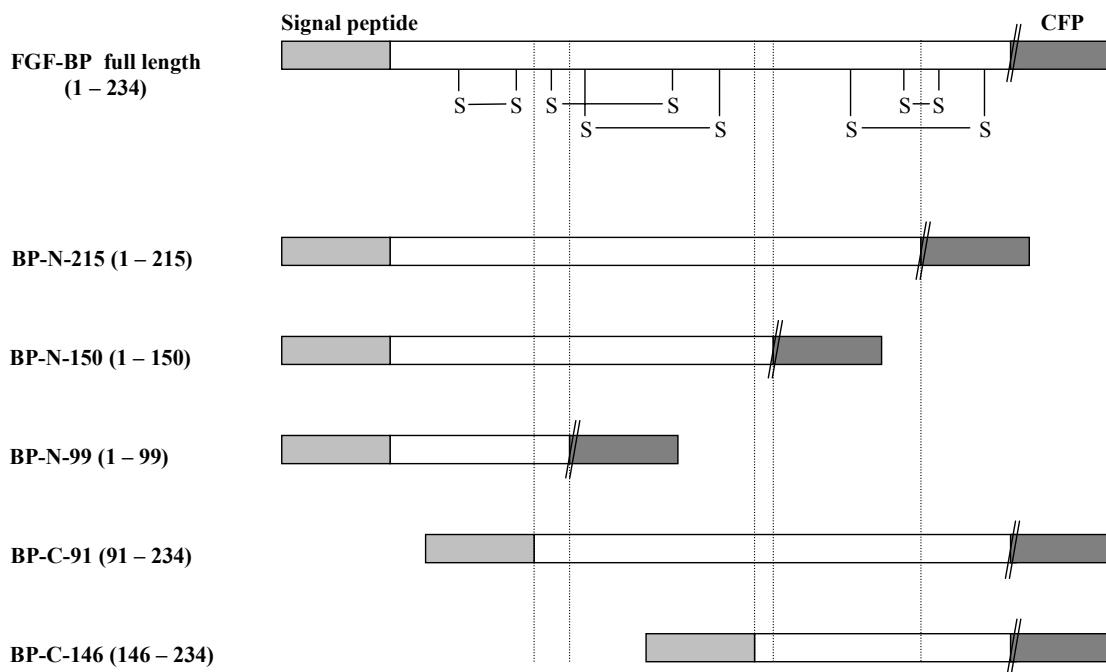
Fig. 14 **Schematic representation of the CFP-tagged full length as well as C- and N-terminally truncated FGF-BP constructs.**

Human full length FGF-BP is 234 residues long. 10 cysteine residues (represented by the symbol S), which are positionally conserved in human, mouse and bovine FGF-BP, form 5 disulfide bonds. The light grey color (left) represents the N-terminal signal peptide and the dark grey color (right) represents the CFP (239 amino acids), which is attached to all constructs. The strategy of the construction of C- and N-terminal truncations of FGF-BP is based on the disruption of certain disulfide bonds of the full length FGF-BP. Numbers listed left in the figure refer to amino acids.

4.2.7 Colocalization and interaction of various truncated FGF-BP constructs with FGF-2 in COS-7 cells

In the first set of experiments, the subcellular localization of various CFP-tagged FGF-BP constructs in COS-7 cells was studied (Fig. 15 a). COS-7 cells were grown on coverslips and transfected after 24 h with expression vectors containing various truncated FGF-BP constructs. At 48 h post transfection, the subcellular localization of various mutants of FGF-BP was analyzed by confocal microscopy. Similar to the subcellular localization of full length FGF-BP, all CFP-tagged FGF-BP constructs showed a primarily cytoplasmic

localization with a particularly strong fluorescence in Golgi area, indicating the localization of various mutants of FGF-BP to ERGIC (Fig. 15 a).

Next, the colocalization of various truncated FGF-BP mutants with FGF-2 in COS-7 cells was examined. COS-7 cells were cotransfected with FGF-2-YFP and various CFP-tagged FGF-BP constructs. After 48 h, the fluorescence of CFP and YFP fusion proteins was detected by confocal microscopy using the appropriate microscope settings for parallel detection of CFP and YFP fluorescence (Fig. 15 b). Upon coexpression with FGF-2, all C-terminally truncated FGF-BP mutants still showed a nuclear colocalization with FGF-2 (Fig. 15 b). In contrast, translocation of FGF-BP into the nucleus was not seen in the case of N-terminally truncated FGF-BP constructs upon coexpression with FGF-2 (Fig. 15 b).

Fig. 15 (next page) **Nuclear colocalization and interaction of FGF-BP with FGF-2 is lost upon N-terminal truncations of FGF-BP.**

A) Subcellular localization of various CFP-tagged FGF-BP constructs (red) upon transfection of COS-7 cells with the corresponding FGF-BP-CFP expression vector. Confocal images revealed for all C- and N-terminally truncated FGF-BP mutants a cytoplasmic distribution similar to full length FGF-BP. B) Fluorescence of CFP (red) and YFP (green) as detected by confocal microscopy after cotransfection of COS-7 cells with FGF-2-YFP and various CFP-tagged mutants of FGF-BP expression vectors. Overlay of red and green color results in yellow indicating the colocalization of FGF-2 and C-terminally truncated FGF-BP mutants in nucleus of COS-7 cells. BP-N-99 construct, which represents the smallest C-terminally truncated mutant of FGF-BP, showed upon coexpression with FGF-2 more CFP fluorescence in cytoplasm of COS-7 cells as compared to other C-terminally truncated FGF-BP constructs, indicating reduced interaction with FGF-2 and decreased nuclear translocation. N-terminally truncated FGF-BP constructs (BP-C-91 and BP-C-146) did not show translocation of FGF-BP into the nucleus upon coexpression with FGF-2. All images are taken at the same setting.

A

B

CFP Channel	Phase contrast

CFP Channel	YFP Channel	Overlay
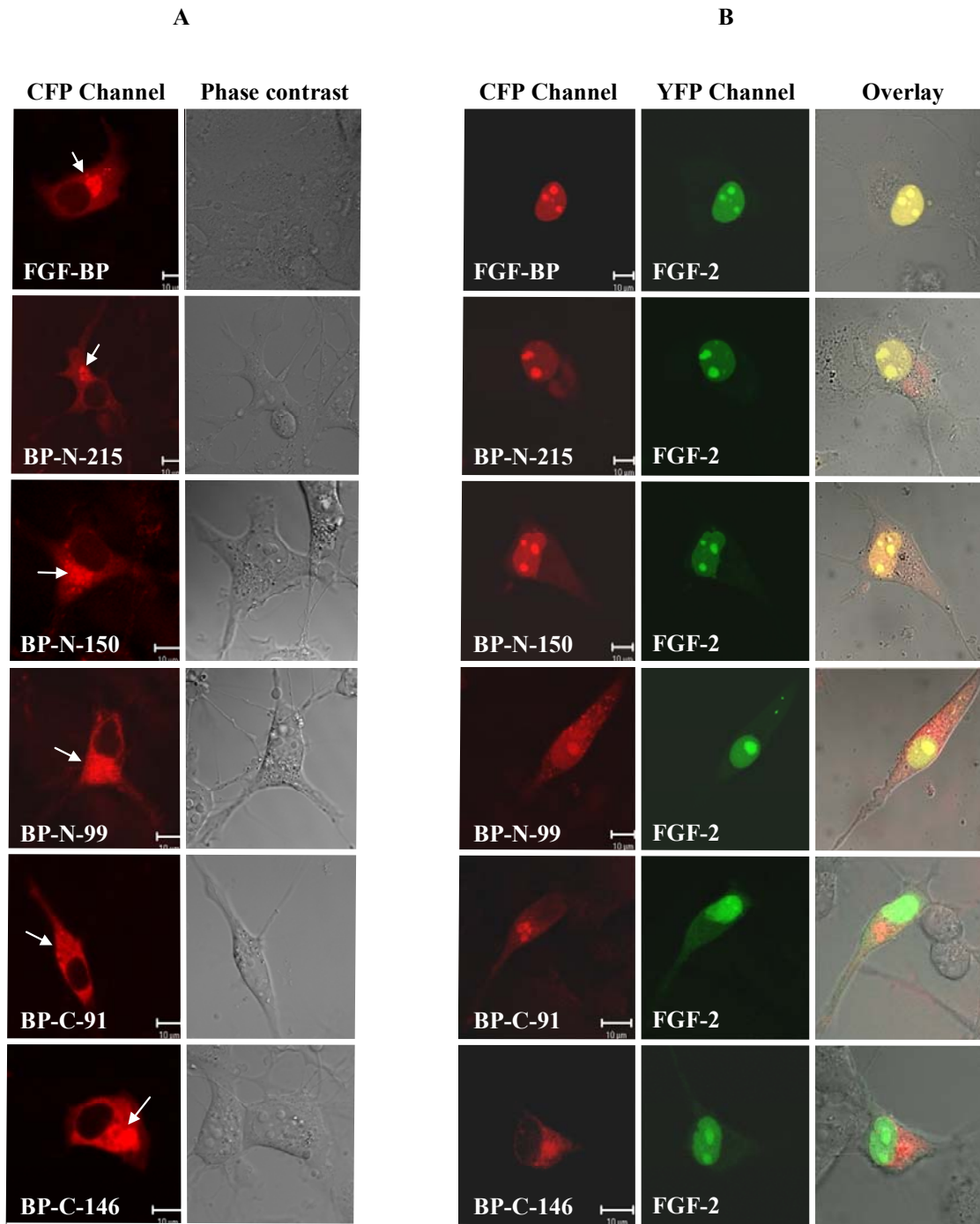
4.2.8 Colony formation of stably transfected SW-13 clones in soft agar

The adrenal carcinoma cell line SW-13 expresses high levels of FGF-2 and lacks expression of the FGF-BP. Furthermore, it has been demonstrated that the stable transfection of SW-13 cells with an FGF-BP expression vector or the addition of FGF-2 induces the colony formation in soft agar [88,307]. For this reason, the analysis of the biological significance of the interaction of various FGF-BP truncations with FGF-2 was performed using this cell line. First, constructs of C- and N-terminally truncated forms of FGF-BP without fusion partner were generated and cloned into pRC/CMV expression plasmids. SW-13 cells were then stably transfected with these constructs or with the empty vector (CMV) as a control.

Soft agar assays were performed to study the anchorage-independent growth of these stably transfected SW-13 cell lines. As expected, full length FGF-BP-transfected SW-13 cells grew more large colonies compared to the control cells stably transfected with the empty vector (CMV) (Fig. 16 lower panel). The similar tendency was also seen in SW-13 clones stably transfected with C-terminally truncated FGF-BP constructs. In contrast, no induction of soft agar colony formation was observed in SW-13 cells stably transfected with constructs containing N-terminal truncations of FGF-BP.
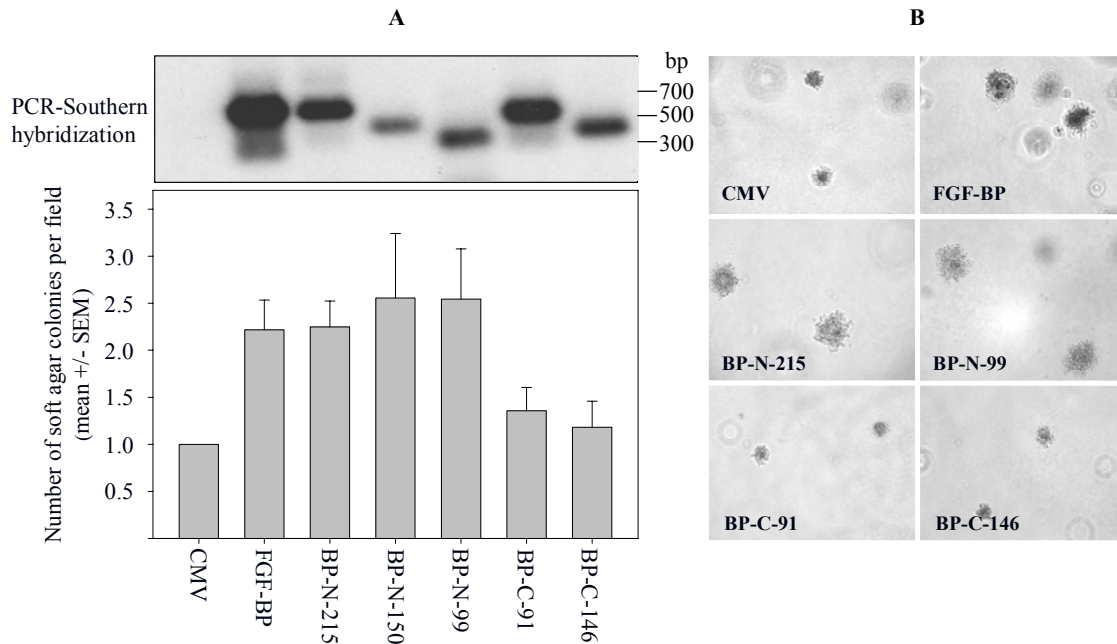
*Fig. 16 **FGF-BP-mediated stimulation of soft agar colony formation is lost upon the N-terminal truncation of FGF-BP.***

A) Stable expression of various C- and N-terminally truncated FGF-BP mutants in SW-13 cells as determined by RT-PCR and PCR-Southern hybridization (upper panel). Total RNA was extracted from cells. The presence of mRNA coding for various truncations of FGF-BP was determined by RT-PCR and PCR-Southern hybridization analysis with the specific primers described in Materials and Methods. The evaluation of the induction of colony formation of SW-13 transfectants in soft agar is shown in the lower panel. Colonies >50 μm were counted after 3 weeks. SW-13 cells transfected with full length or C-terminally truncated FGF-BP constructs grew more colonies >50 μm compared to control cells (CMV). No induction of soft agar colony formation was observed in SW-13 cells stably transfected with constructs containing N-terminal truncations of FGF-BP. Colony numbers of control cells (CMV) were set to 1.0. B) Representative images of counted soft agar colonies.

4.2.9 Effects of FGF-BP and truncated mutants on growth of COS-7 cells in soft agar

To further explore the biological effects of various truncations of FGF-BP in another cell line, COS-7 cells were stably transfected with expression plasmids containing C- and N-terminally truncated FGF-BP constructs without fusion partner, and anchorage-independent growth assays were performed using these various mass transfected COS-7 cells. After 3 weeks, colonies >50 μm were counted. Surprisingly, and in contrast to SW-13 cells,

anchorage-independent cell growth assays revealed an inhibitory effect of full length FGF-BP on the growth of COS-7 cells in soft agar (Fig. 17, lower panel), resulting in a decreased colony formation compared to control cells. Formation of large colonies was observed in COS-7 cells stably transfected with C- and N-terminally truncated FGF-BP constructs, indicating that the loss of the C- and N-terminus of FGF-BP abolished the inhibitory effect of full length FGF-BP on colony formation of COS-7 cells in soft agar.
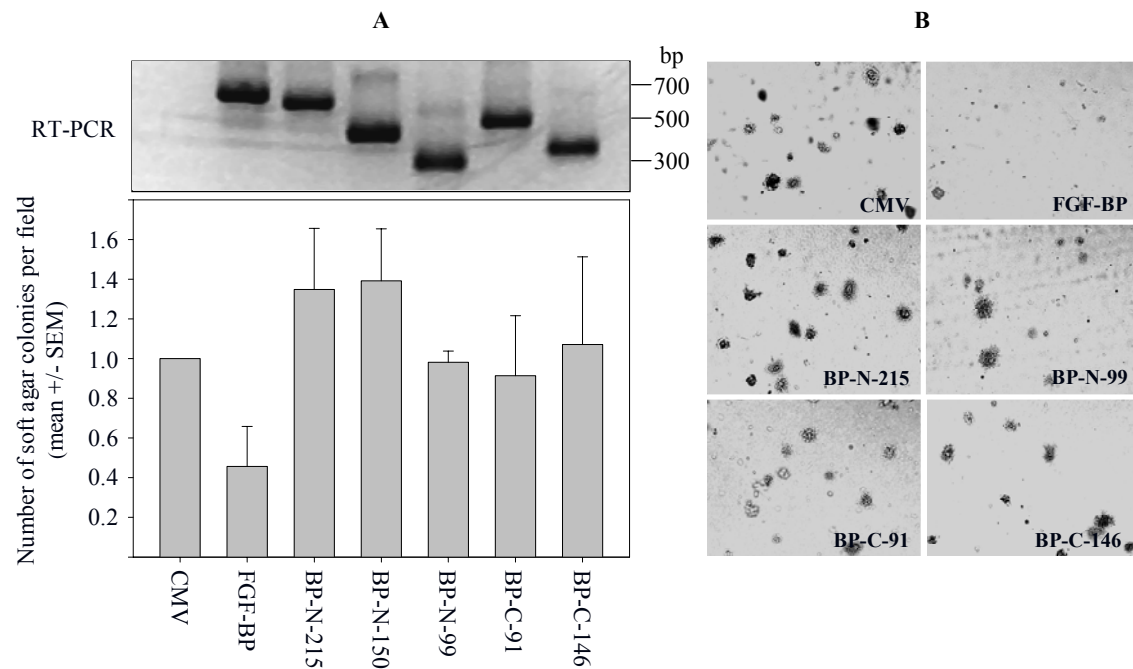
*Fig. 17 **C- and N-terminal truncations of FGF-BP abolish the inhibitory effects of FGF-BP on colony formation of COS-7 cells in soft agar.***

A) Determination of mRNA expression of various C- and N-terminally truncated FGF-BP mutants in stably transfected COS-7 cells by RT-PCR (upper panel). Total RNA was extracted from cells. The presence of mRNA coding for various truncations of FGF-BP was determined by RT-PCR with the specific primers described in Materials and Methods. Soft agar assays show the inhibitory effects of full length FGF-BP on growth of COS-7 cells in soft agar (lower panel). Full length FGF-BP-transfected COS-7 cells grew small colonies compared to control cells transfected with empty vector (CMV). The FGF-BP-mediated inhibition of the growth of COS-7 cells in soft agar was lost upon C- and N-terminal truncation of FGF-BP. Colony numbers of control cells (CMV) were set to 1.0. B) Representative images of counted soft agar colonies.

4.2.10 Inhibition of stimulating effects of FGF-2 on cell growth by endogenously expressed FGF-BP

For characterization of the biological activity of FGF-BP resulting from its interaction with FGF-2, effects of transient transfection of FGF-BP on soft agar colony formation of FGF-2-expressing COS-7 cells on cell growth in soft agar were studied.

First, it was examined if COS-7 cells express FGF receptors. RT-PCR was performed using mRNA from COS-7 cells or human hepatoblastoma cell line HepG2 (as a positive control [308]) in the presence of FGFR1-specific primers. A predicted 530-nucleotide fragment was determined by agarose gel electrophoresis in both cell lines, indicating the expression of FGFR1 mRNA in COS-7 cells (Fig. 18 a). This result was further confirmed by PCR-Southern hybridization analysis (Fig. 18 a).

In further experiments, an FGF-2 construct without fusion partner was generated and stably expressed in COS-7 cells. Control cells stably transfected with empty vector (CMV) and FGF-2 transfectants were transiently transfected with empty vector (CMV) or FGF-BP expression vectors. At 4 h post transfection, a soft agar assay was performed. After 3 weeks, colonies >50 μm were counted. Induction of colony formation in soft agar was shown in the stably FGF-2-transfected COS-7 cells, which were transiently transfected with CMV, compared to control transfectants (Fig. 18 b). In contrast to stably FGF-BP-transfected COS-7 cells, which grew small colonies compared to control cells transfected with the empty vector as shown above (Fig. 17), transient transfection of COS-7 cells with FGF-BP expression vector had no effect on colony formation of COS-7 cells in soft agar. However, the transient expression of FGF-BP in FGF2-expressing COS-7 cells resulted in a decreased colony formation compared to (FGF-2/CMV) cells, indicating the reversal of the stimulatory activity of FGF-2 expression on colony formation in soft agar (Fig. 18 b). These results suggested an FGF-BP-mediated inhibition of the stimulating effects of FGF-2 on growth of COS-7 cell proliferation.
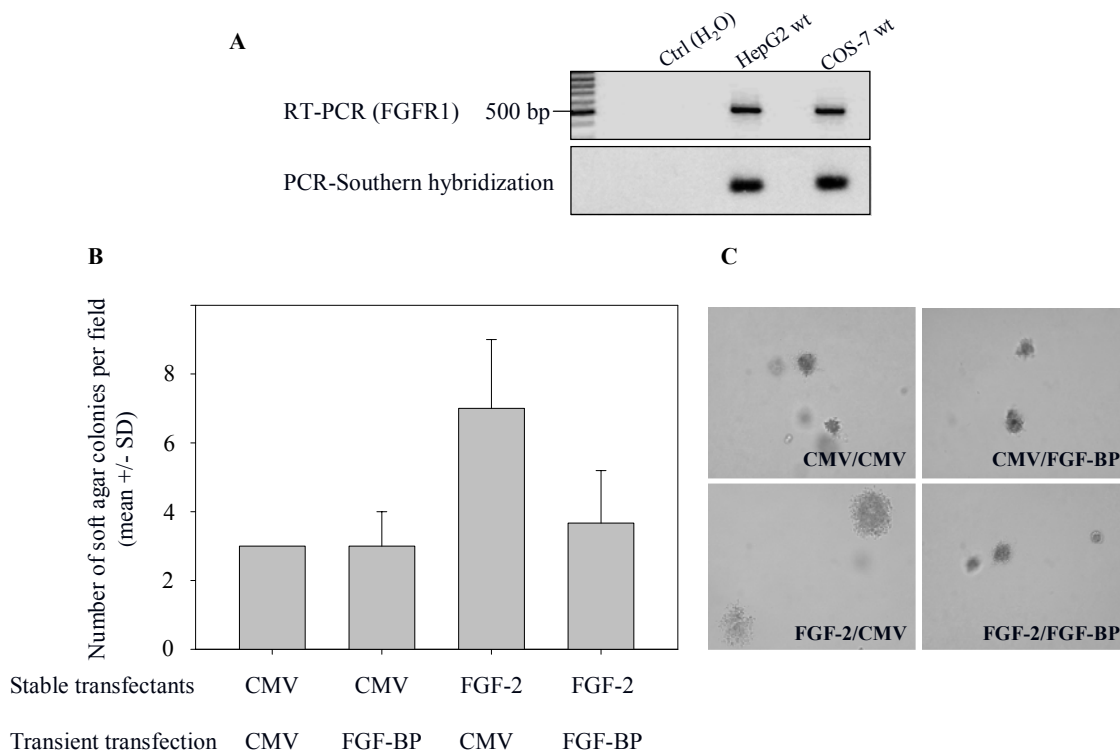
Fig. 18 **FGF-BP-mediated inhibition of stimulating effects of FGF-2 on colony formation of COS-7 cells in soft agar.**

A) Determination of the expression of FGFR1 mRNA by RT-PCR and PCR-Southern hybridization. Total RNA was extracted from COS-7 and HepG2 cells (as a positive control) and RT-PCR was performed using specific primers described in Materials and Methods. The presence of 530-nucleotide fragment (upper panel), which is confirmed by PCR-Southern hybridization (lower panel), demonstrates the expression of FGFR1 in COS-7 cells. B) Soft agar colony formation of FGF-2-expressing and control COS-7 cells. Cells were transiently transfected as indicated in the figure and at 4 h post transfection soft agar assays were performed. After 3 weeks, colonies were counted. The number of colonies >50 μm of (FGF-2/CMV) cells was >2 fold higher than control cells (CMV/CMV), indicating the stimulating effects of FGF-2 on growth of COS-7 cells in soft agar. Transient transfection of stably CMV-transfected COS-78 cells with FGF-BP expression vector had no effect on induction of colony formation compared to control cells (CMV/CMV). In contrast, coexpression of FGF-BP with FGF-2 reversed the stimulatory effects of FGF-2 on colony formation of FGF-2-expressing COS-7 cells. C) Representative images of counted soft agar colonies.

4.2.11 Effect of exogenous recombinant FGF-BP on FGF-2-mediated stimulation of colony formation in soft agar

Previous results demonstrated the inhibitory effects of endogenously expressed FGF-BP on the colony formation of FGF-2-expressing COS-7 cells in soft agar. To test if the inhibitory effects can also be mediated by exogenously added FGF-BP, recombinant FGF-BP was used. This His-tagged recombinant protein was expressed as a non-secreted protein in SF-9 insect cells using BAC-TO-BAC baculovirus expression system [130] and purified under denaturating conditions. Gel electrophoresis with Coomassie staining, as well as Western blotting, revealed a single band (~30 kDa) only in infected SF-9 insect cells, demonstrating the expression of recombinant FGF-BP (Fig. 19 a).

To provide evidence that the recombinant purified FGF-BP can interact with FGF-2 and is biologically active, 0.2 µg recombinant FGF-2 or BSA (as a negative control) were dotted onto a nitrocellulose membrane and a Dot blot was performed as described in Materials and Methods. The Dot blot analysis showed only a signal, where FGF-2 was dotted onto the nitrocellulose membrane, indicating the binding of recombinant FGF-BP to FGF-2 (Fig. 19 b).

In further experiments, soft agar assays were performed using FGF-2-expressing COS-7 cells. COS-7 cells stably transfected with empty vector were used as a control. To analyze the effects of exogenously added recombinant FGF-BP on the colony formation induced by endogenously expressed or exogenously added FGF-2, recombinant FGF-BP and FGF-2 were directly applied onto the solidified agar as indicated in the figure (Fig. 19 c) at final concentrations of 5.0 µg/ml and 1.0 ng/ml, respectively. As expected, colony formation was stimulated by the addition of FGF-2 to control cells, which was comparable to the induction of colony formation in FGF-2-expressing COS-7 cells (Fig. 19 c). While, addition of exogenous FGF-BP did not result in any effects on colony formation of control cells, it inhibited the FGF-2-induced colony formation in FGF-2-expressing COS-7 cells. These experiments confirmed the previously observed growth-inhibitory effects of endogenously expressed FGF-BP.
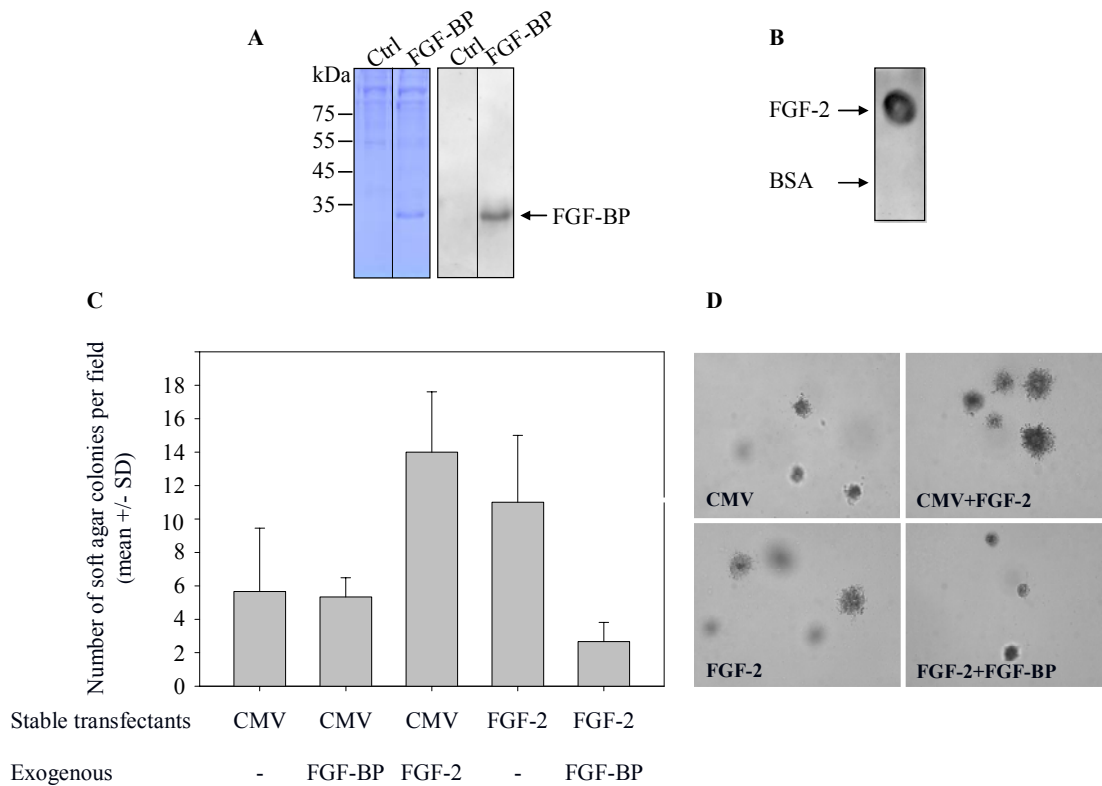
Fig. 19 Growth-inhibitory effects of exogenously added FGF-BP.

A) Gel electrophoresis with Coomassie staining, as well as Western blotting, revealed a single band (~30 kDa) in eluates containing purified FGF-BP expressed in SF-9 insect cells. The control represents non infected SF-9 insect cells, which were subjected to the same FGF-BP purification procedure. B) Detection of the binding of recombinant FGF-BP to FGF-2 by Dot blot analysis. 0.2 µg FGF-2 or BSA were dotted onto a nitrocellulose membrane and a Dot blot was performed as described in Materials and Methods using anti-FGF-BP antibody. C) Induction of colony formation in control and FGF-2-expressing COS-7 cells in soft agar upon exogenous addition of recombinant FGF-BP or FGF-2. 0.5 µg/ml recombinant FGF-BP or 0.1 ng/ml FGF-2 were added immediately onto the solidified agar as indicated in the figure. After 3 weeks, colonies >50 µm were counted. Exogenously added FGF-2 stimulated the colony formation of control cells, indicating the cell growth-inducing bioactivity of FGF-2. This effect was comparable to the effect of endogenously expressed FGF-2. Addition of FGF-BP abolished the effects on stimulation of colony formation in FGF-2-expressing COS-7 cells, indicating the dependence of the growth inhibitory effects of FGF-BP on its interaction with FGF-2. In contrast, FGF-BP had no effects on the induction of colony formation in control cells. D) Representative images of counted soft agar colonies.

4.2.12 Cellular uptake of exogenous FGF-BP is dependent on the expression of and
interaction with FGF-2

The translocation of FGF-BP into the nucleus of COS-7 cells upon coexpression with FGF-2 (Fig. 11) as well as the inhibitory effects of FGF-BP on cell growth in soft agar mediated by exogenously added recombinant FGF-BP (Fig. 19), suggests the uptake of FGF-BP into the cells after its secretion to exert its biological activity. Furthermore, nuclear colocalization of FGF-BP and FGF-2 (Fig. 12) indicates that the uptake of FGF-BP may be dependent on the interaction of FGF-BP with FGF-2.

To study the cellular uptake of FGF-BP in COS-7 cells und its dependence on the expression of FGF-2, COS-7 cells were transiently transfected with CMV (empty vector) or FGF-2 expression vector and at 48 h post transfection, incubated with (5,000 cpm/well) [^{125}I]-labeled FGF-BP for 1 h. The cells were then fractionated by differential centrifugation as described in Materials and Methods. The nuclear and combined mitochondrial and microsomal fractions were measured in a γ-scintillation counter. Radioactivity of both fractions obtained from FGF-2-transfected cells was 2 fold higher than the control cells (Fig. 20 a).

To confirm the dependence of the cellular uptake of exogenous FGF-BP on its interaction with FGF-2, COS-7 cells were transiently transfected with CMV or FGF-2-YFP expression vector and incubated with (3 µg/well) recombinant FGF-BP for 1 h and indirect immunofluorescence was performed using mouse monoclonal anti-FGF-BP antibodies. The primary antibody was visualized with Texas red-conjugated mouse antibodies and the cells were analyzed by confocal microscopy using the appropriate microscope settings for parallel detection of YFP and Texas red (Fig. 20 b). Texas red fluorescence was only detected in the nucleus of FGF-2-YFP-transfected COS-7 cells, which were incubated with the recombinant FGF-BP (Fig. 20 b). The nuclear colocalization of FGF-2 and exogenously added FGF-BP in these cells demonstrated the dependence of cellular uptake of FGF-BP on its interaction with FGF-2 and confirmed previous results regarding the subcellular localization of FGF-BP and FGF-2 obtained from the coexpression of both proteins. Texas red fluorescence was not detectable in the FGF-2-YFP-negative and FGF-2-YFP-transfected COS-7 cells incubated with recombinant FGF-BP or buffer E, respectively (Fig. 20 b). Background fluorescence

was observed in Texas red channel to some extent in FGF-2-YFP-transfected cells (Fig. 20 b).

Fig. 20 (next page) **Dependence of cellular uptake of exogenous recombinant FGF-BP in COS-7 on the expression and interaction with FGF-2.**

A) Uptake of [^{125}I]-labeled FGF-BP in COS-7 cells. COS-7 cells were transiently transfected with the CMV or the FGF-2 expression vector. At 48 h post transfection, (5,000 cpm/well) [^{125}I]-FGF-BP was added to the cells. After washing with PBS, cells were fractioned by differential centrifugation as described in Material and Methods. Radioactivity of nuclear and combined mitochondrial and microsomal fractions obtained from FGF-2-transfected cells was 2 fold higher than the radioactivity of fractions obtained from control cells transfected with the empty vector. B) Detection of the cellular uptake of exogenous FGF-BP in COS-7 cells transiently transfected with the CMV (a) or the FGF-2-YFP (b and c) expression plasmid by confocal immunofluorescence microscopy. COS-7 cells were grown on glass coverslips 24 h before transfection. At 48 h post transfection, cells were either incubated with 30 µl (~3 µg) recombinant FGF-BP diluted in 300 medium (a and c) or with 30 µl buffer E (b) diluted in the same volume of medium for 1 h. The cells were then fixed and immunofluorescence was performed using monoclonal mouse anti-FGF-BP antibodies. For visualization of the primary antibody, a Texas red-labeled anti-mouse antibody was used. The fluorescence of YFP (green) and Texas red (red) was detected by adjustment of microscope configuration for parallel detection of YFP and Texas red. Texas red fluorescence was not detectable in the FGF-2-YFP-negative (a) and in the FGF-2-YFP-transfected (b) COS-7 cells incubated with recombinant FGF-BP or buffer E, respectively. In contrast, confocal images revealed colocalization of FGF-BP with FGF-2 in FGF-2-YFP-transfected COS-7 cells (c) incubated with recombinant FGF-BP, demonstrating the cellular uptake of recombinant FGF-BP and its dependence on the interaction with FGF-2.

A

Nuclear fraction

Mitochondrial and microsomal fraction

B

| | Texas red Channel (FGF-BP) | YFP Channel (FGF-2) | Overlay |
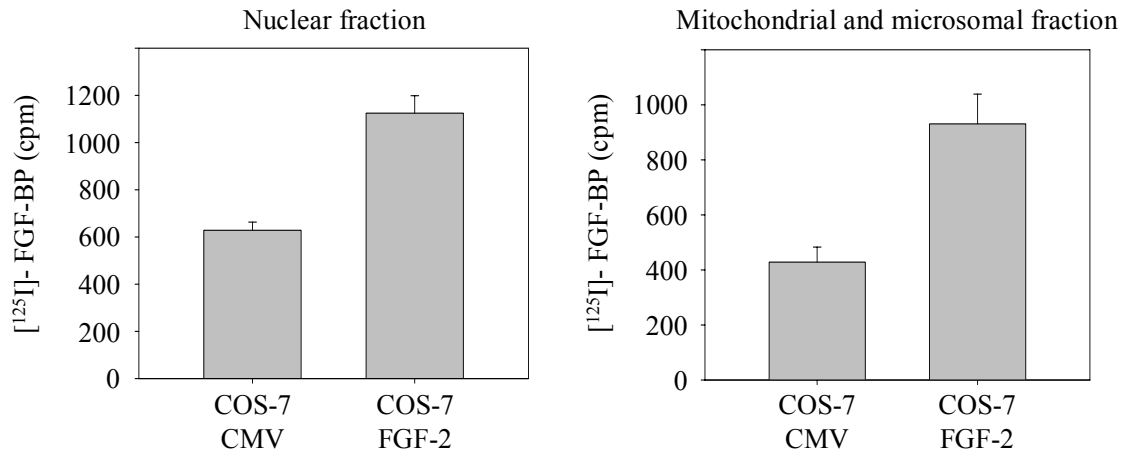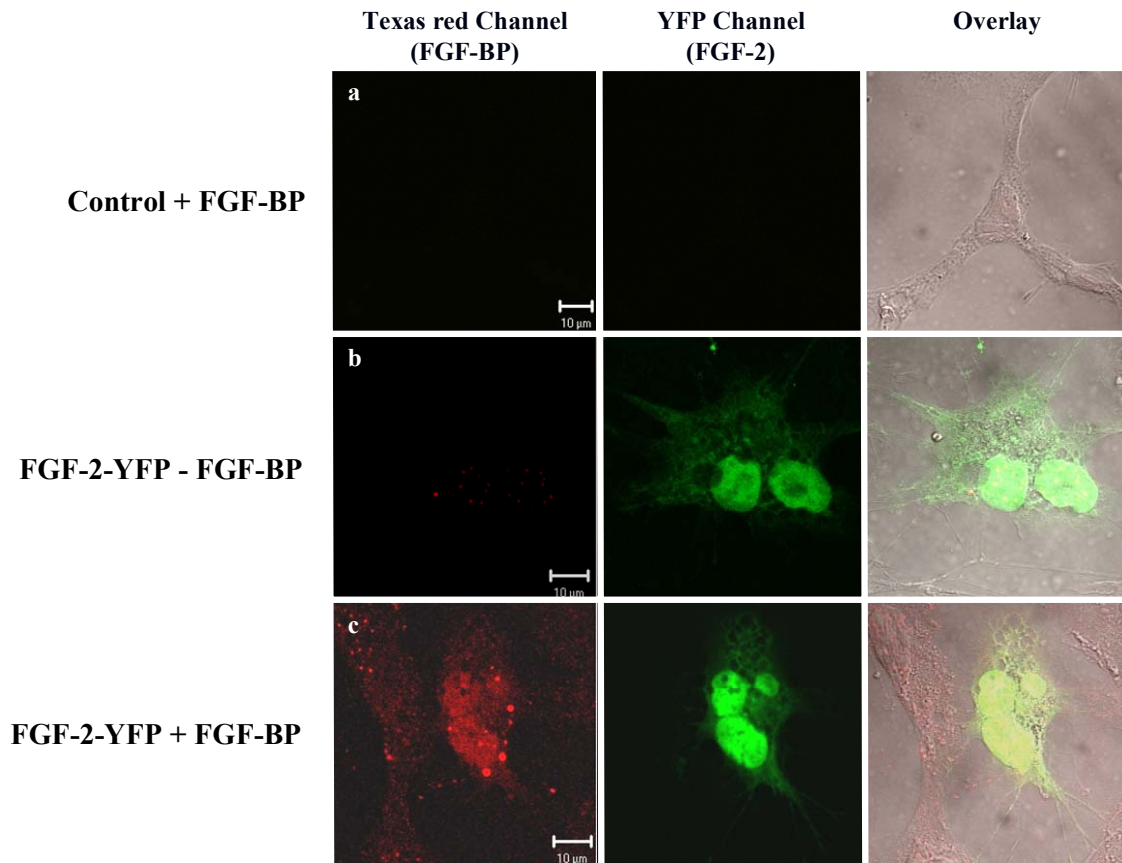
4.3 Effects of riboyzme-mediated HER-2 downregulation on paclitaxel sensitivity in SKOV-3 cells

4.3.1 Effects of HER-2 phosphotyrosine kinase inhibitors D-69491 and D-70166 on cell proliferation

Previous studies showed that treatment with the HER-2 inhibitory antibody trastuzumab (Herceptin), which downregulates HER-2 on the cell surface and is approved and well established for adjuvant therapy of different tumors, results in reduction of cell proliferation as well as markedly increased cellular paclitaxel resistance in human SKOV-3 ovarian cancer cells (see [243] for details).

To investigate the effects of HER-2 inhibition on proliferation of SKOV-3 cells by another different strategy, HER-2 phosphotyrosine kinase inhibitors D-69491 and D-70166 (a gift from Baxter Oncology, Frankfurt/Main, Germany) were used.
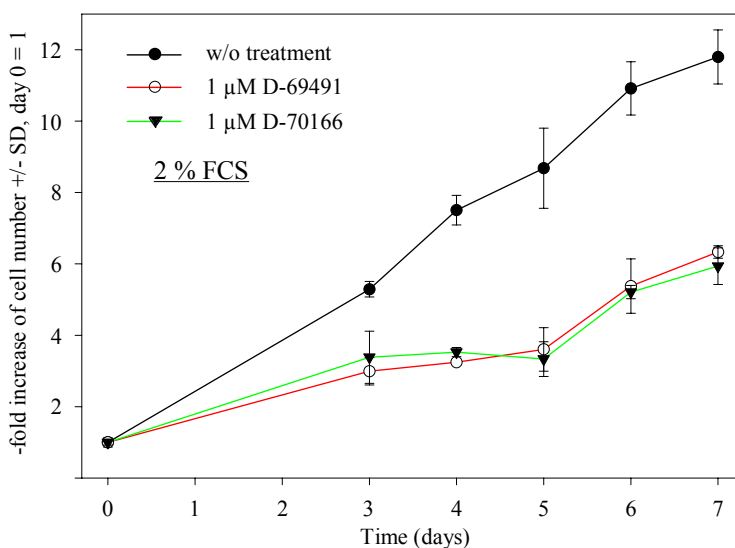
*Fig. 21 **Reduction of proliferation of SKOV-3 cells by the newly developed HER-2 phosphotyrosine kinase inhibitors D-69491 and D-70166.***

Proliferation of SKOV-3 cells (closed circles) was >50 % inhibited upon addition of 1 μM D-69491 (open circles) or D-70166 (inverse triangles).

SKOV-3 cells were cultivated for 7 days in the presence of 1 µM D-69491 or D-70166 and cell numbers were assessed using a colorimetric assay based on the cleavage of the tetrazolium salt WST-1 by dehydrogenases in viable cells. Anchorage-dependent proliferation experiments revealed a >50 % reduction of cell proliferation upon addition of 1 µM D-69491 or D-70166 (Fig. 21).

4.3.2 Effects of HER-2 phosphotyrosine kinase inhibitors D-69491 and D-70166 on Cellular paclitaxel resistance

Next, to study the effects of D-69491- and D-70166-mediated HER-2 inhibition on paclitaxel resistance in SKOV-3 cells, cells were treated with 1 µM D-69491or D-70166, or left untreated, 24 h prior to the addition of paclitaxel at the concentrations indicated (Fig. 22) and numbers of living cells were measured after 3-5 days. Dose-response curves revealed an increase in paclitaxel resistance upon pretreatment with D-69491 or D-70166 (Fig. 22). This effect was identical for both inhibitors with the IC_{50} of paclitaxel being shifted from ~5 nM in untreated cells to ~8 nM.

Treatment	IC_{50} (nM)
untreated	5.0
D-69491	8.0
D-70166	8.0
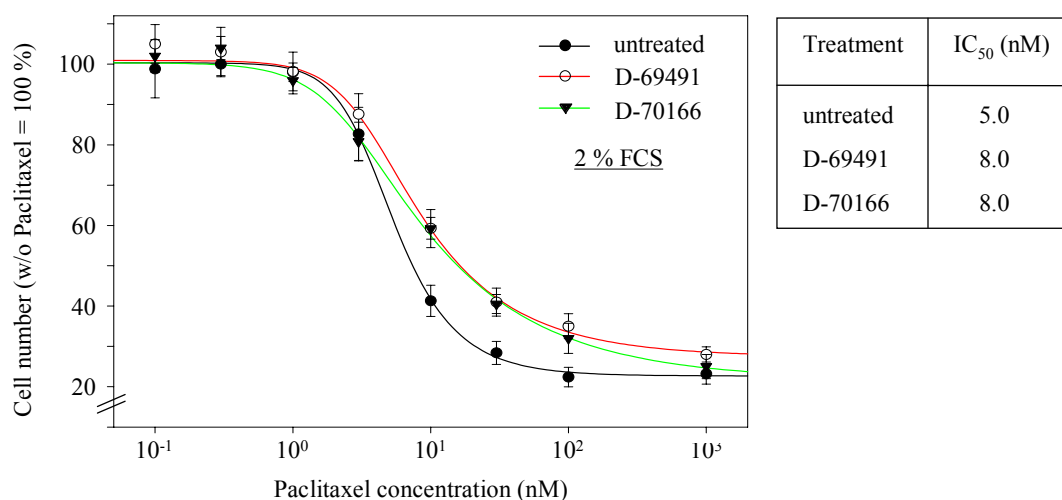
*Fig. 22 **Effects of the newly developed HER-2 phosphotyrosine kinase inhibitors D-69491 and D-70166 on paclitaxel resistance in SKOV-3 cells.***
Treatment of cells with 1 µM D-69491 (open circles) or D-70166 (inverse triangles) 24 h prior to the addition of paclitaxel reveals increased paclitaxel resistance upon HER-2 inhibition compared to untreated cells (closed circles).

4.3.3 Ribozyme-mediated HER-2 depletion leads to reduced cell proliferation

To address a possible HER-2 dependence of proliferation and paclitaxel cytotoxicity in a third, more detailed approach, various stable isogenic SKOV-3 cell lines with ribozyme-mediated reduction of HER-2 expression levels were used. In previous studies, SKOV-3 ovarian carcinoma cells were stably transfected with the ribozyme expression vector RzB containing a ribozyme cloned into the pRc/CMV expression plasmid and designed to cleave 1991 nucleotides downstream of the translation initiation site in the HER-2 mRNA. From the mass-transfected cells, clonal derivative cell lines with various degrees of HER-2 depletion were generated. The clones were termed RzB-3, RzB-7, RzB-8 and show 19.8 %, 50.0 % and 12.5 % residual HER-2 protein levels, respectively, as determined by FACS analysis and Western blot [309].

To study the effects of ribozyme-mediated HER-2 downregulation on cell growth, SKOV-3 wildtype (with 100 % residual HER-2 expression level) and RzB-8 cells (with 12.5% residual HER-2 expression level) were cultivated for 5 days and cell numbers were assessed using a colorimetric assay.

*Fig. 23 **Ribozyme-mediated HER-2 downregulation leads to reduced proliferation of SKOV-3 cells.***
I*n proliferation assays, RzB-8 cells with 12.5% residual HER-2 expression level (open circles) showed a >50% decrease in proliferation compared to SKOV-3 wildtype cells (closed circles).*

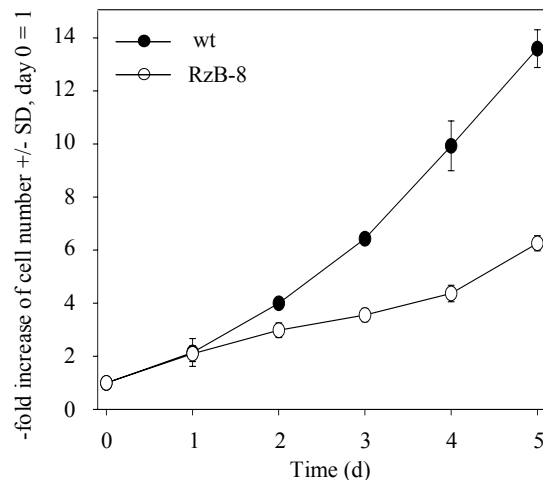Similar to the previous results based on tyrosine kinase inhibitors D-69491 and D-70166 (Fig 21) and Herceptin (see [243] for details), ribozyme-mediated HER-2 downregulation led to reduction of cell growth. A >50% decreased of proliferation of RzB-8 cells on plastic compared to wildtype cells was observed (Fig. 23).

4.3.4 Ribozyme-mediated HER-2 depletion leads to increased resistance towards paclitaxel

Next, the effects of HER-2 expression levels on paclitaxel sensitivity in the different SKOV-3 cell lines wildtype, RzB-7, and RzB-8 were analyzed. Different SKOV-3 cell lines, i.e. wildtype, RzB-7, and RzB-8, were treated with paclitaxel at the concentrations indicated in the figure (Fig. 24) and numbers of living cells were measured after 3-5 days. In agreement with the previous results, ribozyme-mediated reduction of HER-2 expression significantly shifted the paclitaxel dose-response curves to the right with a maximum shift in the case of the RzB-8 cells (IC_{50} = 6.0 nM versus 0.9 nM in wildtype cells; Fig. 24, upper panel).

4.3.5 Doxorubicin or cisplatin cytotoxicity is independent of HER-2 expression levels

To further investigate the effects of ribozyme-mediated HER-2 depletion in human SKOV-3 ovarian cancer cells on the resistance towards other anticancer drugs with different mechanisms of action, doxorubicin (topoisomerase II inhibitor) and cisplatin (intra-DNA strand cross-linker) cytotoxicities were analyzed in the clonal derivative cell line RzB-8 compared to wildtype cells.

SKOV-3 cell lines with 100% (wildtype) and 12.5% (RzB-8) residual HER-2 expression levels were treated with doxorubicin and cisplatin at the concentrations indicated in the figure (Fig. 25) and numbers of living cells were determined after 3-5 days. In contrast to paclitaxel, cytotoxicities of doxorubicin or cisplatin were independent of cellular HER-2 levels in SKOV-3 cells as indicated by very similar dose-response curves for wildtype and RzB-8 cells (Fig. 25).
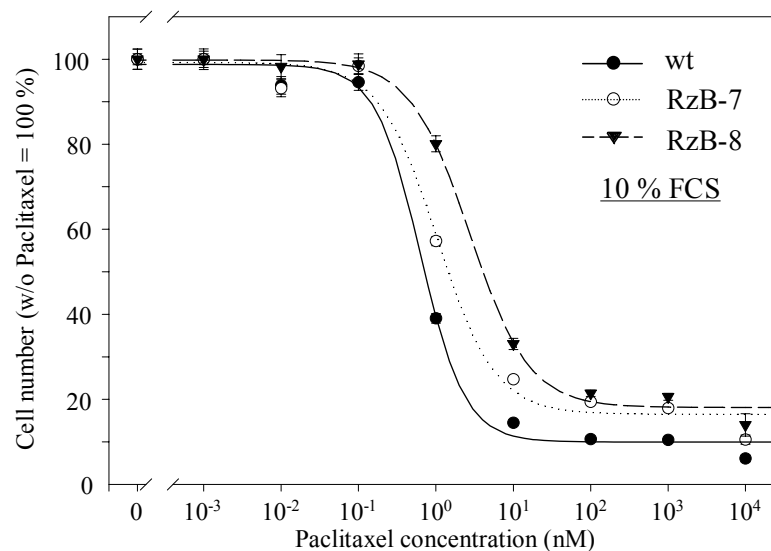
Cell line	HER-2 level (%)	IC$_{50}$ (nM)
wt	100.0	0.9
RzB-7	50.0	2.0
RzB-8	12.5	6.0
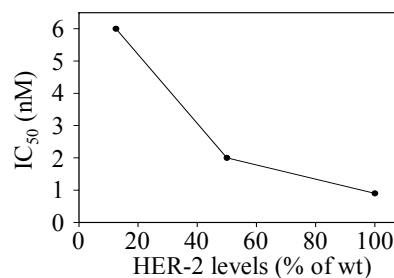
Fig. 24 **Effect of HER-2 expression levels on paclitaxel cytotoxicity in SKOV-3 ovarian carcinoma cells.** *SKOV-3 cell lines with different levels of residual HER-2 expression (see table) as determined by FACS analysis were analyzed for paclitaxel sensitivity. In proliferation assays, SKOV-3 wildtype cells were highly sensitive to paclitaxel treatment (upper panel, closed circles) while cell lines with decreased HER-2 expression levels displayed markedly reduced sensitivity (open circles and inverted triangles). Comparison of IC$_{50}$ values (see table) revealed a direct correlation between HER-2 expression levels and paclitaxel sensitivity (‚HER-2 gene dose effect‘, lower right).*
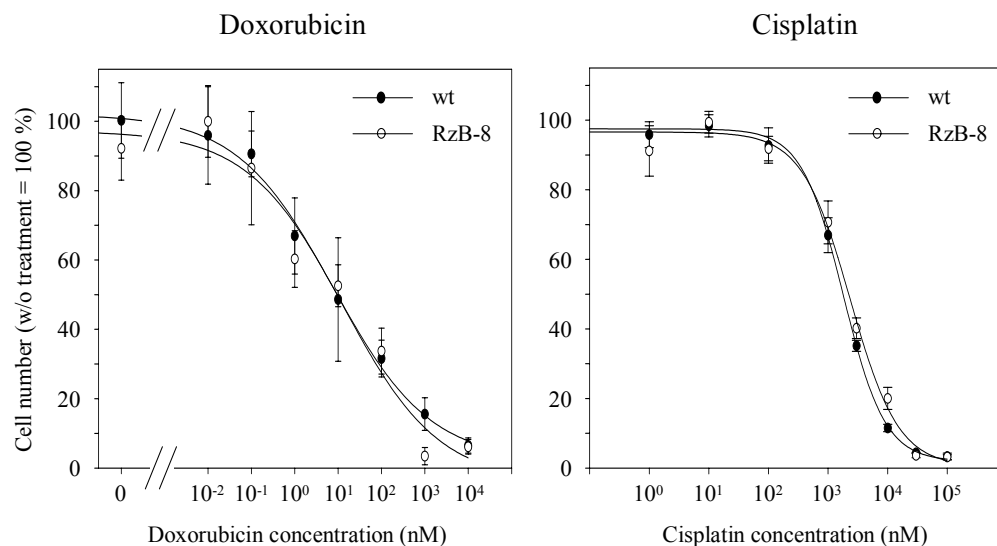
*Fig. 25 **Doxorubicin and cisplatin cytotoxicity is independent of HER-2 expression levels.***
SKOV-3 wildtype cells (with 100 % residual HER-2 expression level) and RzB-8 (with 12.5% residual HER-2
expression level) were treated with doxorubicin and cisplatin at the concentrations indicated. In proliferation
assays, SKOV-3 cell lines wt and RzB-8 showed comparable sensitivities towards doxorubicin (left) and
cisplatin (right).

4.3.6 Paclitaxel cytotoxicity is dependent on serum concentration

In previous studies, a decreased proliferation rate of Herceptin-treated SKOV-3 cells compared to control cells was demonstrated (see [243] for details). It was also shown that D-69491- and D-70166-treated cells (Fig. 21) as well as RzB-8 (Fig. 23) have a lower proliferation rate than control cells. Furthermore, a decreased paclitaxel sensitivity of SKOV-3 cells pretreated with Herceptin or D-69491- and D-70166 as well as of RzB-8 was observed. In all three cases, it seems that the proliferation rate of the cells play a role in paclitaxel sensitivity. To address the correlation between the proliferation rate and paclitaxel sensitivity in SKOV-3 cells, dose-response curve under various serum concentrations was analyzed.

The paclitaxel cytotoxicity on SKOV-3 cells was dependent on the FCS concentration. A ~20-fold or ~200-fold shift of the paclitaxel IC_{50} was observed in SKOV-3 wildtype cells upon the reduction of the FCS concentration from 10 % to 2 % or 0 %, respectively (Fig. 26).
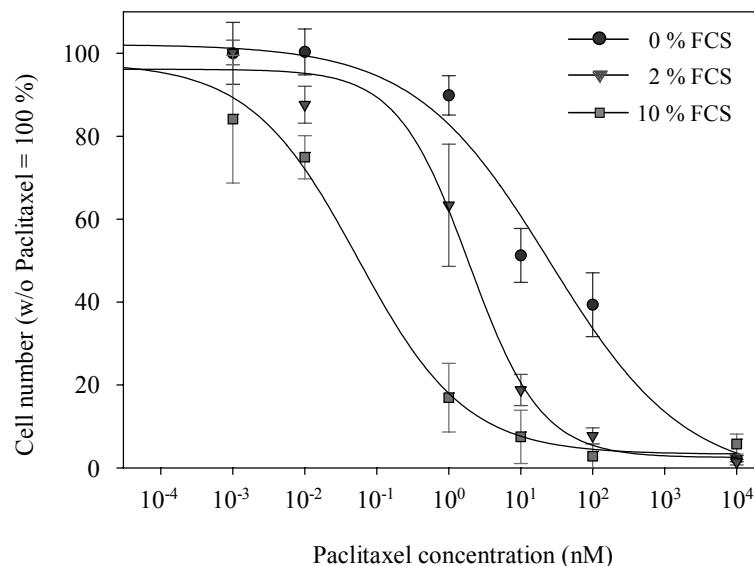
*Fig. 26 **Paclitaxel cytotoxicity in SKOV-3 ovarian carcinoma cells is dependent on the serum concentration.** Under different FCS concentrations, IC_{50} values of paclitaxel cytotoxicity on SKOV-3 wt cells varied. It shifted to ~20-fold (2 % FCS, inverted triangles) or ~200-fold (0 % FCS, circles) higher paclitaxel concentrations as compared to 10 % FCS (squares) indicating a direct correlation between FCS concentration and paclitaxel sensitivity.*

4.3.7 Activation of MAP kinases is dependent on HER-2 expression levels but does not change upon paclitaxel treatment

Because of the importance of mitogen-activated protein kinases (MAPKs) in signaling pathways as well as their implications in a wide array of physiological processes including cell growth, differentiation, and apoptosis, they were examined in the context of this thesis. The activation of the members of MAPK family (Erk1/Erk2, SAPK/JNK, p38) in SKOV-3 ovarian carcinoma cells and the dependence of these effects on HER-2 levels as well as possible changes in response to paclitaxel treatment were analyzed by Western blotting.

SKOV-3 wildtype and RzB-8 cells, which show the highest and the lowest HER-2 expressions levels, respectively, were cultivated for at least 24 h before the direct addition of paclitaxel and basal activity of all tested MAP kinases was detected by Western blotting already without paclitaxel treatment. While basal p42/44 activation was only ~70 % in RzB-8 as compared to wildtype cells, the phosphorylation of p38 and of SAPK/JNK was ~1.8-fold

and ~5-fold higher in ribozyme-transfected cells, respectively (Fig. 27). However, paclitaxel treatment, even at high concentrations (not shown), did not result in statistically significant changes in p42/44, SAPK/JNK or p38 phosphorylation in SKOV-3 wildtype or ribozyme-transfected cells (Fig. 27).
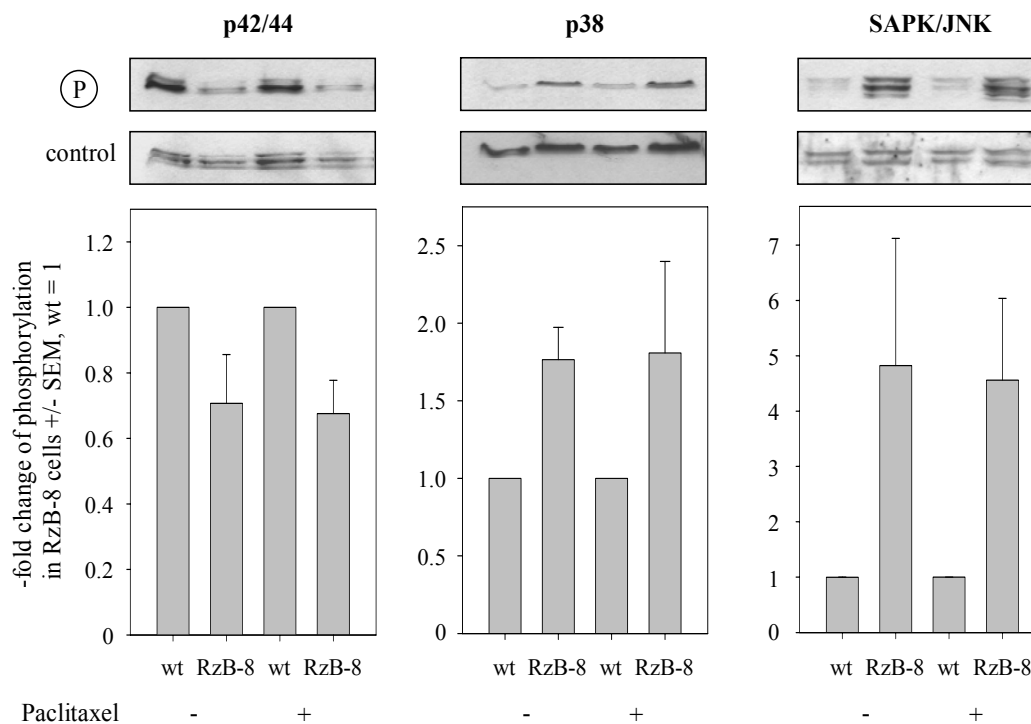
Fig. 27 **Activation of MAP kinases is dependent on HER-2 expression levels but does not change upon Paclitaxel treatment.**

By Western blotting, SKOV-3 cell lines with 100 % (wt) and 12.5 % (RzB-8) residual HER-2 expression levels were assayed for phosphorylated (upper panels) p42/44, p38 and SAPK/JNK after 24 h treatment with 1 nM paclitaxel. The bands detected by the antibodies against the respective unphosphorylated proteins (lower panels) served as loading control. Bars (mean +/- SEM) show the changes in the ratios of phosphorylated/unphosphorylated proteins upon ribozyme-mediated HER-2 deprivation with wt = 1, and represent at least three independent experiments.

4.3.8 Bcl-2 phosphorylation and hyperphosphorylation upon paclitaxel treatment is independent of HER-2 expression levels

Recently, it was reported that one of the proteins that undergoes phosphorylation in paclitaxel treated cells is bcl-2, which is related to apoptosis [264,269,310,311]. In further experiments, changes in bcl-2 in response to paclitaxel treatment of different SKOV-3 cells were studied. Here, SKOV-3 wildtype cells and RzB-8 were treated with 1 nM paclitaxel for 24 h, and phosphorylated and unphosphorylated bcl-2 protein in SKOV-3 wildtype and ribozyme-transfected cells was analyzed by Western blotting (Fig. 28). Paclitaxel treatment induced bcl-2 phosphorylation in both wildtype and RzB-8 cells, which was, however, independent of HER-2 expression levels (Fig. 28).
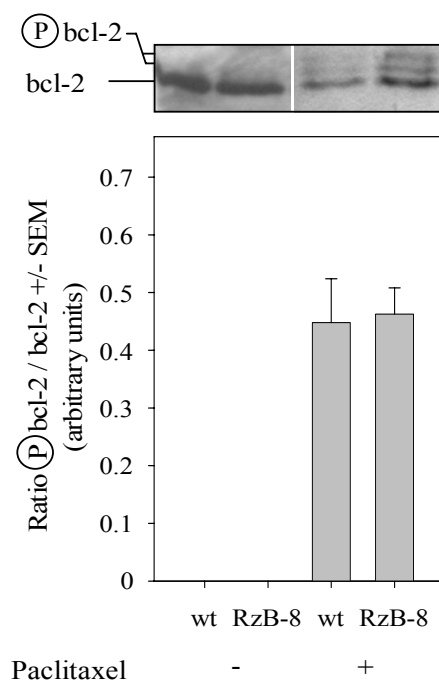
*Fig. 28 **Bcl-2 phosphorylation in SKOV-3 cells upon paclitaxel treatment is independent of HER-2 expression levels.***

By Western blotting, SKOV-3 cell lines with 100 % (wt) and 12.5 % (RzB-8) residual HER-2 expression levels were assayed for bcl-2 after 24 h treatment with 1 nM paclitaxel. The two middle and upper bands represent the phosphorylated and hyperphosphorylated bcl-2. Bars (mean +/- SEM) represent ratios of phosphorylated/unphosphorylated (lower band) bcl-2 in arbitrary units since in untreated SKOV-3 wt cells the phosphorylated bcl-2 was below the limit of detection. The data represent at least three independent experiments.

4.3.9 Paclitaxel utilizes a caspase-independent pathway of induction of apoptosis

The caspase family of cysteine proteases play a key role in apoptosis and inflammation [312]. They are synthesized as inactive proenzymes that are processed in cells undergoing apoptosis by self-proteolysis and/or cleavage by another protease. The processed forms consist of large and small subunits which associate to form an active enzyme. The activation of caspase-3 and caspase-7, which represent effector caspases of two main pathways of induction of apoptosis, upon paclitaxel treatment and its dependence on HER-2 levels was examined. After 24 h treatment with 1 nM paclitaxel, procaspase-7 and -3 expression levels were assayed. Procaspase-7 levels were higher in HER-2-depleted cells compared to wildtype cells and no caspase-7 activation or changes in procaspase-7 levels upon paclitaxel treatment were observed (Fig. 29). Levels of procaspase-3 were similar in SKOV-3 wildtype and ribozyme-transfected cells and similar to caspase-7, no caspase-3 activation was seen (not shown).
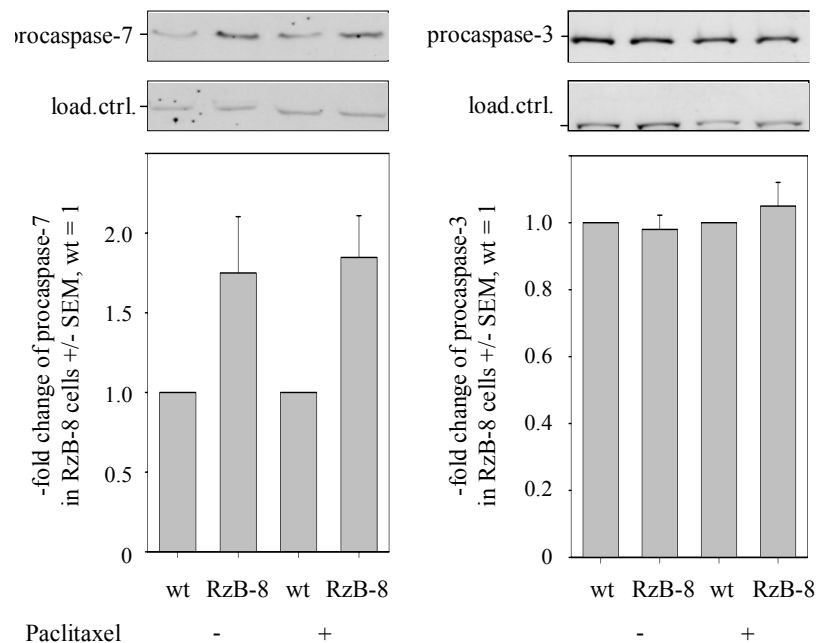
Fig. 29 **Paclitaxel-mediated apoptosis is independent of caspase-7 and -3 in SKOV-3 cells.**
By Western blotting, SKOV-3 cell lines with 100 % (wt) and 12.5 % (RzB-8) residual HER-2 expression levels were assayed for procaspase-7 and procaspase-3 after 24 h treatment with 1 nM paclitaxel. Bars (mean +/- SEM) show the changes in the ratios of procaspase-7 or procaspase-3 (upper band)/loading control (lower band) upon ribozyme-mediated HER-2 deprivation with wt = 1, and represent at least three independent experiments.

4.4 Effects of riboyzme-mediated HER-2 downregulation on rViscumin sensitivity in SKOV-3 cells and its underlying cellular events

4.4.1 Ribozyme-mediated HER-2 depletion leads to increased resistance towards rViscumin

Similar to the effects of Herceptin on paclitaxel sensitivity in SKOV-3 cells, it was observed that upon Herceptin treatment, the cellular rViscumin resistance was markedly increased in SKOV-3 ovarian carcinoma cells (see [313] for details).

To confirm that the effect of ribozyme-mediated HER-2 depletion on SKOV-3 sensitivity towards rViscumin is identical to the Herceptin effect, the sensitivity of SKOV-3 cell lines with various levels of residual HER-2 expression (wildtype, RzB-3, RzB-7, and RzB-8) towards rViscumin was examined in the context of this thesis. Different SKOV-3 cell lines were treated with rViscumin at the concentrations indicated (Fig. 30) and numbers of living cells were measured after 3-5 days. From dose response curves, IC_{50} values for different SKOV-3 cells were evaluated. Interestingly, a ribozyme-mediated >50 % reduction of HER-2 expression significantly shifted the dose-response curves to the right (Fig. 30, left) with a maximum shift in the case of the RzB-8 cells ($IC_{50} = 6.1 \times 10^{-4}$ µg/ml). More strikingly, when comparing the different clonal cell lines with different residual HER-2 levels, a direct correlation between HER-2 expression levels and rViscumin sensitivity was observed: >50 % reduction of HER-2 expression led to decreased sensitivity of SKOV-3 ovarian carcinoma cells (Fig. 30, right and table). Hence, these experiments using HER-2 ribozyme-targeting confirm the data on the changes of rViscumin sensitivity upon Herceptin treatment.
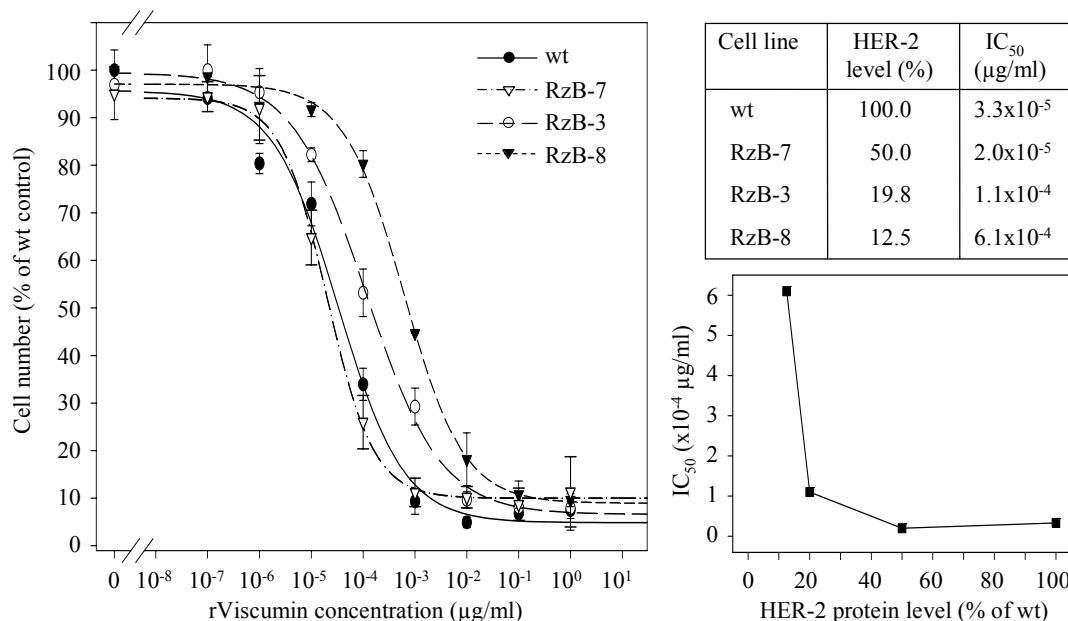
Fig. 30 **Effect of HER-2 expression levels on rViscumin cytotoxicity in SKOV-3 ovarian carcinoma cells.**
SKOV-3 cell lines with various levels of residual HER-2 expression were analyzed by growth assay in presence
of rViscumin at concentrations indicated in the figure. SKOV-3 cells with high HER-2 expression levels (wt and
RzB-7) were highly sensitive to rViscumin treatment (closed circles and open inverted triangles) while cell lines
with >50 % decreased HER-2 expression levels (RzB-3 and RzB-8) displayed markedly reduced sensitivity
(open circles and inverted triangles). Comparison of IC$_{50}$ values (table, upper right) revealed a direct
correlation between HER-2 expression levels and rViscumin sensitivity (‚HER-2 gene dose effect‘, lower right).

4.4.2 rViscumin binding and uptake is independent of HER-2 levels

Binding of rViscumin to tumor cells as well as its cellular uptake is conferred through
interactions of the B-chain of rViscumin with 'viscumin receptor' gangliosides of the
neolacto series on the surface of tumor cells [288,289]. To address the question if the
observed HER-2 dependence of rViscumin cytotoxicity is only a result of differential
rViscumin binding and uptake, SKOV-3 wildtype and various stable isogenic SKOV-3 cell
lines with ribozyme-mediated reduction of HER-2 expression levels were incubated with
[^{125}I]-labeled rViscumin, and at different time points the internalized [^{125}I]-rViscumin was
determined. The comparison between SKOV-3 wildtype and HER-2 depleted cells revealed
no differences in [^{125}I]-rViscumin binding and internalization over the whole time range
indicating that this process is independent of cellular HER-2 levels (Fig. 31).
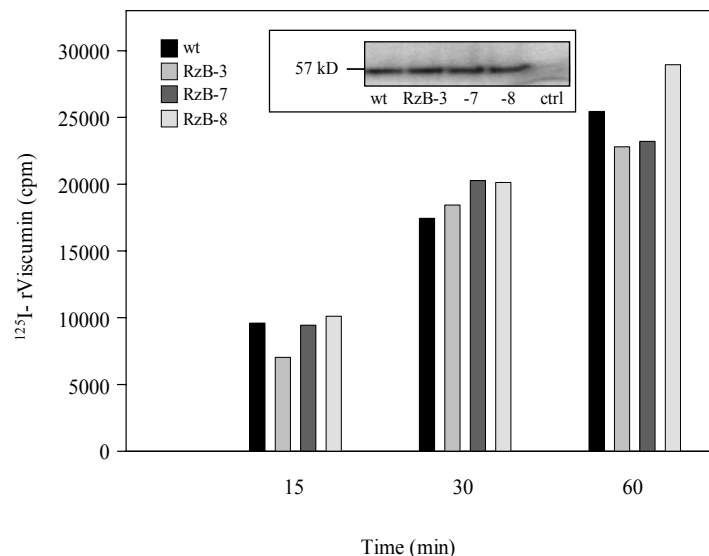
*Fig. 31 **rViscumin binding and uptake is independent of HER-2 levels in SKOV-3 cells.***
SKOV-3 wildtype and HER-2 depleted cells were incubated with [^{125}I]-labeled rViscumin and at different time points analyzed for internalized [^{125}I]-rViscumin. rViscumin uptake was linear for at least 60 min and no differences in [^{125}I]-rViscumin binding and internalization between the different cell lines were observed. SDS gel electrophoresis of cell lysates revealed a single radioactive band at the expected size confirming the integrity of the bound and internalized [^{125}I]-rViscumin (inset). Control: equally treated well without cells.

To confirm the integrity of the bound and internalized [^{125}I]-rViscumin, cell lysates were analysed by SDS gel electrophoresis and autoradiography revealed a single radioactive band at the expected size which was absent in equally treated wells without cells (Fig. 31, inset). Quantitation of the bands by densitometry after 30 min and 60 min again demonstrated the absence of differences between the cells, and the comparison between different time points confirmed for all four cell lines the equally linear uptake kinetics of [^{125}I]-rViscumin. From these experiments, it was concluded that rViscumin binding and uptake is independent of HER-2 levels and therefore is not responsible for the observed HER-2 dependence of rViscumin cytotoxicity in SKOV-3 cells.

4.4.3 Activation of members of the MAPK family upon rViscumin treatment under serumfree conditions or in the presence of 10% FCS

To further elucidate the effects of rViscumin on molecular levels, the activation of the members of the mitogen-activated protein kinase (MAPK) family, Erk1/2, SAPK/JNK and p38 MAPK, upon rViscumin treatment was examined in SKOV-3 wildtype and RzB-8 cells grown under serumfree conditions or in the presence of 10% FCS. Cells were incubated 24 h with rViscumin at concentrations indicated in the figure (Fig. 32). In these experiments, differences between SKOV-3 wildtype and ribozyme-transfected cells were seen in the basal activation of all three signaling pathways as well as in the rViscumin-mediated response. Kinases Erk1/Erk2 in SKOV-3 wildtype cells grown in serum-containing media were activated by rViscumin in a dose-dependent manner (Fig. 32 a). In contrast, in HER-2-depleted cells the basal level of Erk1/Erk2 phosphorylation was somewhat lower and no Erk1/Erk2 activation upon rViscumin treatment was observed even upon treatment with high doses of rViscumin (Fig. 32 a). Under serumfree conditions, in both cell lines basal levels of activated Erk1/Erk2 were similar and rViscumin-induced activation was stronger in SKOV-3 wildtype cells as compared to ribozyme-transfected cells (Fig. 32 b). Since here and in other experiments toxic effects of rViscumin under serumfree conditions were observed already at 5 ng/ml, no higher concentrations were used and decreased Erk1/Erk2 activation in wildtype cells treated with 5ng/ml rViscumin may be due to cell death. SAPK/JNK was activated by rViscumin in a dose-dependent manner in both wildtype and ribozyme-transfected SKOV-3 cells grown in serum-contatining media. However, in wildtype cells levels of phosphorylated SAPK/JNK were always lower as compared to ribozyme-transfected cells (Fig. 32 c). Under serumfree conditions, rViscumin activated SAPK/JNK in a dose-dependent manner while SAPK/JNK phosphorylation in ribozyme-transfected cells reached maximum levels already at 1 ng/ml rViscumin and was again always higher than in wildtype cells (Fig. 32 d). Basal levels of activated SAPK/JNK without rViscumin treatment were below the limit of detection in both cell lines. Finally, for p38 activation results very comparable to SAPK/JNK were obtained (Fig. 32 e). In cells grown in the presence of serum, again an rViscumin dose-dependent activation was observed in both cell lines with signals in wildtype cells always being below levels in ribozyme-transfected cells. Under serumfree conditions, in both cell lines basal levels of p38 were below the limit of detection and maximum p38 phosphorylation was observed already at very low rViscumin concentrations with again ribozyme-transfected cells displaying higher activation (Fig. 32 f)
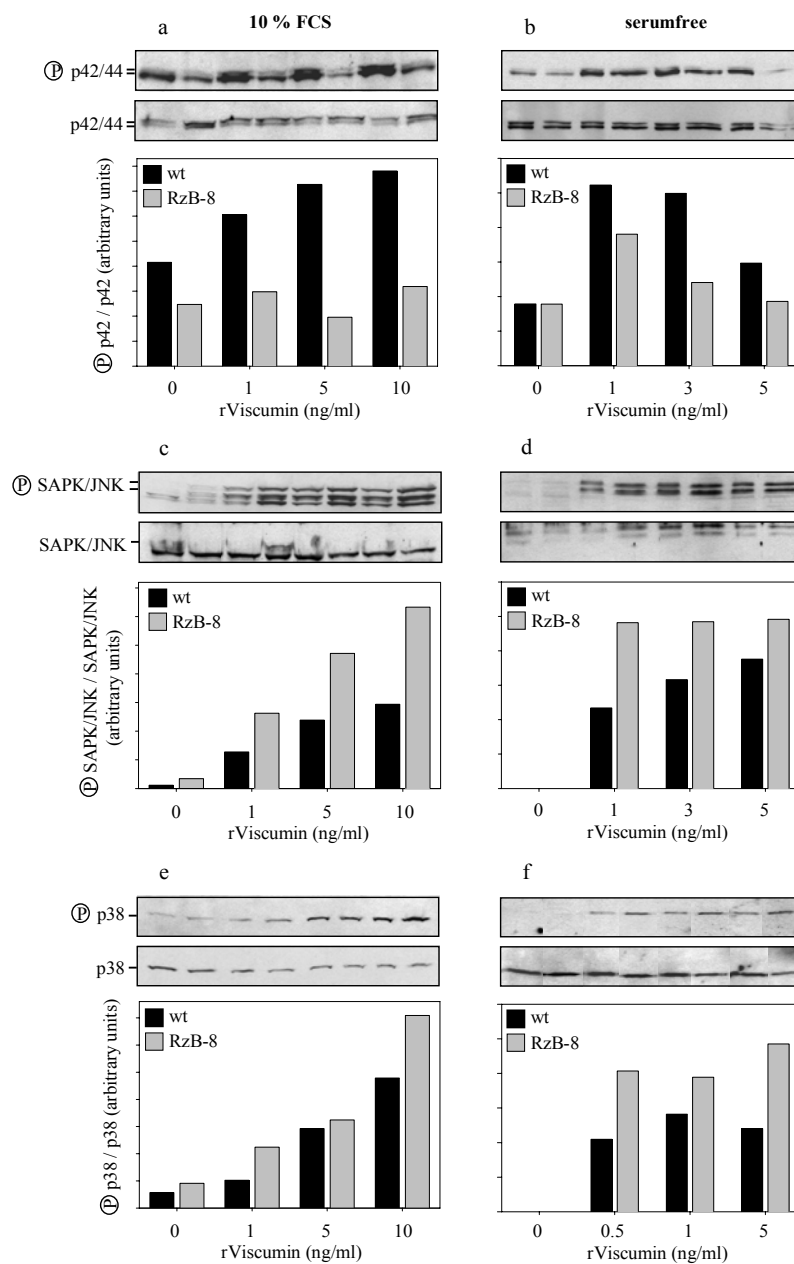
*Fig. 32 **rViscumin activates MAPK signaling pathways dependent on HER-2 expression levels and rViscumin concentrations.***

One representative set of data out of 3 - 6 independent experiments is shown. SKOV-3 wildtype (black bars) and ribozyme-transfected cells (RzB-8, grey bars) were treated for 24 h with rViscumin at the concentrations indicated under 10% FCS (left) or serumfree (right) conditions. Activation of p42/44 (Erk1/Erk2), SAPK/JNK and p38 was determined in Western blots using antibodies specific for phosphorylated proteins (upper panels). For loading control, Western blots were probed with antibodies recognizing the unphosphorylated proteins (lower panels). Bands were quantitated by densitometry and bar graphs represent the ratio upper/lower bands in arbitrary units.

4.4.4 rViscumin-mediated bcl-2 downregulation is dependent on HER-2 levels

   To analyze the effects of rViscumin on molecules related to apoptosis, the changes of bcl-2 upon rViscumin treatment of different SKOV-3 were examined by Western blotting. In contrast to paclitaxel, treatment with 10 ng/ml rViscumin did not lead to phosphorylation of bcl-2, but resulted in a marked, time-dependent down-regulation of the anti-apoptotic molecule bcl-2. Probably due to the limited sensitivity of the bcl-2 Western blot, this effect was not observed at 1 ng/ml rViscumin. In ribozyme-transfected cells, basal bcl-2 levels were comparable but upon rViscumin treatment the decrease was less profound (Fig. 33).
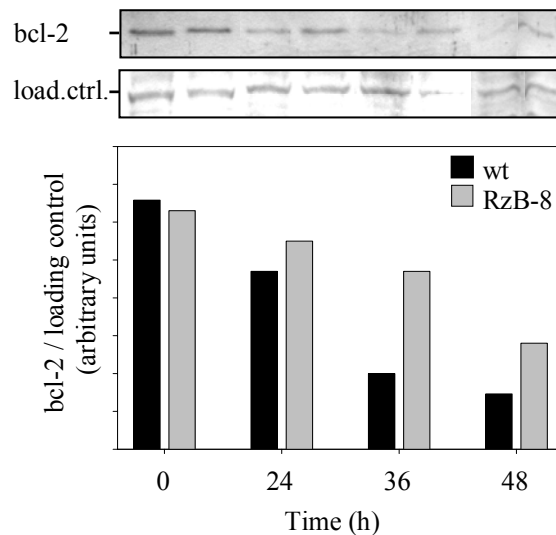
*Fig. 33 **rViscumin-mediated bcl-2 downregulation is dependent on HER-2 expression levels in SKOV-3 cells.** One representative set of data out of 3 - 6 independent experiments is shown. SKOV-3 wildtype (black bars) and ribozyme-transfected cells (RzB-8, grey bars) were treated with 10 ng/ml rViscumin for the time points indicated in the figure. Expression of bcl-2 was determined by Western blotting using specific antibodies (upper panels) and normalized for equal loading (lower panels). Bands were quantitated by densitometry and bar graphs represent the ratio upper/lower bands in arbitrary units.*

4.4.5 Caspase-3 and -7 are not involved in rViscumin-induced apoptosis

To further study the molecular basis of rViscumin-mediated induction of apoptosis in SKOV-3 cells, caspases-3 and -7 were chosen since their activation is the earliest cellular event to integrate the different apoptotic signals. SKOV-3 wildtype and RzB-8 cell lines were treated with 1 ng/ml rViscumin for the time intervals indicated in the figure (Fig. 34) and expression of procaspase-3 and -7 was determined by Western blotting. Treatment of SKOV-3 wildtype cells with 10 ng/ml rViscumin did not result in the activation of caspase-7 or caspase-3 (not shown). While, procaspase-7 expression levels were higher in HER-2-depleted cells compared to wildtype cells, levels of procaspase-3 were similar in SKOV-3 wildtype and ribozyme-transfected cells.
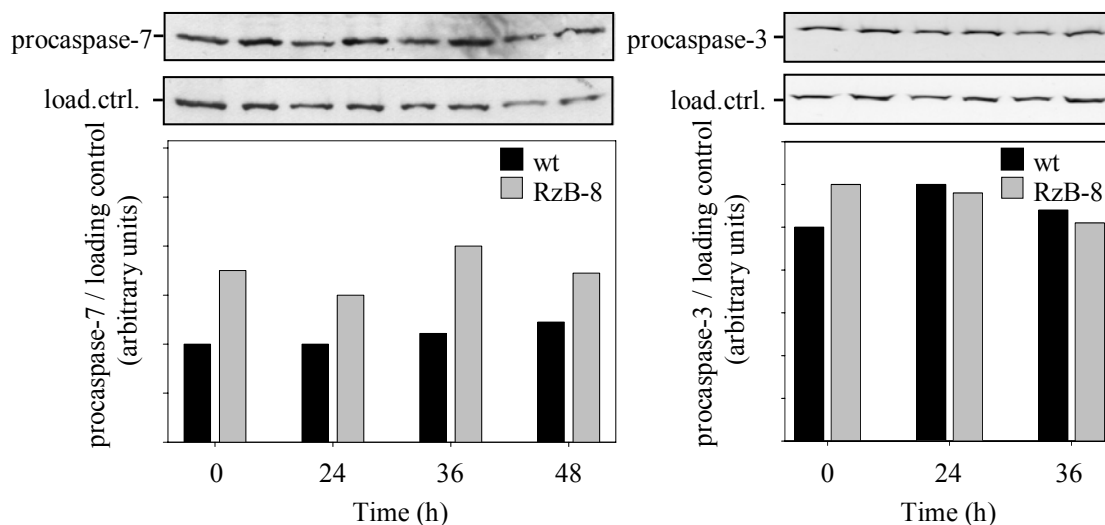
Fig. 34 **rViscumin induces apoptosis independent of caspase-7 and -3 in SKOV-3 cells.**

One representative set of data out of 3 - 6 independent experiments is shown. SKOV-3 wildtype (black bars) and ribozyme-transfected cells (RzB-8, grey bars) were treated with 10 ng/ml rViscumin for the time points indicated. Expression of procaspase-7 and -3 was determined by Westeren blotting using specific antibodies (upper panels) and normalized for equal loading (lower panels). Bands were quantitated by densitometry and bar graphs represent the ratio upper/lower bands in arbitrary units.

5 DISCUSSION

The most lethal type of gynecological cancer in the Western world are ovarian carcinomas [295]. Most ovarian cancer patients present with advanced stage disease, and the overall 5-year survival for these women is less than 30% [314,315]. Although new therapeutic approaches have been developed, these survival statistics have remained largely unchanged for many years. Clearly, there is a need for better understanding of the molecular pathogenesis of ovarian carcinoma in order to identify new biomarkers, which facilitate early detection, and new drug targets that will allow the development of more effective anti-cancer drugs.

The overexpression of a number of oncogenes and growth factors play important roles in the development of ovarian cancer. The main focus of this thesis lies on the analysis of the expression status and cellular functions of two gene products in ovarian carcinomas: the fibroblast growth factor-binding protein (FGF-BP) and human epidermal growth factor receptor-2 (HER-2). While no data are available on the expression status of FGF-BP in ovarian carcinomas, several studies have demonstrated that HER-2 is overexpressed in approximately 20-30% of ovarian carcinomas and that overexpression is significantly correlated with clinical outcome.

Previous studies have investigated the response to and expression of FGF-2 in a variety of ovarian cancer cell lines. An increase in cell proliferation and FGF-2 mRNA expression was observed in several cell lines in response to FGF-2 [316]. Levels of FGF-2 mRNA are also significantly higher in the ovarian tumors in patients with stage III and IV ovarian cancer when compared with normal ovaries [317]. Most recently, it was found that the entire FGF-2 cell surface signaling apparatus (FGF-2, biologically active heparan sulphate, and FGFRs) is present in the ovarian cancer endothelium [318]. These data and other reports describing the activation of extracellular FGF-2 by FGF-BP in different cell lines [88,91], FGF-BP overexpression in some tumors [89,90] as well as the broad similarities in the localization of FGF-2 and FGF-BP in several tissues, e.g. during mouse embryo development [98] led to the analysis of the expression of FGF-BP in normal ovaries and in malignant epithelial carcinomas.

In the context of this thesis, an immunohistochemical approach based on tissue microarrays stained with a monoclonal anti-human FGF-BP (anti-FGF-BP) antibody specific for human FGF-BP was used to determine the expression of FGF-BP in normal ovaries and ovarian carcinomas. The staining pattern of FGF-BP in all different ovarian tissues was heterogeneous, with different staining intensities. While the FGF-BP expression in normal ovarian tissues was negative (0) or weak (1), the FGF-BP IHC staining in ovarian carcinomas ranged from weak (1) to strong (4). This heterogeneity of FGF-BP staining in all different tissues required to set a cutoff in order to distinguish between normal and overexpression of FGF-BP. Hence, staining intensities 0-2 were interpreted as normal expression of FGF-BP, while values 3-4 were considered as overexpression. Although no tissues of normal ovaries showed the value 2, it was considered as normal expression of FGF-BP to produce reliable results regarding the overexpression of FGF-BP in ovarian carcinoma. Using this rating with interpretation of value 2 as normal FGF-BP expression, however, rather underestimates the percentage of FGF-BP-overexpressing ovarian carcinoma tissues.

Ovarian carcinoma is a morphologically and biologically heterogeneous disease, and this fact has likely contributed to difficulties in defining the molecular alterations associated with its development and progression. On the basis of morphological criteria, there are four major types of primary ovarian adenocarcinomas (serous, mucinous, endometrioid, and clear cell). Although various histological types of ovarian carcinoma presumably originate from the ovarian surface epithelium or related cell types such as endometriosis, some studies support the notion that these different histological types of ovarian carcinomas likely represent distinct disease entities (reviewed by [319,320]). In the TMA used in this thesis it was impossible to study the expression of FGF-BP in correlation to different subtypes of ovarian carcinomas since the majority of ovarian carcinoma tissues was indistinguishable regarding the histological type (data not shown). Furthermore, a putatively mixed histology with various subtypes of ovarian carcinoma in one tissue section was observed and data about tumor stage and grade were not available. Therefore, in this thesis the main focus was the comparison between the expression status of FGF-BP in normal ovarian tissues versus ovarian carcinoma tissues.

Generally, the data in this thesis provide evidence that FGF-BP is upregulated in ovarian carcinomas compared to normal ovarian tissues. This provides an excellent starting point for the further investigation of the expression status of FGF-BP in different histological subtypes

of ovarian carcinoma as well as the regulation of FGF-BP in different tumor stages of ovarian cancer.

Several previous studies described only the role of FGF-BP in the extracellular activation of FGF-2 and showed partly contradictory or incomplete data on the mechanism of action of FGF-BP. To gain further insight into the molecular mechanism of action of FGF-BP, its subcellular localization, cellular functions and effects resulting from the interaction of FGF-BP with FGF-2 were studied in greater detail in this thesis by means of confocal laser scanning microscopy and soft agar assays.

The advantage of the green fluorescent protein and its spectral variants cyan (CFP) and yellow (YFP) lies in its ability to act as an N- or C-terminal protein tag. These fluorescent proteins as well as the fusion partner usually retain their functions, and depending on the nature of the fusion partner, GFP-related proteins can be directed specifically to different intracellular compartments. In this thesis, the advantage of this fusion with GFP and its related proteins was taken, which has been proven to be a useful tag for monitoring the subcellular distribution and trafficking of various proteins in living cells [321,322]. Hence, expression vectors for full length as well as various N- or C-terminally truncated FGF-BP mutants were constructed by fusing CFP to the C-terminus. It should be noted that the presence of the N-terminal signal peptide in all N-terminally truncated FGF-BP constructs was retained and guaranteed the analysis of the role of the N-terminal signal peptide in secretion and interaction of various mutants with FGF-2. Thus, the generation of misleading results due to the absence of this signal peptide in some truncated mutants was excluded.

FGF-BP is a soluble secreted protein with an N-terminal signal peptide [32] that promotes co- or post-translational import into the endoplasmic reticulum (ER) [323,324]. Once translocated into the lumen of the ER, secretory proteins are delivered to the cell surface by vesicular transport [325-329]. Transport along the pathway between the endoplasmic reticulum and the Golgi apparatus occurs via an intermediate compartment called ER-Golgi intermediate compartment (ERGIC). The type I transmembrane protein ERGIC-53 is ubiquitously expressed and constitutively cycles between ER and ER-Golgi intermediate compartment (ERGIC) [330]. In the ERGIC the protein segregates from anterograde-directed protein traffic and returns to the ER largely bypassing the Golgi apparatus [331]. The localization of ERGIC, which is described as the first post-ER

compartment in which anterograde (to the Golgi) and retrograde (to the ER) traffic separates, suggests protein sorting as a major function of ERGIC. In this thesis, it was shown for the first time that FGF-BP localizes primarily in cytoplasm and to ERGIC, indicating that FGF-BP is secreted by a pathway employing ERGIC.

For the further analysis of the subcellular colocalization of FGF-BP constructs and FGF-2, and to study the biological significance of the interaction of various FGF-BP mutants with FGF-2, two cell lines were chosen: the normal cell line COS-7 and the adrenal carcinoma cell line SW-13. Due to the lack of FGF-BP expression in both cell lines (see Fig. 16 a and [88]), COS-7 and SW-13 cells appeared to be a good model to study the biological functions and relevance of the interaction of FGF-BP mutants with FGF-2.

One of the best characterized binding partners of FGF-BP is FGF-2. As described in greater detail in the introduction, five isoforms of FGF-2, with molecular weights of 18, 22, 22.5, 24 and 34 kDa, have been identified, all derived from a single messenger RNA (reviewed in [66]). It has been reported that the 18 kDa FGF-2 is primarily a cytosolic protein without a signal sequence [68,332,333]. This protein is exported out of the cells by an unknown mechanism and stored in the ECM. In contrast, the high molecular weight (HMW) isoforms are predominantly located in the nucleus [68,334,335]. It has been shown that NH2-terminal sequences are required for nuclei localization [66,336-338]. Based on these available data on the cytoplasmic localization of 18 kDa FGF-2 and on previous data regarding the activation of extracellular FGF-2 by FGF-BP as well as based on the observed cytoplasmic distribution of FGF-BP in SKOV-3 and COS-7 cells, 18 kDa FGF-2 was chosen to analyze the subcellular colocalization and interaction of FGF-BP constructs with FGF-2.

Surprisingly, the data in this thesis demonstrated that the expressed 18 kDa FGF-2 is primarily localized in the nucleus and clearly enriched in nuclei of COS-7 cells, while fluorescence of the fusion protein (FGF-2-YFP) in the cytoplasm was observed only to some minor extent. Since YFP does not contain any known nuclear localization sequence (NLS) and YFP or CFP alone demonstrates a faint nuclear and cytoplasmic fluorescence (not shown), the nuclear localization of the fusion protein represents a property of FGF-2 rather than a property of YFP. Recently and in agreement with these results, it was shown by confocal microscopy that the nucleus and the cytoplasm are positive for the 18 kDa FGF-2 expressed as FGF-GFP fusion protein in CHO cells [339]. Furthermore, corneal endothelial

cells (CEC) accumulate the 18 kDa in the nucleus during the early stage of cell growth [340] and the expressed 18 kDa FGF-2 was directly translocated from the cytoplasmatic synthetic site to the nucleus [341]. Others reported that exogenous 18 kDa FGF-2 is internalized via high and low-affinity FGF receptors [342-344], and that it is translocated to the nucleus [345]. Taken together, the solely subcellular localization of 18 kDa FGF-2 in the cytoplasm and extracellular matrix (ECM) may not be accepted as a general rule.

Since the mechanism of release of the 18 kDa FGF-2 which lacks a signal peptide for secretion remains to be elucidated, it is unknown whether the 18 kDa FGF-2 is translocated after synthesis directly from cytoplasm to the nucleus or whether it is secreted first, internalized later and subsequently translocated to the nuclei. The nuclear localization of the 18 kDa FGF-2 suggests that the intracellular 18 kDa FGF-2 can be targeted to the nucleus via NLS-independent pathways. Alternatively, the existence of another NLS in FGF-2 located within the 18 kDa FGF-2 may be responsible for the nuclear localization of 18 kDa FGF-2. The last suggestion may explain why the mutagenesis of individual putative nuclear localization domains in FGF-1 and FGF-2 has not always prevented nuclear localization [346,347].

Interestingly, upon coexpression with FGF-2 the cytoplasmic FGF-BP was translocated into the nucleus of COS-7 cells. In further experiments, the nuclear colocalization of FGF-2 and FGF-BP was confirmed, suggesting an intracellular function of FGF-BP based on its interaction with 18 kDa FGF-2 in the nucleus.

To confirm the dependence of nuclear translocation of FGF-BP on FGF-2, the subcellular localization of FGF-BP was examined in SW-13 cells, which already express high levels of endogenous FGF-2. FGF-BP was concentrated in the nucleus of SW-13 cells and showed a similar nuclear localization to FGF-2.

The data presented in this thesis on the translocation of FGF-BP into the nucleus as well as the dependence of the cellular uptake of exogenous [125I]-labeled FGF-BP on FGF-2 suggest the uptake of secreted or exogenously added FGF-BP into the cells and its dependence on the interaction with FGF-2. This was confirmed by confocal microscopy of COS-7 cells, which were transiently transfected with an FGF-2-YFP expression vector and incubated with recombinant FGF-BP. These data indicated the internalization of FGF-BP,

which may follow and depend on the binding of FGF-BP to FGF-2, by a pathway that allows its uptake into the cytoplasm and subsequent translocation to the nucleus. While, the observation of the uptake and nuclear localization of FGF-BP and their dependence on FGF-2 suggest that both processes can occur in a ligand-dependent manner, it is unknown if FGF-BP was internalized as a complex with FGF-2 and/or with other molecules and translocated in the nucleus. Furthermore, in the case of endogenous coexpression of FGF-BP and FGF-2 it cannot be excluded that FGF-BP interacts with FGF-2 in the cytoplasm prior to its secretion, and that it is only then translocated into the nucleus.

The colocalization data of FGF-BP with ERGIC suggest that the secreted FGF-BP is transported in a direction passing from the endoplasmic reticulum to the Golgi apparatus and then to the cell surface. Recently, it is becoming clear that proteins can move in the opposite direction in a process termed retrograde transport, eventually ending up in the cytoplasm (for reviews, see [348,349]. Although this pathway is poorly understood, it provides a possibility for the translocation of secreted FGF-BP from endoplasmic reticulum into the cytosol, where the interaction with FGF-2 may take place and may result in the translocation of FGF-BP into the nucleus.

Probably, the majority of intracellular molecules that interact with endogenous 18 kDa FGF-2 is still unkown. Recently, Bossard et al. [350] showed that a cytoplasmic protein called Translokin interacts specifically with the 18 kDa FGF-2 and is involved in the intracellular trafficking of the internalized growth factor. In addition, using the radiation inactivation method Prats et al. [351] reported that FGF-2 is present in the nucleus in two complexes: HMW FGF-2 in a complex of 320 kDa and 18 kDa FGF-2 in a complex of 130 kDa. In agreement with these results, it was also shown that the various isoforms of FGF-2 exist as relatively large protein complexes with one or more protein species, which was confirmed by immunoprecipitation assay [352]. These results indicate that intracellular FGF-2 may associate with other molecules. The observed nuclear translocation of FGF-BP upon coexpression with FGF-2 as well as the nuclear colocalization of both proteins suggest that FGF-BP is one of the molecules that interact with intracellular FGF-2 and may play a role in the intracellular trafficking pathways of FGF-2 and hence in the modulation of its biological activity.

Data on the FGF-binding site of FGF-BP are still lacking. Using various C- and N-terminally truncated FGF-BP mutants, the segment(s) of FGF-BP, which are responsible for the interaction with FGF-2 and the nuclear translocation, were explored. Confocal microscopy revealed that the nuclear colocalization and interaction of FGF-BP with FGF-2 is lost upon the N-terminal truncation of FGF-BP. These data demonstrated for the first time the importance of the N-terminal segment of FGF-BP in the interaction with FGF-2.

Anchorage-independent growth assay correlates strongly with tumorigenicity and invasiveness in several cell types, e.g. small-cell lung carcinoma [353]. For this reason soft agar assays were performed using SW-13 and COS-7 cells stably transfected with various FGF-BP constructs to analyze the biological significance of the interaction of full length and various truncated FGF-BP mutants with FGF-2. As expected, stimulating effects of full length FGF-BP on the colony formation of SW-13 cells were observed. The similar effects have been demonstrated in previous studies [88,93]. Furthermore, through the blocking of colony formation of FGF-BP-transfected SW-13 cells by a specific antibody against FGF-2 it was demonstrated that the tumorgenic potential of FGF-BP is FGF-2-dependent [88]. These previous studies provide indirect evidence that FGF-BP can stimulate tumor growth by releasing and activating endogenous FGF-2 from the extracellular matrix (ECM). Based on the confocal microscopy data regarding the nuclear localization of FGF-BP in SW-13 cells, an intracellular mechanism of the stimulating function of FGF-BP based on its interaction with nuclear FGF-2 cannot be excluded. This suggestion is supported by the loss of FGF-BP-mediated colony formation of SW-13 cells upon stable transfection with N-terminal truncated FGF-BP constructs (BP-C-91 and BP-C-146), which in confocal microscopy did not show nuclear colocalization and interaction with FGF-2.

Previously, it was shown that the recombinant FGF-BP displays bioactivity in terms of induction of tumor cell proliferation. Upon exogenous addition of recombinant FGF-BP, a dose-dependent stimulation of colony formation of SW-13 cells in soft agar was seen [130]. Based on the fact that two different neutralizing anti-FGF-2 antibodies added to the cells in soft agar reversed the stimulating effect of FGF-BP it was suggested that the recombinant FGF-BP is highly unlikely internalized by the cells and the mechanism of FGF-BP action seems to be confined to the extracellular matrix. The data of nuclear localization of FGF-BP in SW-13 cells as well as the cellular uptake of [^{125}I]-labeled FGF-BP in SW-13 (data not shown) or in COS-7 cells suggest another mechanism of FGF-BP-action relying on the

internalization of FGF-BP and subsequent cellular stimulation through intracellular mechanism(s) seems possible. Furthermore, the inhibition of stimulating effects of FGF-BP on colony formation of SW-13 cells in soft agar after exogenous addition of two different neutralizing anti-FGF-2 antibodies indicate that the internalization of FGF-BP seems to be dependent on the interaction with FGF-2 in the extracellular matrix.

To explore the biological functions of FGF-BP and various mutants, COS-7 cells were used as another model system in this thesis. Surprisingly, inhibitory rather than stimulating effects were shown in soft agar assays with COS-7 cells stably transfected with full length FGF-BP. In agreement with this, Chen et al. [133] showed that FGF-BP at high medium concentrations inhibits DNA synthesis and cell growth in mouse fibroblast 3T3 cells. Based on the previously described data on the role of FGF-BP-binding to FGF-1 and FGF-2 in inhibiting their biological activities, they suggested that the inhibitory effects are probably due to the formation of FGF-BP/FGF complexes leading to the reduction of free FGF-1 and FGF-2 concentrations hence leading to insufficient stimulation of DNA synthesis and cell growth in these cells. These data and the results of this thesis regarding the cytoplasmic localization of FGF-BP in COS-7 cells indicate that FGF-BP may play specific physiological roles in addition to its function as extracellular carrier protein.

The FGF-BP-mediated inhibition of the growth of COS-7 cells in soft agar was lost upon C- and N-terminal truncations of FGF-BP, indicating that the complete sequence of full length FGF-BP is required to exert its inhibitory function. Furthermore, it is noteworthy that the inhibitory effects were not seen by the transient transfection with an FGF-BP expression vector or by exogenous addition of FGF-BP on COS-7 wild-type cells in soft agar. This difference in the effects could be explained by the short time and level of FGF-BP expression in transient transfection or by decreased stability in case of exogenous addition of FGF-BP, which is probably not sufficient to inhibit the cell growth in soft agar as seen in the stable transfection with the FGF-BP expression vector.

To examine the consequences of the nuclear interaction of FGF-BP and FGF-2 on the cell proliferation of COS-7 cells, the expression of the FGFR1 receptor as well as the stimulating effects of FGF-2 in COS-7 wild type cells were analyzed. COS-7 cells are FGFR1 positive as determined by RT-PCR and PCR-Southern blotting and stimulation of cell proliferation of COS-7 cells by endogenously expressed or exogenously added FGF-2 in soft agar was also

demonstrated. Upon coexpression of FGF-BP, the stimulation of colony formation of COS-7 cells induced by FGF-2 was inhibited. Similar effects were obtained upon exogenous addition of recombinant FGF-BP that can bind to FGF-2 as evidenced by Dot blotting. It is noteworthy that the necessary concentrations of exogenously added FGF-BP to reverse the stimulating effects of FGF-2 were comparably high (5 µg/ml). This can be explained by the several steps included in the process of uptake of FGF-BP after its interaction with secreted FGF-2: 1) diffusion of FGF-BP to FGF-2 immobilized in the extracellular matrix (ECM), 2) binding of FGF-BP with FGF-2 before/after the interaction of FGF-2 with its receptor, 3) internalization of FGF-BP alone or as a complex with FGF-2 and/or other molecules, 4) translocation into the nucleus. Another possibility is that the FGF-BP used in these experiments was purified under strongly denaturing conditions, which may lead to partially inactive preparations.

Studies in ovarian neoplasms reported that HER-2 oncogene is overexpressed in approximately 20-30% of ovarian carcinomas [188,189,354-356] and found that HER-2-gene amplification, as determined by Southern blotting, and HER-2 overexpression, as determined by immunohistochemistry (IHC) significantly correlated with clinical outcome. Recently, it has been shown that tumor cell lines established *in vitro* from ovarian carcinoma, as well as ovarian carcinoma cells harvested from ascites fluid, frequently express the HER-2 protein on their surface, suggesting that cells expressing this protein have a selective growth advantage over HER-2-negative cells [188,357,358].

Although treatment of ovarian cancer has improved over recent years with the introduction of taxane-based chemotherapy, it is still a difficult clinical situation, since the majority of patients will relapse and the disease in the majority of these patients remains incurable. Clearly, there is a need for alternative chemotherapeutics with higher tumor cell specificity and lower side effects which preferably display cytotoxicity through mechanisms different from current cytostatic drugs. While there are clinical and experimental data indicating a role of HER-2 overexpression in tumor cell sensitivity to chemotherapy, results are conflicting as to whether elevated HER-2 levels lead to increased resistance or higher sensitivity of tumors, especially in ovarian carcinomas and in ovarian carcinoma cell lines, where HER-2 overexpression has been found in considerable percentages. Interestingly, highly drug-specific HER-2 effects have been previously described. It was found that

paclitaxel cytotoxicity, but not of other chemotherapeutics like cisplatin, vinblastine or doxorubicin is dependent on HER-2 levels in SKOV-3 ovarian carcinoma cells [210].

Human SKOV-3 ovarian cancer cells overexpress HER-2 and express HER-1 but only very low levels of HER-3 and HER-4 [359]. Thus, they were chosen in the context of this thesis to analyze the HER-2 effects on paclitaxel and rViscumin cytotoxicity aside from the complex signaling network of other HER receptors. For this purpose, different and independent strategies were thereby used, including treatment with the HER-2 inhibitory antibody trastuzumab (Herceptin), phosphotyrosine kinase inhibitors, and downregulation of HER-2 expression by ribozyme-targeting. Finally, the underlying effects of the observed correlation between ribozyme-mediated HER-2 downregulation and paclitaxel and rViscumin sensitivity on cellular and molecular levels were analyzed.

Interestingly, in previous studies, the treatment with a HER-2 inhibitory humanized antibody (Herceptin), leads to increased paclitaxel resistance in SKOV-3 ovarian carcinoma cells. These results are in agreement with report that described the differentially expressed genes associated with paclitaxel resistance using cDNA array technology [211] and with other earlier studies [210]. On the other hand, there are other studies demonstrating the opposite observations e.g. HER-2 overexpressing breast cancer cells are more resistant than other cells towards certain chemotherapeutic agents inluding paclitaxel ([360] for review) and show the contrary to the observation of E1A-medited paclitaxel sensitization in HER-2-overexpressing SKOV-3.ip1 cells [209].

In the context of this thesis, two newly developed low molecular weight inhibitors of HER tyrosine kinase activity, D-69491 and D-70166, were used to confirm the previous results obtained by Herceptin treatment of SKOV-3 ovarian carcinoma cells. Previously, it was shown that D-69491 and D-70166 inhibit HER-2 phosphorylation almost completely or completely at concentrations above 10µM [243] by acting through intracellular inhibition of HER-2-mediated signal transduction as seen before in A431 epidermoid carcinoma cells for HER-1 [361]. In agreement with previous results based on Herceptin, D-69491 and D-70166 reduced the proliferation of SKOV-3 cells >50% upon addition of 1 µM, although the mechanism of action being completely unrelated to Herceptin. In the experiments, where the effects of D-69491 and D-70166 on proliferation and paclitaxel sensitivity were examined, the concentration of serum in medium was reduced to 0 - 2 %, since the solubility of both

HER tyrosine kinase inhibitor seems to be somewhat lower in 10 % FCS containing medium (unpublished data).

Since a >50% reduction of anchorage-dependent cell proliferation was observed upon addition of 1µM D-69491 or D-70166, this concentration was chosen to study the effects of these HER tyrosine kinase inhibitors on paclitaxel sensitivity in SKOV-3 cells. By examination of paclitaxel sensitivity after treatment of SKOV-3 cells with D-69491 and D-70166, the similar tendency of increased resistance of cells towards paclitaxel, as seen before by Herceptin treatment, was observed. It should be mentioned that although SKOV-3 cells mainly express HER-2 and only much lower (HER-1) or very low (HER-3, HER-4) levels of the other HER receptors [359], effects through inhibition of receptors different from HER-2 cannot be completely ruled out [361].

To address in more detail the underlying effects of the inverse correlation between HER-2 expression levels and paclitaxel resistance on molecular levels as well as to exclude the possibility of interferences resulting from the inhibition of different HER receptors by D-69491 and D-70166 kinase inhibitors, stable isogenic SKOV-3 cell lines with ribozyme-mediated reduction of HER-2 expression levels were used. Selection of different clones with various levels of residual HER-2 expression excluded clonal artifacts non-related to HER-2 expression and allowed to establish a 'HER-2 gene dose effect' of paclitaxel sensitivity. Hence, by using three independent strategies to transiently or constitutively inhibit HER-2-mediated signal transduction, the HER-2 dependence of paclitaxel cytotoxicity in SKOV-3 cells was demonstrated.

It is notably that by comparison of the paclitaxel IC_{50} values, which resulted from different experiments in this thesis as well as in previous studies [362], IC_{50} values increase with lower serum concentrations (this point is discussed in detail below) or reduced time of cells being exposed to the drug. Nevertheless, the effect of increased resistance upon HER-2 inhibition was observed under each condition independently of incubation times or serum concentrations.

Targeting of HER-2 expression levels or signal transduction by Herceptin was previously shown to decrease proliferation of SKOV-3 cells (see [243] for details). Similarly, HER-2 ribozyme-targeting and tyrosine kinase inhibitors reduced the proliferation of SKOV-3 cells.

Treatment of SKOV-3 cells with Herceptin or tyrosine kinase inhibitors prior to the addition of paclitaxel as well as HER-2 downregulation by ribozyme-targeting render the cells more resistant to paclitaxel. These results indicate that reduced proliferation may be the underlying cellular effect that determines the increased paclitaxel resistance of SKOV-3 cells. This could merely be because cells take a longer time to reach mitosis, where the lethal event upon paclitaxel treatment occurs. The active paclitaxel might be metabolized in this time and therefore the slower growing cells may be subjected to a lower effective dose by the time they reach mitosis. The correlation between proliferation rate and sensitivity towards paclitaxel is further supported by the fact that serum-starving conditions attenuate paclitaxel-induced cell death in this cell system as well. On the other hand, doxorubicin or cisplatin cytotoxicities are independent of HER-2 levels as shown here and previously [210] demonstrating that HER-2 targeting does not result in a general increase in resistance towards all drugs only due to reduced cell proliferation. Taken together, these data indicate that HER-2 has an effect on cell cycle progression and proliferation which determines the cytotoxicity of paclitaxel, but not of doxorubicin or cisplatin.

Extracellular signals are transduced into the cell by a complex network of signaling pathways. Specificity of the cellular response is determined by an equilibrium existing between distinct pathways which in turn is dependent on the duration and strength of a signal. Previous data have shown that paclitaxel can activate several MAPK pathways, associated with Erk1/2, p38, and SAPK/JNK kinases [262,363-366]. These pathways are implicated in different, often opposite, cellular effects such as proliferation, differentiation, stress response, and apoptosis. To further explore the consequences of HER-2 downregulation on molecular levels, especially with regard to paclitaxel sensitivity in SKOV-3 ovarian carcinoma cells, the activation of members of the mitogen-activated protein kinase (MAPK) familiy was examined. In Western blot experiments, basal (i.e. without paclitaxel treatment) levels of active MAP kinases indicated a decreased p42/p44 phosphorylation as well as increased levels of phosphorylated SAPK/JNK and p38 upon HER-2 depletion. This reduced p42/p44 activation is in agreement with the decreased proliferation rate, which was observed in ribozyme-transfected cells with reduced HER-2 expression. The higher phosphorylation of SAPK/JNK, which is activated by a variety of (environmental) stress factors, in ribozyme-transfected cells may result from the impairment of the cells upon HER-2 depletion. This is also reflected by the increased basal apoptosis rate, as seen previously [243]. Interactions between the MAPK pathways seem to be cell

specific. Although the involvement of p38 and SAPK/JNK kinases in promoting cell death and Erk1/Erk2 in proliferation has been demonstrated in many cell types, in some cells the opposite picture has been reported. For instance, in B lymphocytes p38 is required for proliferation and not for apoptosis [367], while in leukemic cells Erk1/Erk2 kinases rather than p38 have been reported to potentiate apoptosis [368].

In contrast to previous data of paclitaxel-mediated activation of members of MAPK family, which seems to be cell specific, no significant activation/deactivation of these kinases was observed in SKOV-3 cells upon paclitaxel treatment and the differences in basal levels cannot fully explain the HER-2 dependence of SKOV-3 paclitaxel sensitivity.

Both caspase-3 and caspase-7, which represent effector caspases of two main pathways of induction of apoptosis, are known to be activated in paclitaxel-induced apoptosis [369,370]; therefore, the relationship between caspase activities and HER-2 expression levels as well as paclitaxel-induced apoptosis in different SKOV-3 cells were examined in the context of this thesis. Caspases-3 and caspase-7 independently of HER-2 levels were not activated in SKOV-3 cells upon paclitaxel treatment, indicating that paclitaxel may utilize a caspase-independent pathway of induction of apoptosis in SKOV-3 ovarian carcinoma cells. Conflicting data have been published as to whether paclitaxel induces caspase-3 in SKOV-3 cells [209,371]. The discrepancy between the data of caspase-3 activation in this thesis as well as previous data [371] on the one hand and the earlier observation [209] on the other hand could be explained by the use of the HER-2-overexpressing subtype SKOV-3.ip1 in the latter study rather than the wildtype cells or by approach of repressing the HER-2 promoter via the adenovirus type 5 E1A gene. Indeed, IC_{50} values of paclitaxel estimated from Uneo et al. [209] are ~4 – 5 fold higher as compared to the data in this thesis and, since other studies in different cell lines have shown E1A-mediated enhanced sensitivity to other cytostatic agents being independent of HER-2 expression levels [372,373], it is possible that E1A-mediated paclitaxel sensitization relies on a mechanism unrelated to HER-2.

Interaction among p53, the cyclin-dependent kinase inhibitors p21 and p16, and pRb has been shown to be crucial in cell cycle progression and apoptosis. p21^{Cip1} encodes a 21 kDa protein and was discovered as a Cdk inhibitor [374] as well as a wild type p53-inducable gene [375]. In breast cancer cells overexpression of HER-2 upregulates p21^{Cip1} leading to inhibition of paclitaxel-mediated activation of p34^{cdc2} and of subsequent apoptosis [197].

SKOV-3 cells, however, do not express widtype p53 protein [362]. Therefore, p21^{Cip1} was not studied.

Furthermore, bcl-2, which blocks or delays apoptosis in many cell systems and exerts its antiapoptotic effect mainly through stabilization of mitochondrial membranes was studied. Previously, in different cancer types paclitaxel was shown to either diminish bcl-2 transcription or to modify bcl-2 via phosphorylation [376,377], hereby inactivating bcl-2 and inducing apoptosis ([264] for review). In Western blotting experiments, paclitaxel time-dependently induced the phosphorylation of the antiapoptotic protein bcl-2, which likely reflects the inactivation of bcl-2 and the onset of apoptosis. However, bcl-2 phosphorylation and hyperphosphorylation in SKOV-3 cells was independent of HER-2 expression levels.

The molecular network for the evolving paclitaxel resistance in SKOV-3 ovarian cancer cells seems to be complex as recently suggested in the same cell line [378]. In summary, a HER-2 dose dependence of SKOV-3 paclitaxel resistance was established in this thesis and cell proliferation was identified as an underlying cellular event.

rViscumin is a recombinantly expressed mistletoe lectin heterodimer which shows a completely different mechanism of action as compared to other cytotoxic compounds. To analyze the role of HER-2 expression in cellular chemoresistance towards this novel anti-cancer drug, a strategy similar to paclitaxel was employed.

Initially, by ribozyme-targeting, a dramatic alteration of sensitivity to rViscumin in the HER-2-depleted cells was found. Moreover, by comparing cell lines with different residual HER-2 levels, a direct correlation between HER-2 levels and cellular sensitivity towards rViscumin in SKOV-3 cells was established. These results are in agreement with previous results based on Herceptin [313]. Interestingly, these findings are comparable to data on the sensitivity of SKOV-3 cells towards paclitaxel, although both drugs display cytotoxicity through completely different mechanisms (rViscumin: inhibition of translation; Paclitaxel: cell cycle arrest).

It has been described that the interaction of the rViscumin B-chain with 'viscumin receptor' gangliosides of the neolacto series on the surface of tumor cells is responsible for cellular rViscumin uptake in the cells, which is necessary for rViscumin to exert its effects

[288]. Using [^{125}I]-labeled rViscumin, it was demonstrated that rViscumin uptake is independent of cellular HER-2 expression levels. Moreover, a linear rViscumin uptake over a time range of at least 60 min in all clonal derivative cells of SKOV-3, which was comparable, was observed. These data firmly rule out that HER-2 ribozyme-mediated alterations in rViscumin binding and/or uptake are responsible for the observed HER-2 dependence of rViscumin cytotoxicity in SKOV-3 cells and clearly points towards intracellular mechanisms.

To explore the effects of rViscumin on molecular levels und their dependence on HER-2 expression levels, MAPK-dependent signal transduction pathways were investigated. In this thesis, it was shown for the first time that rViscumin activates members of the MAPK family and that this activation follows a complex pattern which is dependent on cellular HER-2 expression levels and on the rViscumin concentration. As seen before, without rViscumin treatment, the observed differences between wildtype and HER-2-ribozyme-transfected cells may be due to impaired activation by growth factors (p42/p44) and increased stress response (SAPK/JNK, p38) upon HER-2 depletion. Upon rViscumin treatment, however, the precise roles of the activated kinases remain somewhat obscure. It seems likely that activation of different MAP kinases by rViscumin treatment may be an attempt of the cells to maintain cellular homeostasis prior to and/or independent of apoptosis as hypothesized earlier for paclitaxel-treated cells [379].

In further experiments, the changes in bcl-2 were studied. Bcl-2 was time-dependently downregulated in SKOV-3 wildtype cells upon rViscumin treatment. Interestingly, in HER-2 depleted cells bcl-2 levels remained significantly higher after rViscumin treatment as compared to the wildtype cells, which may account for the low rViscumin sensitivity in ribozyme-transfected cells compared to wildtype cells.

Finally, to further study the molecular basis of rViscumin-mediated induction of apoptosis in SKOV-3 cells, procaspases-3 and -7 and their changes upon rViscumin treatment were analyzed. While basal procaspase-7 expression was ~2-fold higher in SKOV-3 cells upon HER-2 depletion, no activation of caspases-3 or -7 was observed after rViscumin treatment. In contrast, activation of caspases-3, -8, and -9 after treatment with different mistletoe lectins has been described in leukemic cell lines [380,381]. These earlier studies were mostly done in blood cells and employed various natural mistletoe preparations rather than the pure

recombinant protein, which could explain the lack in caspase activation upon rViscumin treatment. However, Hostanska et al. [287] have shown in a mouse tumor cell system that the rViscumin-mediated induction of apoptosis is independent of p53 and leads to caspase-3 activation [287]. Regarding the role of p53, SKOV-3 cells do not express wildtype p53, however, no caspase-3 activation was observed in these cells. Also, the results in this thesis indicate that in SKOV-3 cells rViscumin-mediated induction of apoptosis is independent of the activation of caspases-3, -7, as well as caspases-8, -9, or -10.

In conclusion, the inverse correlation between HER-2 expression and rViscumin-mediated bcl-2 downregulation may well account for the HER-2 dependence of cellular rViscumin sensitivity and determination of HER-2 expression levels in tumor cells as well as the further clarification of the mechanistic details of rViscumin-induced activation of downstream signalling pathways which may involve known or yet unknown modulators of MAPKs may open new avenues to better predict the efficacy of the new chemotherapeutic rViscumin.

6 SUMMARY

Ovarian cancer is one of the most widespread and lethal gynecological malignancies with so far limited treatment options. A better understanding of the genetic changes in ovarian pathogenesis is of critical importance. In this thesis, two gene products were studied: the fibroblast growth factor-binding protein (FGF-BP) and the human epidermal growth factor receptor-2 (HER-2).

FGF-BP is a heparin-binding protein which interacts with FGFs releasing them from the extracellular matrix and hence playing a significant role in extracellular FGF bioactivation. In this work, the immunohistochemical analysis of tissue microarrays (TMAs) revealed for the first time FGF-BP overexpression in 40% of invasive ovarian carcinomas. Since none of the normal ovarian tissues showed similar FGF-BP immunopositivity, these data suggest that FGF-BP overexpression may represent an acquired malignant phenotypic feature of ovarian carcinoma.

To further explore the molecular mechanism of FGF-BP action, confocal microscopy was employed. Dependent on the cell line, FGF-BP was either localized in the cytoplasm and released through a classic secretion pathway employing ERGIC or, despite a classical signal peptide, showed a nuclear localization. Interestingly, upon coexpression with nuclear FGF-2, cytoplasmic FGF-BP was translocated and colocalized with FGF-2 in the nucleus. Additionally, the dependence of the cellular uptake of exogenous FGF-BP on the expression of and interaction with FGF-2 was demonstrated. Various truncated FGF-BP mutant constructs showed that extensive truncations at the C-terminal end of FGF-BP had no effect on the subcellular localization and FGF-2 interaction, while upon N-terminal truncations nuclear colocalization and interaction of FGF-BP with FGF-2 was lost. Proliferation assays provided evidence that biological effects of FGF-BP depend on the cell line. While in SW-13 adrenal carcinoma cells the stable transfection of FGF-BP induced cell proliferation, inhibitory activity of FGF-BP in COS-7 cells was demonstrated. Moreover, FGF-BP-mediated stimulation of colony formation in soft agar was lost upon N-terminal truncations of FGF-BP in SW-13 cells, whereas C- or N-terminal truncations abolished the inhibitory effect of FGF-BP on COS-7 cell proliferation. The induction of cell proliferation resulting

from the expression of FGF-2 in COS-7 cells, which also express FGF receptors, was lost upon endogenous expression or exogenous addition of FGF-BP.

Hence, in addition to its already published extracellular role, FGF-BP exerts intracellular, nuclear functions. More specifically, dependent on the cell line FGF-BP displays inhibitory or stimulating activities upon interaction with FGF-2 in the nucleus.

HER-2 belongs to the epidermal growth factor (EGF) receptor family and plays an important role in human tumors. However, clinical and experimental data indicating effects of HER-2 overexpression on tumor cell sensitivity towards chemotherapy are conflicting as to whether elevated HER-2 levels lead to increased resistance or higher sensitivity of tumors. This is particularly true for ovarian carcinomas and ovarian carcinoma cell lines, where HER-2 overexpression has been found in considerable percentages. In this work, the role of HER-2 expression and signaling levels pertaining to paclitaxel and rViscumin chemoresistance were explored.

Treatment of SKOV-3 cells with two newly developed low molecular weight inhibitors of HER-2 tyrosine kinase activity resulted in a decrease in the cellular paclitaxel sensitivity. These data confirmed previous data regarding treatment with the HER-2 inhibitory antibody trastuzumab (Herceptin), which is well established in tumor therapy. Using various isogenic SKOV-3 cell lines with ribozyme-mediated stable reduction of HER-2 expression levels, a 'HER-2 gene dose effect' of paclitaxel cytotoxicity was established, while doxorubicin and cisplatin cytotoxicity remained unchanged. To elucidate the underlying mechanisms of this effect, paclitaxel- or HER-2-mediated alterations in phosphorylation of MAP kinase p42/44, stress-activated protein kinase/Jun-terminal kinase (SAPK/JNK), and p38, and effects on the activation of caspase-3, caspase-7, and bcl-2 were analyzed. Activation of MAP kinases was dependent on HER-2 expression levels but did not change upon paclitaxel treatment. Paclitaxel-induced bcl-2 phosphorylation and hyperphosphorylation was independent of HER-2 expression levels. Finally, it was shown that paclitaxel utilizes a caspase-independent pathway of induction of apoptosis in SKOV-3 ovarian carcinoma cells.

The selective depletion of HER-2 by ribozyme-targeting also decreased the cellular sensitivity of SKOV-3 cells towards the recombinant cytostatic mistletoe rViscumin, establishing a 'HER-2 gene dose' dependence of rViscumin cytotoxicity, which is not

mediated by altered cellular rViscumin binding/internalization. The analysis of the underlying molecular effects of rViscumin treatment demonstrated that members of the MAPK family, p42/44, SAPK/JNK, and p38 are activated in a HER-2 and rViscumin concentration-dependent manner. While no rViscumin-mediated activation of caspase-3 and caspase-7 were observed, HER-2-dependent downregulation of the anti-apoptotic molecule bcl-2 was demonstrated.

In conclusion, by focusing on two cancer-relevant genes, this work establishes FGF-BP as a new potential target molecule in ovarian cancer therapy and explores its intracellular mechanism of action. Furthermore, this thesis provides new insights into the role of HER-2 in ovarian cancer sensitivity towards cytostatic drugs like paclitaxel or rViscumin which may allow to better assess the efficacy of both drugs in a clinical setting.

7 ZUSAMMENFASSUNG

Ovarialkarzinome gehören zu den weitverbreitetsten und lebensgefährlichsten gynäkologischen Tumoren mit bislang begrenzten Behandlungsmöglichkeiten. Ein besseres Verständnis der genetischen Änderungen in der Pathogenese des Ovarialkarzinoms ist von entscheidender Bedeutung. Im Rahmen dieser Doktorarbeit wurden zwei Genprodukte analysiert: das Fibroblasten-Wachstumsfaktor-bindende Protein (FGF-BP) und der epidermale Wachstumsfaktor-Rezeptor-2 (HER-2).

FGF-BP ist ein Heparin-bindendes Protein, das mit FGFs wechselwirkt, sie von der extrazellulären Matrix freisetzt und folglich eine bedeutende Rolle in der extrazellulären FGF-Bioaktivität spielt. In dieser Doktorarbeit wurde mittels immunhistochemischer Untersuchungen an Tissue Microarrays (TMAs) erstmals gezeigt, dass FGF-BP in 40% aller Ovarialkarzinome überexprimiert ist. Da keines der normalen Ovarialgewebe eine vergleichbar starke immunhistochemische Färbung zeigte, deuten diese Daten an, dass die Überexpression von FGF-BP eine bösartige phänotypische Eigenschaft des Ovarialkarzinoms darstellen kann.

Um die molekularen Mechanismen der FGF-BP-Wirkung weiter zu untersuchen, wurde konfokale Mikroskopie eingesetzt. Abhängig von der Zellinie war FGF-BP entweder im Zytoplasma lokalisiert und wurde durch einen klassischen Sekretionsweg über ERGIC sekretiert, oder es wurde, trotz eines klassischen Signalpeptides, eine nukleäre Lokalisation gefunden. Bei der Koexpression mit nukleärem FGF-2 wurde interessanterweise das zytoplasmatische FGF-BP in den Zellkern transloziert und eine nukleäre Kolokalisation von FGF-BP und FGF-2 beobachtet. Zusätzlich wurde die Abhängigkeit der zellulären Aufnahme von exogenem FGF-BP von der Expression und Interaktion mit FGF-2 demonstriert. Verschiedene Verkürzungsmutanten des FGF-BP zeigten, dass Verkürzungen am C-terminalen Ende keinen Effekt auf die subzelluläre Lokalisation und FGF-2-Wechselwirkung haben, während bei N-terminalen Verkürzungsmutanten die nukleäre Kolokalisation und Interaktion des FGF-BP mit FGF-2 nicht mehr auftrat. In Proliferationsassays wurde beobachtet, dass die biologischen Effekte von FGF-BP von der jeweiligen Zellinie abhängen. Während in SW-13-Nebennierenkarzinom-Zellen die konstitutive Expression des FGF-BP Zellproliferation induzierte, wurde in COS-7 Zellen ein Proliferations-hemmender Effekt

demonstriert. Außerdem unterblieb in Soft Agar-Assays bei N-terminalen Verkürzungsmutanten in SW-13-Zellen die FGF-BP-vermittelte Stimulation der Kolonienbildung, während bei C- und N-terminalen Verkürzungsmutanten in COS-7-Zellen der hemmende Effekt des FGF-BP auf die Zellproliferation aufgehoben wurde. Die durch FGF-2 vermittelte Induktion des Zellwachstums in den FGF-Rezeptor-positiven COS-7-Zellen wurde durch endogene Expression oder exogene Zugabe des FGF-BP inhibiert.

Zusätzlich zu seiner bereits beschriebenen extrazellulären Rolle entfaltet FGF-BP somit auch intrazelluläre, nukleäre Funktionen. Insbesondere zeigt FGF-BP, abhängig von der jeweiligen Zellinie, hemmende oder stimulierende Aktivitäten, die offensichtlich auf der Wechselwirkung mit FGF-2 im Zellkern beruhen.

HER-2 gehört zur Familie der epidermalen Wachstumsfaktor-Rezeptoren und spielt eine wichtige Rolle in menschlichen Tumoren. Die klinischen und experimentellen Daten bezüglich der Effekte der HER-2-Überexpression auf die zelluläre Sensitivität von Tumoren gegenüber Chemotherapie sind jedoch widersprüchlich, insbesondere, ob eine erhöhte HER-2-Expression zu einer höheren Resistenz oder einer erhöhten Sensitivität von Tumoren führt. Dies gilt besonders für Ovarialkarzinome und Ovarialkarzinom-Zellinien, in denen HER-2-Überexpression zu einem hohen Prozentsatz gefunden wird. Im Rahmen dieser Arbeit wurde die Rolle der HER-2-Expression und HER-2-vermittelten Signaltransduktion in der zellulären Resistenz gegenüber Paclitaxel und rViscumin untersucht.

Die Behandlung von SKOV-3-Zellen mit zwei neu entwickelten niedermolekularen HER-2-Tyrosinkinase-Inhibitoren führte zu erhöhter zellulärer Resistenz gegenüber Paclitaxel. Diese Daten bestätigten vorherige Ergebnisse bezüglich der Behandlung mit Anti-HER-2 Antikörpern (Herceptin), die in der Tumortherapie etabliert sind. Anhand verschiedener SKOV-3-Zellinien mit ribozymbedingt verminderter HER-2-Expression wurde ein „HER-2-Gen-Dosis-Effekt" etabliert, während Doxorubicin- und Cisplatin-Zytotoxitäten unverändert blieben. Zur näheren molekularen Charakterisierung der zugrundeliegenden Mechanismen dieses Effektes wurden Paclitaxel- oder HER-2-vermittelte Veränderungen in der Phosphorylierung der MAP-Kinasen p42/p44, der stress-activated protein kinase/Jun-terminal kinase SAPK/JNK und der p38 MAP-Kinase, sowie des Effekts auf die Aktivierung von Caspase-3 und Caspase-7 und bcl-2 analysiert. Die Aktivierung der MAP-Kinasen war abhängig von der HER-2-Expressions, aber änderte sich nicht unter Paclitaxel-Behandlung.

Eine beobachtete Paclitaxel-induzierte bcl-2-Phosphorylierung und -Hyperphosphorylierung war HER-2-unabhängig. Schließlich wurde gezeigt, dass Paclitaxel in SKOV-3 Zellen über einen Caspase-unabhängigen Weg Apoptose induziert.

Die selektive HER-2-Reduktion durch Ribozyme-Targeting führte in SKOV-3-Zellen auch zur Verminderung der Sensitivität gegenüber dem rekombinanten zytostatischen Mistellektin rViscumin. Wiederum wurde eine „HER-2-Gen-Dosis"-abhängige Sensitivität der Zellen gegenüber rViscumin beobachtet, die nicht durch eine geänderte zelluläre rViscumin-Bindung oder -Internalisierung vermittelt wird. Die Analyse der zugrundeliegenden molekularen Effekte zeigte, dass die Mitglieder der MAPK-Familie p42/p44, SAPK/JNK und p38 in HER-2- und rViscumin-konzentrationsabhängiger Weise aktiviert werden. Während keine rViscumin-vermittelte Aktivierung der Caspasen-3 und -7 beobachtet wurde, zeigte sich eine HER-2-abhängige Herunterregulation des antiapoptotischen Moleküls bcl-2.

Zusammenfassend konzentriert sich diese Arbeit auf zwei Krebs-relevante Gene. FGF-BP wird als neues mögliches Zielmolekül in Ovarialkarzinom-Therapie etabliert und bezüglich seiner intrazellulären Wirkmechanismen analysiert. Die hier vorgestellten Untersuchungen zeigen ferner neue Daten zur Rolle der HER-2-Expression bezüglich der Sensitivität von Ovarialkarzinomen gegenüber Zytostatika wie Paclitaxel oder rViscumin, was für die Bewertung der Wirksamkeit dieser Chemotherapeutika in der klinischen Verwendung relevant sein könnte.

8 ABBREVIATIONS

aFGF (FGF-1)	acidic fibroblast growth factor
APS	ammonium peroxodisulfate
bFGF (FGF-2)	basic fibroblast growth factor
BSA	bovine serum albumin
cDNA	complementary DNA
CFP	cyan fluorescent protein
cpm	counts per minute
DAB	diaminobenzidine tetrahydochloride
ddH$_2$O	bidestilled H$_2$o
DEPC	diethylpyrocarbonate
DMBA	dimethyl benz (a) anthracene
DMSO	dimethyl sulfoxide
ECL	enhanced chemiluminescence
ECM	extracellular matrix
EDTA	ethylenediamine tetraacetic acid
EGF	epidermal growth factor
ELISA	enzyme-linked immunosorbent assay
ERGIC	enoplasmic reticulum-Golgi intermediate compartment
Erk	extracellular signal-regulated kinase
FBS	fetal bovine serum
FGF-BP	fibroblast growth factor-bindingprotein
FGFRs	fibroblast growth factor receptors
FGFs	fibroblast growth factors
HER	human epidermal growth factor receptor
HER-2	human epidermal growth factor receptor-2
HLGAGs	heparan-like glycosaminoglycans
HMW	high molecular weight
HSPGs	heparan sulphate proteoglycans
IC$_{50}$	inhibitory concentration 50%
IHC	immunohistochemistry
IMDM	Iscove's Modified Eagle's Medium

kb	kilo base
kDa	kilo dalton
LB	Luria-Bertani
MAPK	mitogen-activated protein kinase
ML I	mistletoe lectin I
Ni-NTA	nickel-nitrilotriacetic acid
NLS	nuclear localizing sequence
PBS	phosphate-buffered saline
PCR	polymerase chain reaction
PKC	protein kinase C
PTB	phosphotyrosine binding domain
PTK	protein tyrosine kinases
RIPs	ribosome-inactivating proteins
RT-PCR	reverse transcription-polymerase chain reaction
SAP	Shrimp alkaline phosphatase
SCC	squamous cell carcinoma
SDS	sodium dodecyl sulfate
SDS-PAGE	sodium dodecyl sulphate-polyacrylamide gel electrophoresis
SSC	sodium chloride-sodium citrate
TAE	tris-acetate-EDTA
TBST	tris-buffered saline tween
TEMED	tetramethylethylendiamine
TKIs	tyrosine kinase inhibitors
TMA	tissue microarrays
TPA	12-O-tetradecanoylphorbol-13-acetate
tRA	all-trans retinoic acid
Tris-HCl	tris(hydroxymethyl)aminomethane hydrochloride
U	unit
UV	ultraviolet
VEGF	vascular endothelial growth factor
YFP	yellow fluorescent protein

9 REFERENCES

1.   Folkman, J. (1995) *Nature Medicine* **1**, 27-31
2.   Stancovski, I., Sela, M., and Yarden, Y. (1994) *Cancer Treat Res* **71**, 161-191
3.   Yamanaka, Y., Friess, H., Kobrin, M. S., Buchler, M., Kunz, J., Beger, H. G., and Korc, M. (1993) *Hum Pathol* **24**(10), 1127-1134
4.   Lengauer, C., Kinzler, K. W., and Vogelstein, B. (1998) *Nature* **396**(6712), 643-649
5.   Rabbitts, T. H. (1999) *J Pathol* **187**(1), 39-42
6.   Hanahan, D., and Weinberg, R. A. (2000) *Cell* **100**(1), 57-70
7.   Hyder, S. M., and Stancel, G. M. (1999) *Mol Endocrinol* **13**(6), 806-811
8.   Hanahan, D. (1998) *Nat Med* **4**(1), 13-14
9.   Gasparini, G. (1999) *Drugs* **58**(1), 17-38
10. Baird, A., and Klagsbrun, M. (1991) *Cancer Cells* **3**(6), 239-243
11. Kim, K. J., Li, B., Winer, J., Armanini, M., Gillett, N., Phillips, H. S., and Ferrara, N. (1993) *Nature* **362**, 841-844
12. Weidner, K. M., Hartmann, G., Sachs, M., and Birchmeier, W. (1993) *Am.J Respir.Cell Mol.Biol* **8**, 229-237
13. Schreiber, A. B., Winkler, M. E., and Derynck, R. (1986) *Science* **232**(4755), 1250-1253.
14. Fang, W., Hartmann, N., Chow, D. T., Riegel, A. T., and Wellstein, A. (1992) *J.Biol.Chem.* **267**, 25889-25897
15. O'Reilly, M. S., Holmgren, L., Shing, Y., Chen, C., Rosenthal, R. A., Moses, M., Lane, W. S., Cao, Y., Sage, E. H., and Folkman, J. (1994) *Cell* **79**, 315-328
16. O'Reilly, M. S., Holmgren, L., Chen, C., and Folkman, J. (1996) *Nat Med* **2**(6), 689-692
17. O'Reilly, M. S., Boehm, T., Shing, Y., Fukai, N., Vasios, G., Lane, W. S., Flynn, E., Birkhead, J. R., Olsen, B. R., and Folkman, J. (1997) *Cell* **88**, 277-285
18. Pepper, M. S. (1997) *Arterioscler Thromb Vasc Biol* **17**(4), 605-619
19. Mukhopadhyay, D., Tsiokas, L., Zhou, X. M., Foster, D., Brugge, J. S., and Sukhatme, V. P. (1995) *Nature* **375**, 577-581
20. Jiang, B. H., Agani, F., Passaniti, A., and Semenza, G. L. (1997) *Cancer Res* **57**(23), 5328-5335
21. Kerbel, R. S., Viloria-Petit, A., Okada, F., and Rak, J. (1998) *Mol Med* **4**(5), 286-295
22. Okada, F., Rak, J. W., Croix, B. S., Lieubeau, B., Kaya, M., Roncari, L., Shirasawa, S., Sasazuki, T., and Kerbel, R. S. (1998) *Proc Natl Acad Sci U S A* **95**(7), 3609-3614
23. Arbiser, J. L., Moses, M. A., Fernandez, C. A., Ghiso, N., Cao, Y., Klauber, N., Frank, D., Brownlee, M., Flynn, E., Parangi, S., Byers, H. R., and Folkman, J. (1997) *Proc.Natl.Acad.Sci.U.S.A.* **94**, 861-866
24. Talarico, D., and Basilico, C. (1991) *Mol.Cell Biol.* **11**, 1138-1145
25. Kleiner, D. E., and Stetler-Stevenson, W. G. (1999) *Cancer Chemother Pharmacol* **43 Suppl**, S42-51
26. Burgess, W. H., and Maciag, T. (1989) *Annu.Rev.Biochem.* **58**, 575-606
27. Gospodarowicz, D. (1974) *Nature* **249**, 123-127
28. Ornitz, D. M., and Itoh, N. (2001) *Genome Biol* **2**(3), REVIEWS3005
29. Basilico, C., and Moscatelli, D. (1992) *Adv.Cancer Res.* **59**, 115-165
30. Rubin, J. S., Osada, H., Finch, P. W., Taylor, W. G., Rudikoff, S., and Aaronson, S. A. (1989) *Proc.Natl.Acad.Sci.U.S.A.* **86**, 802-806
31. Ornitz, D. M. (2000) *Bioessays* **22**(2), 108-112
32. Wu, D., Kan, M., Sato, G. H., Okamoto, T., and Sato, J. D. (1991) *J.Biol.Chem.* **266**, 16778-16785
33. Tassi, E., Al-Attar, A., Aigner, A., Swift, M. R., McDonnell, K., Karavanov, A., and Wellstein, A. (2001) *J Biol Chem* **16**, 16
34. Johnson, D. E., and Williams, L. T. (1993) *Adv.Cancer Res.* **60**, 1-41
35. Ornitz, D. M., Xu, J., Colvin, J. S., McEwen, D. G., MacArthur, C. A., Coulier, F., Gao, G., and Goldfarb, M. (1996) *J Biol Chem* **271**(25), 15292-15297
36. Givol, D., and Yayon, A. (1992) *FASEB J.* **6**, 3362-3369
37. Dionne, C. A., Jaye, M., and Schlessinger, J. (1991) *Ann N Y Acad Sci* **638**, 161-166
38. Jaye, M., Schlessinger, J., and Dionne, C. A. (1992) *Biochim Biophys Acta* **1135**(2), 185-199
39. Lobb, R. R. (1988) *Biochemistry.* **27**, 2572-2578
40. Sommer, A., and Rifkin, D. B. (1989) *J Cell Physiol* **138**(1), 215-220.
41. Saksela, O., Moscatelli, D., Sommer, A., and Rifkin, D. B. (1988) *J Cell Biol* **107**, 743-751
42. Presta, M., Moscatelli, D., Joseph-Silverstein, J., and Rifkin, D. B. (1986) *Mol Cell Biol* **6**(11), 4060-4066
43. Goldfarb, M. (1996) *Cytokine Growth Factor Rev* **7**(4), 311-325

44.   Abud, H. E., Skinner, J. A., Cohn, M. J., and Heath, J. K. (1996) *Biochem Soc Symp* **62**, 39-50
45.   Wiedlocha, A., and Sorensen, V. (2004) *Curr Top Microbiol Immunol* **286**, 45-79
46.   Yoshimura, S., Takagi, Y., Harada, J., Teramoto, T., Thomas, S. S., Waeber, C., Bakowska, J. C., Breakefield, X. O., and Moskowitz, M. A. (2001) *Proc Natl Acad Sci U S A* **98**(10), 5874-5879
47.   Cohn, M. J., Izpisua-Belmonte, J. C., Abud, H., Heath, J. K., and Tickle, C. (1995) *Cell* **80**(5), 739-746
48.   Crossley, P. H., Minowada, G., MacArthur, C. A., and Martin, G. R. (1996) *Cell* **84**(1), 127-136
49.   Feldman, B., Poueymirou, W., Papaioannou, V. E., DeChiara, T. M., and Goldfarb, M. (1995) *Science* **267**(5195), 246-249.
50.   Sun, X., Meyers, E. N., Lewandoski, M., and Martin, G. R. (1999) *Genes Dev* **13**(14), 1834-1846.
51.   Sekine, K., Ohuchi, H., Fujiwara, M., Yamasaki, M., Yoshizawa, T., Sato, T., Yagishita, N., Matsui, D., Koga, Y., Itoh, N., and Kato, S. (1999) *Nat Genet* **21**(1), 138-141.
52.   Fiore, F., Planche, J., Gibier, P., Sebille, A., deLapeyriere, O., and Birnbaum, D. (1997) *Int J Dev Biol* **41**(4), 639-642
53.   Ortega, S., Ittmann, M., Tsang, S. H., Ehrlich, M., and Basilico, C. (1998) *Proc Natl Acad Sci U S A* **95**(10), 5672-5677.
54.   Zhou, M., Sutliff, R. L., Paul, R. J., Lorenz, J. N., Hoying, J. B., Haudenschild, C. C., Yin, M., Coffin, J. D., Kong, L., Kranias, E. G., Luo, W., Boivin, G. P., Duffy, J. J., Pawlowski, S. A., and Doetschman, T. (1998) *Nat Med* **4**(2), 201-207.
55.   Dono, R., Texido, G., Dussel, R., Ehmke, H., and Zeller, R. (1998) *Embo J* **17**(15), 4213-4225.
56.   Ichimura, T., Finch, P. W., Zhang, G., Kan, M., and Stevens, J. L. (1996) *Am J Physiol* **271**(5 Pt 2), F967-976
57.   Ay, I., Sugimori, H., and Finklestein, S. P. (2001) *Brain Res Mol Brain Res* **87**(1), 71-80
58.   Kondo, S., Yin, D., Aoki, T., Takahashi, J. A., Morimura, T., and Takeuchi, J. (1994) *Exp Cell Res* **213**(2), 428-432
59.   Shaulian, E., Resnitzky, D., Shifman, O., Blandino, G., Amsterdam, A., Yayon, A., and Oren, M. (1997) *Oncogene* **15**(22), 2717-2725
60.   Song, S., Wientjes, M. G., Gan, Y., and Au, J. L. (2000) *Proc Natl Acad Sci U S A* **97**(15), 8658-8663
61.   Takahashi, J. A., Fukumoto, M., Igarashi, K., Oda, Y., Kikuchi, H., and Hatanaka, M. (1992) *J Neurosurg* **76**(5), 792-798
62.   Kornmann, M., Ishiwata, T., Beger, H. G., and Korc, M. (1997) *Oncogene* **15**(12), 1417-1424
63.   Samaniego, F., Markham, P. D., Gendelman, R., Watanabe, Y., Kao, V., Kowalski, K., Sonnabend, J. A., Pintus, A., Gallo, R. C., and Ensoli, B. (1998) *Am J Pathol* **152**(6), 1433-1443
64.   Gospodarowicz, D. (1975) *J.Biol.Chem.* **250**, 2515-2520
65.   Bikfalvi, A., Klein, S., Pintucci, G., and Rifkin, D. B. (1997) *Endocr Rev* **18**(1), 26-45
66.   Arnaud, E., Touriol, C., Boutonnet, C., Gensac, M. C., Vagner, S., Prats, H., and Prats, A. C. (1999) *Mol Cell Biol* **19**(1), 505-514
67.   Bugler, B., Amalric, F., and Prats, H. (1991) *Mol Cell Biol* **11**, 573-577
68.   Renko, M., Quarto, N., Morimoto, T., and Rifkin, D. B. (1990) *J.Cell Physiol.* **144**, 108-114
69.   Mignatti, P., Morimoto, T., and Rifkin, D. B. (1991) *Proc Natl Acad Sci U S A* **88**(24), 11007-11011
70.   Jouanneau, J., Plouet, J., Moens, G., and Thiery, J. P. (1997) *Oncogene* **14**(6), 671-676
71.   McNeil, P. L., Muthukrishnan, L., Warder, E., and D'Amore, P. A. (1989) *J.Cell Biol.* **109**, 811-822
72.   Haimovitz-Friedman, A., Vlodavsky, I., Chaudhuri, A., Witte, L., and Fuks, Z. (1991) *Cancer Res* **51**(10), 2552-2558
73.   Lorenzet, R., Sobel, J. H., Bini, A., and Witte, L. D. (1992) *Thromb Haemost* **68**(3), 357-363
74.   Mignatti, P., Morimoto, T., and Rifkin, D. B. (1992) *J Cell Physiol* **151**(1), 81-93
75.   Jackson, R. L., Busch, S. J., and Cardin, A. D. (1991) *Physiol Rev* **71**(2), 481-539.
76.   Wong, P., Hampton, B., Szylobryt, E., Gallagher, A. M., Jaye, M., and Burgess, W. H. (1995) *J Biol Chem* **270**(43), 25805-25811.
77.   Baird, A., Schubert, D., Ling, N., and Guillemin, R. (1988) *Proc Natl Acad Sci USA* **85**, 2324-2328
78.   Faham, S., Hileman, R. E., Fromm, J. R., Linhardt, R. J., and Rees, D. C. (1996) *Science* **271**(5252), 1116-1120.
79.   Vlodavsky, I., Eldor, A., Bar-Ner, M., Fridman, R., Cohen, I. R., and Klagsbrun, M. (1988) *Adv.Exp.Med.Biol* **233**, 201-210
80.   Bashkin, P., Doctrow, S., Klagsbrun, M., Svahn, C. M., Folkman, J., and Vlodavsky, I. (1989) *Biochemistry.* **28**, 1737-1743
81.   Moscatelli, D. (1992) *J.Biol.Chem.* **267**, 25803-25809
82.   Vlodavsky, I., Friedmann, Y., Elkin, M., Aingorn, H., Atzmon, R., Ishai-Michaeli, R., Bitan, M., Pappo, O., Peretz, T., Michal, I., Spector, L., and Pecker, I. (1999) *Nat Med* **5**(7), 793-802.
83.   Hulett, M. D., Freeman, C., Hamdorf, B. J., Baker, R. T., Harris, M. J., and Parish, C. R. (1999) *Nat Med* **5**(7), 803-809.

84.   Dennis, P. A., Saksela, O., Harpel, P., and Rifkin, D. B. (1989) *J Biol Chem* **264**(13), 7210-7216.
85.   Beer, H. D., Bittner, M., Niklaus, G., Munding, C., Max, N., Goppelt, A., and Werner, S. (2005) *Oncogene* **24**(34), 5269-5277
86.   Ogawa, K., Tanaka, K., Ishii, A., Nakamura, Y., Kondo, S., Sugamura, K., Takano, S., Nakamura, M., and Nagata, K. (2001) *J Immunol* **166**(10), 6404-6412.
87.   Schmidt, J. (2003) A novel binding Protein for Fibroblast Growth Factors (FGF-2): Cloning, Expression Profile, Tumorigenic Activity, and Regulation of Gene Expression by Fetal Bovine Serum and Retinoic Acid., Department of Pharmacology and Toxicology, Philipps-University, Marburg. PhD. Thesis
88.   Czubayko, F., Smith, R. V., Chung, H. C., and Wellstein, A. (1994) *J.Biol.Chem.* **269**, 28243-28248
89.   Li, W. M., and Chen, W. B. (2004) *Chin Med J (Engl)* **117**(4), 621-623
90.   Kagan, B. L., Henke, R. T., Cabal-Manzano, R., Stoica, G. E., Nguyen, Q., Wellstein, A., and Riegel, A. T. (2003) *Cancer Res* **63**(7), 1696-1705
91.   Czubayko, F., Liaudet-Coopman, E. D. E., Aigner, A., Tuveson, A. T., Berchem, G., and Wellstein, A. (1997) *Nature Medicine* **3**, 1137-1140
92.   Aigner, A., Renneberg, H., Bojunga, J., Apel, J., Nelson, P. S., and Czubayko, F. (2002) *Oncogene* **21**(37), 5733-5742
93.   Liaudet-Coopman, E. D. E., Schulte, A. M., Cardillo, M., and Wellstein, A. (1996) *Biochem.Biophys.Res.Commun.* **229**, 930-937
94.   Kurtz, A., Darwiche, N., Harris, V., Wang, H. L., and Wellstein, A. (1997) *Oncogene* **14**, 2671-2681
95.   Yuspa, S. (1994) *Cancer Research* **54**, 1178-1189
96.   Kurtz, A., Aigner, A., Cabal-Manzano, R. H., Butler, R. E., Hood, D. R., Sessions, R. B., Czubayko, F., and Wellstein, A. (2004) *Neoplasia* **6**(5), 595-602
97.   Ray, R., Cabal-Manzano, R., Moser, A. R., Waldman, T., Zipper, L. M., Aigner, A., Byers, S. W., Riegel, A. T., and Wellstein, A. (2003) *Cancer Res* **63**(23), 8085-8089
98.   Aigner, A., Ray, P. E., Czubayko, F., and Wellstein, A. (2002) *Histochem Cell Biol* **117**(1), 1-11
99.   McDonnell, K., Bowden, E. T., Cabal-Manzano, R., Hoxter, B., Riegel, A. T., and Wellstein, A. (2005) *Lab Invest* **85**(6), 747-755
100. Liu, X. H., Aigner, A., Wellstein, A., and Ray, P. E. (2001) *Kidney Int* **59**(5), 1717-1728.
101. Napoli, C., de Nigris, F., Welch, J. S., Calara, F. B., Stuart, R. O., Glass, C. K., and Palinski, W. (2002) *Circulation* **105**(11), 1360-1367
102. Blumberg, P. M. (1988) *Cancer Res* **48**, 1-8
103. Harris, V. K., Liaudet-Coopman, E. D., Boyle, B. J., Wellstein, A., and Riegel, A. T. (1998) *J Biol Chem* **273**(30), 19130-19139
104. Harris, V. K., Coticchia, C. M., Kagan, B. L., Ahmad, S., Wellstein, A., and Riegel, A. T. (2000) *J Biol Chem* **275**(15), 10802-10811.
105. Harris, V. K., Kagan, B. L., Ray, R., Coticchia, C. M., Liaudet-Coopman, E. D., Wellstein, A., and Tate Riegel, A. (2001) *Oncogene* **20**(14), 1730-1738.
106. Lippman, S. M., Kessler, J. F., and F.L.JR., M. (1987) *Cancer Treat.Rep.* **71**, 493-515
107. Lippman, S. M., Kessler, J. F., and Meyskens, F. L. J. (1987) *Cancer Treat.Rep.* **71**, 391-405
108. Jetten, A. M., Kim, J. S., Sacks, P. G., Rearick, J. I., Lotan, D., Hong, W. K., and Lotan, R. (1990) *Int J Cancer* **45**(1), 195-202
109. Lotan, R. (1994) *Cancer Res.* **54**, 1987s-1990s
110. Bertram, J. S., Kolonel, L. N., and Meyskens, F. R. J. (1987) *Cancer Res.* **47**, 3012-3031
111. Moon, R. C., and Mehta, R. G. (1990) *Chemistry and Biology of Synthetic Retinoids*, CRC Press, Boca Raton,FL
112. Pollard, M., Luckert, P., and Sporn, M. (1991) *Cancer Res.* **51**, 3610-3611
113. Shklar, G., Schwartz, J., Grau, D., Trickler, D., and Wallace, K. D. (1980) *Oral Surgery* **50**, 45-52
114. Abemayor, E. (1992) *Laryngoscope* **102**, 1133-1149
115. Dmitrovsky, E., and Bosl, G. J. (1992) *J Natl Cancer Inst* **84**(4), 218-219.
116. Lippman, S. M., Heyman, R. A., Kurie, J. M., Benner, S. E., and Hong, W. K. (1995) *J Cell Biochem Suppl* **22**, 1-10
117. Tallman, M. S., and Wiernik, P. H. (1992) *J Clin Pharmacol* **32**(10), 868-888.
118. Khuri, F. R., Lippman, S. M., Spitz, M. R., Lotan, R., and Hong, W. K. (1997) *J Natl Cancer Inst* **89**(3), 199-211.
119. Kim, J. W., Kim, Y. T., Choi, S. M., Kim, D. K., and Song, C. H. (1996) *Am J Clin Oncol* **19**(5), 442-444.
120. Aigner, A., Malerczyk, C., Houghtling, R., and Wellstein, A. (2000) *Growth Factors* **18**(1), 51-62
121. Liaudet-Coopman, E. D. E., and Wellstein, A. (1996) *J.Biol.Chem.* **271**, 21303-21308

122.   Liaudet-Coopman, E. D. E., Berchem, G. J., and Wellstein, A. (1997) *Clinical Cancer Research* **3**, 179-184

123.   Boyle, B. J., Harris, V. K., Liaudet-Coopman, E. D., Riegel, A. T., and Wellstein, A. (2000) *Biochem Pharmacol* **60**(11), 1677-1684.

124.   Rosini, P., Bonaccorsi, L., Baldi, E., Chiasserini, C., Forti, G., De Chiara, G., Lucibello, M., Mongiat, M., Iozzo, R. V., Garaci, E., Cozzolino, F., and Torcia, M. G. (2002) *Prostate* **53**(4), 310-321

125.   Lametsch, R., Rasmussen, J. T., Johnsen, L. B., Purup, S., Sejrsen, K., Petersen, T. E., and Heegaard, C. W. (2000) *J Biol Chem* **275**(26), 19469-19474

126.   Barr, P. J. (1991) *Cell* **66**(1), 1-3

127.   Wang, X. C., Chen, J. H., Crab, J. W., and Sato, J. D. (1998) *Biochem Mol Biol Int* **46**(1), 81-87

128.   Mongiat, M., Otto, J., Oldershaw, R., Ferrer, F., Sato, J. D., and Iozzo, R. V. (2001) *J Biol Chem* **276**(13), 10263-10271.

129.   Cardin, A. D., and Weintraub, H. J. (1989) *Arteriosclerosis* **9**(1), 21-32

130.   Aigner, A., Butscheid, M., Kunkel, P., Krause, E., Lamszus, K., Wellstein, A., and Czubayko, F. (2001) *Int J Cancer* **92**(4), 510-517.

131.   Sauter, E. R., Nesbit, M., Tichansky, D., Liu, Z. J., Shirakawa, T., Palazzo, J., and Herlyn, M. (2001) *Int J Cancer* **92**(3), 374-381

132.   Wellstein, A., and Czubayko, F. (1996) *Breast Cancer Res.Treat.* **38**, 109-119

133.   Chen, J. H., Wang, X. C., and Sato, J. D. (2001) *Cell Biol Int* **25**(6), 567-570

134.   Rak, J., and Kerbel, R. S. (1997) *Nat Med* **3**(10), 1083-1084.

135.   Yamamoto, T., Ikawa, S., Akiyama, T., Semba, K., Nomura, N., Miyajima, N., Saito, T., and Toyoshima, K. (1986) *Nature* **319**(6050), 230-234.

136.   Bargmann, C. I., Hung, M. C., and Weinberg, R. A. (1986) *Cell* **45**, 649-657

137.   Schechter, A. L., Stern, D. F., Vaidyanathan, L., Decker, S. J., Drebin, J. A., Greene, M. I., and Weinberg, R. A. (1984) *Nature* **312**(5994), 513-516.

138.   Shih, C., Padhy, L. C., Murray, M., and Weinberg, R. A. (1981) *Nature* **290**(5803), 261-264

139.   Ullrich, A., Coussens, L., Hayflick, J. S., Dull, T. J., Gray, A., Tam, A. W., Lee, J., Yarden, Y., Libermann, T. A., Schlessinger, J., and et al. (1984) *Nature* **309**(5967), 418-425.

140.   Riese, D. J., 2nd, and Stern, D. F. (1998) *Bioessays* **20**(1), 41-48

141.   Lupu, R., Cardillo, M., Harris, L., Hijazi, M., and Rosenberg, K. (1995) *Semin Cancer Biol* **6**(3), 135-145

142.   van der Geer, P., Hunter, T., and Lindberg, R. A. (1994) *Annu Rev Cell Biol* **10**, 251-337

143.   Earp, H. S., Dawson, T. L., Li, X., and Yu, H. (1995) *Breast Cancer Res Treat* **35**(1), 115-132

144.   Guy, P. M., Platko, J. V., Cantley, L. C., Cerione, R. A., and Carraway, K. L., 3rd. (1994) *Proc Natl Acad Sci U S A* **91**(17), 8132-8136

145.   Carraway III, K. L., and Cantley, L. C. (1994) *Cell* **78**, 5-8

146.   Marmor, M. D., Skaria, K. B., and Yarden, Y. (2004) *Int J Radiat Oncol Biol Phys* **58**(3), 903-913

147.   Akiyama, T., Saito, T., Ogawara, H., Toyoshima, K., and Yamamoto, T. (1988) *Mol Cell Biol* **8**(3), 1019-1026

148.   Kokai, Y., Myers, J. N., Wada, T., Brown, V. I., LeVea, C. M., Davis, J. G., Dobashi, K., and Greene, M. I. (1989) *Cell* **58**(2), 287-292

149.   Connelly, P. A., and Stern, D. F. (1990) *Proc Natl Acad Sci U S A* **87**(16), 6054-6057

150.   Burgess, A. W., Cho, H. S., Eigenbrot, C., Ferguson, K. M., Garrett, T. P., Leahy, D. J., Lemmon, M. A., Sliwkowski, M. X., Ward, C. W., and Yokoyama, S. (2003) *Mol Cell* **12**(3), 541-552

151.   Garrett, T. P., McKern, N. M., Lou, M., Elleman, T. C., Adams, T. E., Lovrecz, G. O., Zhu, H. J., Walker, F., Frenkel, M. J., Hoyne, P. A., Jorissen, R. N., Nice, E. C., Burgess, A. W., and Ward, C. W. (2002) *Cell* **110**(6), 763-773

152.   Ogiso, H., Ishitani, R., Nureki, O., Fukai, S., Yamanaka, M., Kim, J. H., Saito, K., Sakamoto, A., Inoue, M., Shirouzu, M., and Yokoyama, S. (2002) *Cell* **110**(6), 775-787

153.   Cho, H. S., and Leahy, D. J. (2002) *Science* **297**(5585), 1330-1333

154.   Ferguson, K. M., Berger, M. B., Mendrola, J. M., Cho, H. S., Leahy, D. J., and Lemmon, M. A. (2003) *Mol Cell* **11**(2), 507-517

155.   Garrett, T. P., McKern, N. M., Lou, M., Elleman, T. C., Adams, T. E., Lovrecz, G. O., Kofler, M., Jorissen, R. N., Nice, E. C., Burgess, A. W., and Ward, C. W. (2003) *Mol Cell* **11**(2), 495-505

156.   Cho, H. S., Mason, K., Ramyar, K. X., Stanley, A. M., Gabelli, S. B., Denney, D. W., Jr., and Leahy, D. J. (2003) *Nature* **421**(6924), 756-760

157.   Hynes, N. E., and Lane, H. A. (2005) *Nat Rev Cancer* **5**(5), 341-354

158.   Heldin, C. H. (1995) *Cell* **80**(2), 213-223.

159.   Hubbard, S. R., Mohammadi, M., and Schlessinger, J. (1998) *J Biol Chem* **273**(20), 11987-11990

160.   Schlessinger, J. (2000) *Cell* **103**(2), 211-225

161. Pinkas-Kramarski, R., Soussan, L., Waterman, H., Levkowitz, G., Alroy, I., Klapper, L., Lavi, S., Seger, R., Ratzkin, B. J., Sela, M., and Yarden, Y. (1996) *EMBO J* **15**, 2452-2467

162. Tzahar, E., Waterman, H., Chen, X., Levkowitz, G., Karunagaran, D., Lavi, S., Ratzkin, B. J., and Yarden, Y. (1996) *Mol Cell Biol* **16**, 5276-5287

163. Lenferink, A. E., Pinkas-Kramarski, R., van de Poll, M. L., van Vugt, M. J., Klapper, L. N., Tzahar, E., Waterman, H., Sela, M., van Zoelen, E. J., and Yarden, Y. (1998) *Embo J* **17**(12), 3385-3397

164. Worthylake, R., Opresko, L. K., and Wiley, H. S. (1999) *J Biol Chem* **274**(13), 8865-8874

165. Karunagaran, D., Tzahar, E., Beerli, R. R., Chen, X., Graus-Porta, D., Ratzkin, B. J., Seger, R., Hynes, N. E., and Yarden, Y. (1996) *EMBO J* **15**, 254-264

166. Sliwkowski, M. X., Schaefer, G., Akita, R. W., Lofgren, J. A., Fitzpatrick, V. D., Nuijens, A., Fendly, B. M., Cerione, R. A., Vandlen, R. L., and Carraway, K. L., III. (1994) *J.Biol.Chem.* **269**, 14661-14665

167. Pinkas-Kramarski, R., Shelly, M., Glathe, S., Ratzkin, B. J., and Yarden, Y. (1996) *J.Biol.Chem.* **271**, 19029-19032

168. Riese, D. J., II., van Raaij, T. M., Plowman, G. D., Andrews, G. C., and Stern, D. F. (1995) *Molecular and Cellular Biology* **15**, 5770-5776

169. Jones, J. T., Akita, R. W., and Sliwkowski, M. X. (1999) *FEBS Lett* **447**(2-3), 227-231

170. Alimandi, M., Romano, A., Curia, M. C., Muraro, R., Fedi, P., Aaronson, S. A., Di Fiore, P. P., and Kraus, M. H. (1995) *Oncogene* **10**, 1813-1821

171. Yen, L., Benlimame, N., Nie, Z. R., Xiao, D., Wang, T., Al Moustafa, A. E., Esumi, H., Milanini, J., Hynes, N. E., Pages, G., and Alaoui-Jamali, M. A. (2002) *Mol Biol Cell* **13**(11), 4029-4044

172. Holbro, T., Civenni, G., and Hynes, N. E. (2003) *Exp Cell Res* **284**(1), 99-110

173. Carpenter, G. (1999) *J Cell Biol* **146**(4), 697-702

174. Blume-Jensen, P., and Hunter, T. (2001) *Nature* **411**(6835), 355-365

175. Prenzel, N., Fischer, O. M., Streit, S., Hart, S., and Ullrich, A. (2001) *Endocr Relat Cancer* **8**(1), 11-31

176. Bos, J. L. (1989) *Cancer Res* **49**(17), 4682-4689

177. Johnson, G. L., and Vaillancourt, R. R. (1994) *Curr Opin Cell Biol* **6**(2), 230-238

178. Salomon, D. S., Brandt, R., Ciardiello, F., and Normanno, N. (1995) *Crit Rev Oncol Hematol* **19**(3), 183-232.

179. Lonardo, F., Di Marco, E., King, C. R., Pierce, J. H., Segatto, O., Aaronson, S. A., and Di Fiore, P. P. (1990) *New Biol* **2**(11), 992-1003.

180. Di Fiore, P. P., Pierce, J. H., Kraus, M. H., Segatto, O., King, C. R., and Aaronson, S. A. (1987) *Science* **237**, 178-182

181. Di Marco, E., Pierce, J. H., Knicley, C. L., and Di Fiore, P. P. (1990) *Mol Cell Biol* **10**(6), 3247-3252

182. Segatto, O., King, C. R., Pierce, J. H., Di Fiore, P. P., and Aaronson, S. A. (1988) *Mol Cell Biol* **8**(12), 5570-5574

183. Siegel, P. M., Ryan, E. D., Cardiff, R. D., and Muller, W. J. (1999) *Embo J* **18**(8), 2149-2164

184. Cohen, B. D., Kiener, P. A., Green, J. M., Foy, L., Fell, H. P., and Zhang, K. (1996) *J Biol Chem* **271**(48), 30897-30903

185. Zhang, K., Sun, J., Liu, N., Wen, D., Chang, D., Thomason, A., and Yoshinaga, S. K. (1996) *J Biol Chem* **271**(7), 3884-3890

186. Gilbertson, R. J., Perry, R. H., Kelly, P. J., Pearson, A. D., and Lunec, J. (1997) *Cancer Res* **57**(15), 3272-3280

187. Xia, W., Lau, Y. K., Zhang, H. Z., Xiao, F. Y., Johnston, D. A., Liu, A. R., Li, L., Katz, R. L., and Hung, M. C. (1999) *Clin Cancer Res* **5**(12), 4164-4174

188. Hellstrom, I., Goodman, G., Pullman, J., Yang, Y., and Hellstrom, K. E. (2001) *Cancer Res* **61**(6), 2420-2423

189. Slamon, D. J., Godolphin, W., Jones, L. A., Holt, J. A., Wong, S. G., Keith, D. E., Levin, W. J., Stuart, S. G., Udove, J., and Ullrich, A. (1989) *Science* **244**, 707-712

190. Yu, D., and Hung, M. C. (2000) *Oncogene* **19**(53), 6115-6121.

191. Baselga, J., Seidman, A. D., Rosen, P. P., and Norton, L. (1997) *Oncology (Huntingt)* **11**(3 Suppl 2), 43-48.

192. Pegram, M. D., Finn, R. S., Arzoo, K., Beryt, M., Pietras, R. J., and Slamon, D. J. (1997) *Oncogene* **15**(5), 537-547.

193. Burke, H. B., Hoang, A., Iglehart, J. D., and Marks, J. R. (1998) *Cancer* **82**(5), 874-877.

194. Pirollo, K. F., Hao, Z., Rait, A., Ho, C. W., and Chang, E. H. (1997) *Biochem Biophys Res Commun* **230**(1), 196-201.

195. Tsai, C. M., Chang, K. T., Chen, J. Y., Chen, Y. M., Chen, M. H., and Perng, R. P. (1996) *Cancer Res* **56**(4), 794-801

196. Yu, D., Jing, T., Sun, D., Price, J. E., Singletary, S. E., Ibrahim, N., Hortobagyi, G. N., and Hung, M. C. (1998) *Oncogene* **16 (16)**, 2087-2094

197. Yu, D., Jing, T., Liu, B., Yao, J., Tan, M., McDonnell, T. J., and Hung, M. C. (1998) *Mol Cell* **2**(5), 581-591.

198. Colomer, R., Lupu, R., Bacus, S. S., and Gelman, E. P. (1994) *Br.J Cancer* **70**, 819-825

199. Baselga, J., Norton, L., Albanell, J., Kim, Y. M., and Mendelsohn, J. (1998) *Cancer Research* **58 (13)**, 2825-2831

200. Hancock, M. C., Langton, B. C., Chan, T., Toy, P., Monahan, J. J., Mischak, R. P., and Shawver, L. K. (1991) *Cancer Res* **51**(17), 4575-4580

201. Pietras, R. J., Fendly, B. M., Chazin, V. R., Pegram, M. D., Howell, S. B., and Slamon, D. J. (1994) *Oncogene.* **9**, 1829-1838

202. Slamon, D. J., Leyland-Jones, B., Shak, S., Fuchs, H., Paton, V., Bajamonde, A., Fleming, T., Eiermann, W., Wolter, J., Pegram, M., Baselga, J., and Norton, L. (2001) *N Engl J Med* **344**(11), 783-792

203. Gusterson, B. A., Gelber, R. D., Goldhirsch, A., Price, K. N., Save-Soderborgh, J., Anbazhagan, R., Styles, J., Rudenstam, C. M., Golouh, R., and Reed, R. (1992) *Journal of Clinical Oncology* **10**, 1049-1056

204. Muss, H. B., Thor, A. D., Berry, D. A., Kute, T., Liu, E. T., Koerner, F., Cirrincione, C. T., Budman, D. R., Wood, W. C., Barcos, M., and Henderson, I. C. (1994) *N.Engl.J Med.* **330**, 1260-1266

205. Tetu, B., and Brisson, J. (1994) *Cancer* **73**(9), 2359-2365

206. Fehm, T., Maimonis, P., Weitz, S., Teramoto, Y., Katalinic, A., and Jager, W. (1997) *Breast Cancer Res Treat* **43**(1), 87-95

207. Mehta, R. R., McDermott, J. H., Hieken, T. J., Marler, K. C., Patel, M. K., Wild, L. D., and Das Gupta, T. K. (1998) *J Clin Oncol* **16**(7), 2409-2416

208. Brader, K. R., Wolf, J. K., Hung, M. C., Yu, D., Crispens, M. A., van Golen, K. L., and Price, J. E. (1997) *Clin Cancer Res* **3**(11), 2017-2024

209. Ueno, N. T., Bartholomeusz, C., Herrmann, J. L., Estrov, Z., Shao, R., Andreeff, M., Price, J., Paul, R. W., Anklesaria, P., Yu, D., and Hung, M. C. (2000) *Clin Cancer Res* **6**(1), 250-259

210. Aigner, A., Hsieh, S. S., Malerczyk, C., and Czubayko, F. (2000) *Toxicology* **144**(1-3), 221-228

211. Duan, Z., Feller, A. J., Penson, R. T., Chabner, B. A., and Seiden, M. V. (1999) *Clin Cancer Res* **5**(11), 3445-3453

212. Drebin, J. A., Stern, D. F., Link, V. C., Weinberg, R. A., and Greene, M. I. (1984) *Nature* **312**(5994), 545-548

213. Flanagan, J. G., and Leder, P. (1988) *Proc Natl Acad Sci U S A* **85**(21), 8057-8061

214. Kasprzyk, P. G., Song, S. U., Di Fiore, P. P., and King, C. R. (1992) *Cancer Res* **52**(10), 2771-2776

215. Shepard, H. M., Lewis, G. D., Sarup, J. C., Fendly, B. M., Maneval, D., Mordenti, J., Figari, I., Kotts, C. E., Palladino, M. A., Jr., Ullrich, A., and et al. (1991) *J Clin Immunol* **11**(3), 117-127.

216. Pegram, M. D., Lipton, A., Hayes, D. F., Weber, B. L., Baselga, J. M., Tripathy, D., Baly, D., Baughman, S. A., Twaddell, T., Glaspy, J. A., and Slamon, D. J. (1998) *Journal of Clinical Oncology* **16 (8)**, 2659-2671

217. Dickman, S. (1998) *Science* **280**(5367), 1196-1197

218. Baselga, J., Tripathy, D., Mendelsohn, J., Baughman, S., Benz, C. C., Dantis, L., Sklarin, N. T., Seidman, A. D., Hudis, C. A., Moore, J., Rosen, P. P., Twaddell, T., Henderson, I. C., and Norton, L. (1996) *J Clin Oncol* **14**(3), 737-744

219. Pietras, R. J., Pegram, M. D., Finn, R. S., Maneval, D. A., and Slamon, D. J. (1998) *Oncogene* **17**(17), 2235-2249

220. McKeage, K., and Perry, C. M. (2002) *Drugs* **62**(1), 209-243

221. Bookman, M. A., Darcy, K. M., Clarke-Pearson, D., Boothby, R. A., and Horowitz, I. R. (2003) *J Clin Oncol* **21**(2), 283-290

222. Uhlenbeck, O. C. (1987) *Nature* **328**, 596-600

223. Thomson, J. B., Sigurdsson, S. T., Zeuch, A., and Eckstein, F. (1996) *Nucleic Acids Res* **24**(22), 4401-4406

224. Scott, W. G., and Klug, A. (1996) *Trends Biochem Sci* **21**(6), 220-224

225. Doherty, E. A., and Doudna, J. A. (2000) *Annu Rev Biochem* **69**, 597-615

226. Takagi, Y., Warashina, M., Stec, W. J., Yoshinari, K., and Taira, K. (2001) *Nucleic Acids Res* **29**(9), 1815-1834

227. Tekur, S., and Ho, S. M. (2002) *Mol Carcinog* **33**(1), 44-55

228. Kashani-Sabet, M., and Scanlon, K. J. (1995) *Cancer Gene Ther* **2**(3), 213-223

229. Lin, J. S., Song, Y. H., Kong, X. J., Li, B., Liu, N. Z., Wu, X. L., and Jin, Y. X. (2003) *World J Gastroenterol* **9**(3), 572-577

230. Zheng, Y., Zhang, J., and Qu, L. (2002) *Chin Med J (Engl)* **115**(10), 1501-1506

231.   Castanotto, D., Li, J. R., Michienzi, A., Langlois, M. A., Lee, N. S., Puymirat, J., and Rossi, J. J. (2002) *Biochem Soc Trans* **30**(Pt 6), 1140-1145
232.   Tong, Q., Zhao, J., Chen, Z., Zeng, F., and Lu, G. (2003) *Chin Med J (Engl)* **116**(10), 1515-1518
233.   Goodchild, J. (2002) *Expert Opin Ther Targets* **6**(2), 235-247
234.   Goodchild, J. (2000) *Curr Opin Mol Ther* **2**(3), 272-281
235.   Suzuki, T., Anderegg, B., Ohkawa, T., Irie, A., Engebraaten, O., Halks-Miller, M., Holm, P. S., Curiel, D. T., Kashani-Sabet, M., and Scanlon, K. J. (2000) *Gene Ther* **7**(3), 241-248
236.   Wiechen, K., Zimmer, C., and Dietel, M. (1998) *Cancer Gene Ther* **5**(1), 45-51
237.   Czubayko, F., Downing, S. G., Hsieh, S. S., Goldstein, D. J., Lu, P. Y., Trapnell, B. C., and Wellstein, A. (1997) *Gene Therapy* **4**, 943-949
238.   Juhl, H., Downing, S., Hssieh, S., Wellstein, A., and Czubayko, F. (1997) *Langenbecks.Arch.Chir.Suppl.Kongressbd.* **114**, 41-45
239.   Slichenmyer, W. J., and Fry, D. W. (2001) *Semin Oncol* **28**(5 Suppl 16), 67-79
240.   Ciardiello, F., Caputo, R., Bianco, R., Damiano, V., Fontanini, G., Cuccato, S., De Placido, S., Bianco, A. R., and Tortora, G. (2001) *Clin Cancer Res* **7**(5), 1459-1465
241.   Sirotnak, F. M., Zakowski, M. F., Miller, V. A., Scher, H. I., and Kris, M. G. (2000) *Clin Cancer Res* **6**(12), 4885-4892
242.   Ciardiello, F., Caputo, R., Bianco, R., Damiano, V., Pomatico, G., De Placido, S., Bianco, A. R., and Tortora, G. (2000) *Clin Cancer Res* **6**(5), 2053-2063
243.   Abuharbeid, S., Apel, J., Zugmaier, G., Knabbe, C., Sander, M., Gilbert, S., Czubayko, F., and Aigner, A. (2005) *Naunyn Schmiedebergs Arch Pharmacol* **371**(2), 141-151
244.   Rait, A. S., Pirollo, K. F., Ulick, D., Cullen, K., and Chang, E. H. (2003) *Ann N Y Acad Sci* **1002**, 78-89
245.   Roh, H., Pippin, J., and Drebin, J. A. (2000) *Cancer Res* **60**(3), 560-565
246.   Faltus, T., Yuan, J., Zimmer, B., Kramer, A., Loibl, S., Kaufmann, M., and Strebhardt, K. (2004) *Neoplasia* **6**(6), 786-795
247.   Urban-Klein, B., Werth, S., Abuharbeid, S., Czubayko, F., and Aigner, A. (2005) *Gene Ther* **12**(5), 461-466
248.   Offterdinger, M., Schneider, S. M., Huber, H., and Grunt, T. W. (1998) *Biochem Biophys Res Commun* **251**(3), 907-913
249.   Grunt Th, W., Dittrich, E., Offterdinger, M., Schneider, S. M., Dittrich, C., and Huber, H. (1998) *Br J Cancer* **78**(1), 79-87
250.   Lu, H., Qin, H., and Zhang, Y. (2000) *Zhonghua Zhong Liu Za Zhi* **22**(5), 370-373
251.   Zang, R. Y., Shi, D. R., Lu, H. J., Cai, S. M., Lu, D. R., Zhang, Y. J., and Qin, H. L. (2001) *Int J Gynecol Cancer* **11**(1), 18-23
252.   Ueno, N. T., Yu, D., and Hung, M. C. (1997) *Oncogene* **15**(8), 953-960
253.   Deshane, J., Grim, J., Loechel, S., Siegal, G. P., Alvarez, R. D., and Curiel, D. T. (1996) *Cancer Gene Ther* **3**(2), 89-98
254.   Neve, R. M., Nielsen, U. B., Kirpotin, D. B., Poul, M. A., Marks, J. D., and Benz, C. C. (2001) *Biochem Biophys Res Commun* **280**(1), 274-279
255.   George Gi, C. T., Ojima i, Vyas DM. (1995) *Taxane anticancer agents: basic science and current status*, Washington DC. American chemical Sociaty.
256.   M., S. (1995) *Taxol: science and applications*, New York: CRC Press
257.   Horwitz, S. B., Cohen, D., Rao, S., Ringel, I., Shen, H. J., and Yang, C. P. (1993) *J Natl Cancer Inst Monogr* (15), 55-61
258.   Jordan, M. A., Toso, R. J., Thrower, D., and Wilson, L. (1993) *Proc Natl Acad Sci U S A* **90**(20), 9552-9556
259.   Rao, S., Orr, G. A., Chaudhary, A. G., Kingston, D. G., and Horwitz, S. B. (1995) *J Biol Chem* **270**(35), 20235-20238
260.   Combeau, C., Commercon, A., Mioskowski, C., Rousseau, B., Aubert, F., and Goeldner, M. (1994) *Biochemistry* **33**(21), 6676-6683
261.   Parness, J., and Horwitz, S. B. (1981) *J Cell Biol* **91**(2 Pt 1), 479-487
262.   Ding, A., Sanchez, E., and Nathan, C. F. (1993) *J Immunol* **151**(10), 5596-5602
263.   Wolfson, M., Yang, C. P., and Horwitz, S. B. (1997) *Int J Cancer* **70**(2), 248-252
264.   Blagosklonny, M. V., Schulte, T., Nguyen, P., Trepel, J., and Neckers, L. M. (1996) *Cancer Res* **56**(8), 1851-1854
265.   Fan, W. (1999) *Biochem Pharmacol* **57**(11), 1215-1221
266.   Tudor, G., Aguilera, A., Halverson, D. O., Laing, N. D., and Sausville, E. A. (2000) *Cell Death Differ* **7**(6), 574-586
267.   Haldar, S., Chintapalli, J., and Croce, C. M. (1996) *Cancer Res* **56**(6), 1253-1255

268. Ding, A. H., Porteu, F., Sanchez, E., and Nathan, C. F. (1990) *Science* **248**(4953), 370-372

269. Basu, A., and Haldar, S. (1998) *Int J Oncol* **13**(4), 659-664

270. Blagosklonny, M. V., Schulte, T. W., Nguyen, P., Mimnaugh, E. G., Trepel, J., and Neckers, L. (1995) *Cancer Res* **55**(20), 4623-4626

271. Hajto, T., Hostanska, K., and Gabius, H. J. (1989) *Cancer Res* **49**(17), 4803-4808.

272. Beuth, J., Ko, H. L., Gabius, H. J., Burrichter, H., Oette, K., and Pulverer, G. (1992) *Clin Investig* **70**(8), 658-661

273. Kleinen, J., and Knipschild, P. (1994) *Phytomedicine* **1**, 255-260

274. Endo, Y., Tsurugi, K., and Franz, H. (1988) *FEBS Lett* **231**(2), 378-380.

275. Williams, J. M., Lea, N., Lord, J. M., Roberts, L. M., Milford, D. V., and Taylor, C. M. (1997) *Toxicol Lett* **91**(2), 121-127

276. Brooks, S. A., and Leathem, A. J. (1998) *Invasion Metastasis* **18**(3), 115-121

277. Mockel, B., Schwarz, T., Zinke, H., Eck, J., Langer, M., and Lentzen, H. (1997) *Arzneimittelforschung* **47**(10), 1145-1151

278. Baxevanis, C. N., Voutsas, I. F., Soler, M. H., Gritzapis, A. D., Tsitsilonis, O. E., Stoeva, S., Voelter, W., Arsenis, P., and Papamichail, M. (1998) *Immunopharmacol Immunotoxicol* **20**(3), 355-372

279. Hajto, T. (1986) *Oncology* **43 Suppl 1**, 51-65

280. Vehmeyer, K., Hajto, T., Hostanska, K., Konemann, S., Loser, H., Saller, R., and Wormann, B. (1998) *Eur J Haematol* **60**(1), 16-20

281. Eck, J., Langer, M., Mockel, B., Witthohn, K., Zinke, H., and Lentzen, H. (1999) *Eur J Biochem* **265**(2), 788-797.

282. Eck, J., Langer, M., Mockel, B., Baur, A., Rothe, M., Zinke, H., and Lentzen, H. (1999) *Eur J Biochem* **264**(3), 775-784.

283. Langer, M., Mockel, B., Eck, J., Zinke, H., and Lentzen, H. (1999) *Biochem Biophys Res Commun* **264**(3), 944-948.

284. Hajto, T., Hostanska, K., Weber, K., Zinke, H., Fischer, J., Mengs, U., Lentzen, H., and Saller, R. (1998) *Nat Immun* **16**(1), 34-46

285. Schumacher, U., Feldhaus, S., and Mengs, U. (2000) *Cancer Lett* **150**(2), 171-175.

286. Schaffrath, B., Mengs, U., Schwarz, T., Hilgers, R. D., Beuth, J., Mockel, B., Lentzen, H., and Gerstmayer, B. (2001) *Anticancer Res* **21**(6A), 3981-3987

287. Hostanska, K., Vuong, V., Rocha, S., Soengas, M. S., Glanzmann, C., Saller, R., Bodis, S., and Pruschy, M. (2003) *Br J Cancer* **88**(11), 1785-1792

288. Muthing, J., Burg, M., Mockel, B., Langer, M., Metelmann-Strupat, W., Werner, A., Neumann, U., Peter-Katalinic, J., and Eck, J. (2002) *Glycobiology* **12**(8), 485-497

289. Muthing, J., Meisen, I., Bulau, P., Langer, M., Witthohn, K., Lentzen, H., Neumann, U., and Peter-Katalinic, J. (2004) *Biochemistry* **43**(11), 2996-3007

290. Elsasser-Beile, U., Ruhnau, T., Freudenberg, N., Wetterauer, U., and Mengs, U. (2001) *Cancer* **91**(5), 998-1004.

291. Schumer, J., Klocker, J., Tidstrand, J., Rab, B., and Allmayer, H. (1990) *Onkologie.* **13**, 310-312

292. Schoffski, P., Breidenbach, I., Krauter, J., Bolte, O., Stadler, M., Ganser, A., Wilhelm-Ogunbiyi, K., and Lentzen, H. (2005) *Eur J Cancer* **41**(10), 1431-1438

293. Brinton, L. A., Moghissi, K. S., Scoccia, B., Westhoff, C. L., and Lamb, E. J. (2005) *Fertil Steril* **83**(2), 261-274; quiz 525-266

294. Swenerton, K. D., Hislop, T. G., Spinelli, J., LeRiche, J. C., Yang, N., and Boyes, D. A. (1985) *Obstet Gynecol* **65**(2), 264-270

295. Scully, R. E., Young, R. H., and Clement, P. B. (1998) *Tumors of the ovary, maldeveloped gonads, fallopian tube, and broad ligament*, 3rd series, Atlas of tumor pathology, fasc 23. Armed Forces Institute of Pathology, Washington, DC

296. Kurmann, R. J. (1994) *Blaustein's Pathology of the Female Genital Tract*, 4th Ed., Springer-Verlag, New York

297. Gompel, C., and Silverberg, S. G. (1994) *Pathology in Gynecology and Obstetrics*, 4th Ed., Lippincott, Philadelphia

298. Weinberg, R. A. (1996) *Sci Am* **275**(3), 62-70

299. Stratton, J. F., Gayther, S. A., Russell, P., Dearden, J., Gore, M., Blake, P., Easton, D., and Ponder, B. A. (1997) *N Engl J Med* **336**(16), 1125-1130

300. Struewing, J. P., Hartge, P., Wacholder, S., Baker, S. M., Berlin, M., McAdams, M., Timmerman, M. M., Brody, L. C., and Tucker, M. A. (1997) *N Engl J Med* **336**(20), 1401-1408

301. Bast, R. C., Jr., Jacobs, I., and Berchuck, A. (1992) *J Natl Cancer Inst* **84**(8), 556-558

302. Laemmli, U. K. (1970) *Nature* **227**(5259), 680-685

303.   Butscheid, M. (2003) Untersuchungen zu einem tumorrelevanten, FGF-bindenden Protein (FGF-BP), Department of Phamacology and Toxicology, Philipps-University, Marburg, PhD. Thesis
304.   Helenius, A., Marquardt, T., and Braakman, I. (1992) *Trends Cell Biol* **2**(8), 227-231
305.   Gething, M. J., and Sambrook, J. (1992) *Nature* **355**(6355), 33-45
306.   Helenius, A. (1994) *Mol Biol Cell* **5**(3), 253-265
307.   Wellstein, A., Lupu, R., Zugmaier, G., Flamm, S. L., Cheville, A. L., Delli Bovi, P., Basilico, C., Lippman, M. E., and Kern, F. G. (1990) *Cell Growth Differ.* **1**, 63-71
308.   Asada, N., Tanaka, Y., Hayashido, Y., Toratani, S., Kan, M., Kitamoto, M., Nakanishi, T., Kajiyama, G., Chayama, K., and Okamoto, T. (2003) *In Vitro Cell Dev Biol Anim* **39**(7), 321-328
309.   Hsieh, S. S., Malerczyk, C., Aigner, A., and Czubayko, F. (2000) *Int J Cancer* **86**(5), 644-651
310.   Kroning, R., and Lichtenstein, A. (1998) *Leuk Res* **22**(3), 275-286
311.   Srivastava, R. K., Sasaki, C. Y., Hardwick, J. M., and Longo, D. L. (1999) *J Exp Med* **190**(2), 253-265
312.   Patel, T., Gores, G. J., and Kaufmann, S. H. (1996) *Faseb J* **10**(5), 587-597
313.   Abuharbeid, S., Apel, J., Sander, M., Fiedler, B., Langer, M., Zuzarte, M. L., Czubayko, F., and Aigner, A. (2004) *Biochem Biophys Res Commun* **321**(2), 403-412
314.   Landis, S. H., Murray, T., Bolden, S., and Wingo, P. A. (1999) *CA Cancer J Clin* **49**(1), 8-31, 31
315.   Holschneider, C. H., and Berek, J. S. (2000) *Semin Surg Oncol* **19**(1), 3-10
316.   Crickard, K., Gross, J. L., Crickard, U., Yoonessi, M., Lele, S., Herblin, W. F., and Eidsvoog, K. (1994) *Gynecol Oncol* **55**(2), 277-284
317.   Fujimoto, J., Ichigo, S., Hori, M., Hirose, R., Sakaguchi, H., and Tamaya, T. (1997) *Cancer Lett* **111**(1-2), 21-26
318.   Whitworth, M. K., Backen, A. C., Clamp, A. R., Wilson, G., McVey, R., Friedl, A., Rapraeger, A. C., David, G., McGown, A., Slade, R. J., Gallagher, J. T., and Jayson, G. C. (2005) *Clin Cancer Res* **11**(12), 4282-4288
319.   Feeley, K. M., and Wells, M. (2001) *Histopathology* **38**(2), 87-95
320.   Aunoble, B., Sanches, R., Didier, E., and Bignon, Y. J. (2000) *Int J Oncol* **16**(3), 567-576
321.   Michigami, T., Suga, A., Yamazaki, M., Shimizu, C., Cai, G., Okada, S., and Ozono, K. (1999) *J Biol Chem* **274**(47), 33531-33538
322.   Moede, T., Leibiger, B., Pour, H. G., Berggren, P., and Leibiger, I. B. (1999) *FEBS Lett* **461**(3), 229-234
323.   Walter, P., Gilmore, R., and Blobel, G. (1984) *Cell* **38**(1), 5-8
324.   Rapoport, T. A., Jungnickel, B., and Kutay, U. (1996) *Annu Rev Biochem* **65**, 271-303
325.   Palade, G. (1975) *Science* **189**(4200), 347-358
326.   Rothman, J. E., and Wieland, F. T. (1996) *Science* **272**(5259), 227-234
327.   Schekman, R., and Orci, L. (1996) *Science* **271**(5255), 1526-1533
328.   Mellman, I., and Warren, G. (2000) *Cell* **100**(1), 99-112
329.   Nickel, W., Brugger, B., and Wieland, F. T. (2002) *J Cell Sci* **115**(Pt 16), 3235-3240
330.   Hauri, H. P., Kappeler, F., Andersson, H., and Appenzeller, C. (2000) *J Cell Sci* **113 (Pt 4)**, 587-596
331.   Klumperman, J., Schweizer, A., Clausen, H., Tang, B. L., Hong, W., Oorschot, V., and Hauri, H. P. (1998) *J Cell Sci* **111 (Pt 22)**, 3411-3425
332.   Monzat, V., Ratovo, G., Estival, A., Fanjul, M., Bertrand, C., Clement, B., Vaysse, N., Hollande, E., and Clemente, F. (1996) *Eur J Cell Biol* **69**(4), 316-326
333.   Bugler, B., Amalric, F., and Prats, H. (1991) *Mol Cell Biol* **11**(1), 573-577
334.   Florkiewicz, R. Z., Baird, A., and Gonzalez, A. M. (1991) *Growth Factors* **4**(4), 265-275
335.   Mason, I. J. (1994) *Cell* **78**, 547-552
336.   Delrieu, I. (2000) *FEBS Lett* **468**(1), 6-10
337.   Quarto, N., Finger, F. P., and Rifkin, D. B. (1991) *J.Cell Physiol.* **147**, 311-318
338.   Amalric, F., Bouche, G., Bonnet, H., Brethenou, P., Roman, A. M., Truchet, I., and Quarto, N. (1994) *Biochem Pharmacol* **47**(1), 111-115
339.   Engling, A., Backhaus, R., Stegmayer, C., Zehe, C., Seelenmeyer, C., Kehlenbach, A., Schwappach, B., Wegehingel, S., and Nickel, W. (2002) *J Cell Sci* **115**(Pt 18), 3619-3631
340.   Gu, X., and Kay, E. P. (1998) *Invest Ophthalmol Vis Sci* **39**(12), 2252-2258
341.   Choi, J., Ko, M. K., and Kay, E. P. (2000) *Mol Vis* **6**, 222-231
342.   Roghani, M., and Moscatelli, D. (1992) *J Biol Chem* **267**(31), 22156-22162
343.   Rusnati, M., Urbinati, C., and Presta, M. (1993) *J Cell Physiol* **154**(1), 152-161
344.   Murono, E. P., Washburn, A. L., Goforth, D. P., and Wu, N. (1993) *Mol.Cell Endocrinol.* **98**, 81-90
345.   Bouche, G., Gas, N., Prats, H., Baldin, V., Tauber, J. P., Teissi:e, J., and Amalric, F. (1987) *Proc Natl.Acad Sci.USA* **84**, 6770-6774
346.   Friedman, S., Zhan, X., and Maciag, T. (1994) *Biochem.Biophys.Res Commun.* **198**, 1203-1208

347.   Gualandris, A., Coltrini, D., Bergonzoni, L., Isacchi, A., Tenca, S., Ginelli, B., and Presta, M. (1993) *Growth Factors* **8**(1), 49-60
348.   Sandvig, K., and van Deurs, B. (2002) *FEBS Lett* **529**(1), 49-53
349.   Tsai, B., Ye, Y., and Rapoport, T. A. (2002) *Nat Rev Mol Cell Biol* **3**(4), 246-255
350.   Bossard, C., Laurell, H., Van den Berghe, L., Meunier, S., Zanibellato, C., and Prats, H. (2003) *Nat Cell Biol* **5**(5), 433-439
351.   Prats, H., Party, V., Vagner, S., Van den Berghe, L., Bugler, A., Barlet, A., Bayard, F., Amalric, F., and Prats, A. C. (1994) Human bFGF: regulation of expression, protein/protein interaction. In: EMBO Worckshop on the Molecular and Cellular Biology of FGF and their receptors. Capri, Italy, (Abstract)
352.   Patry, V., Bugler, B., Maret, A., Potier, M., and Prats, H. (1997) *Biochem J* **326 (Pt 1)**, 259-264
353.   Carney, D. N., Gazdar, A. F., and Minna, J. D. (1980) *Cancer Res* **40**(6), 1820-1823
354.   McKenzie, S. J., DeSombre, K. A., Bast, B. S., Hollis, D. R., Whitaker, R. S., Berchuck, A., Boyer, C. M., and Bast, R. C., Jr. (1993) *Cancer* **71**(12), 3942-3946
355.   Berchuck, A. (1995) *J Cell Biochem Suppl* **23**, 223-226
356.   Cirisano, F. D., and Karlan, B. Y. (1996) *J Soc Gynecol Investig* **3**(3), 99-105
357.   Mills, G. B., May, C., Hill, M., Campbell, S., Shaw, P., and Marks, A. (1990) *J Clin Invest* **86**(3), 851-855
358.   Xu, Y., Gaudette, D. C., Boynton, J. D., Frankel, A., Fang, X. J., Sharma, A., Hurteau, J., Casey, G., Goodbody, A., Mellors, A., and et al. (1995) *Clin Cancer Res* **1**(10), 1223-1232
359.   Xu, F., Yu, Y., Le, X. F., Boyer, C., Mills, G. B., and Bast, R. C. (1999) *Clin.Cancer Res.* **5**, 3653-3660.
360.   Yu, D., and Hung, M. C. (2000) *Bioessays* **22**(7), 673-680
361.   Gilbert, S., Schachtele, C., Weinberger, H., and Reissmann, T. (2002) *Eur.J.Cancer* **38**(Suppl.7)
362.   Gibb, R. K., Taylor, D. D., Wan, T., O'Connor, D. M., Doering, D. L., and Gercel-Taylor, C. (1997) *Gynecol Oncol* **65**(1), 13-22
363.   Shtil, A. A., Mandlekar, S., Yu, R., Walter, R. J., Hagen, K., Tan, T. H., Roninson, I. B., and Kong, A. N. (1999) *Oncogene* **18**(2), 377-384
364.   Wang, T. H., Wang, H. S., Ichijo, H., Giannakakou, P., Foster, J. S., Fojo, T., and Wimalasena, J. (1998) *J Biol Chem* **273**(9), 4928-4936
365.   Han, J., Lee, J. D., Bibbs, L., and Ulevitch, R. J. (1994) *Science* **265**(5173), 808-811
366.   Lee, L. F., Li, G., Templeton, D. J., and Ting, J. P. (1998) *J Biol Chem* **273**(43), 28253-28260
367.   Craxton, A., Shu, G., Graves, J. D., Saklatvala, J., Krebs, E. G., and Clark, E. A. (1998) *J Immunol* **161**(7), 3225-3236
368.   Jarvis, W. D., Fornari, F. A., Jr., Tombes, R. M., Erukulla, R. K., Bittman, R., Schwartz, G. K., Dent, P., and Grant, S. (1998) *Mol Pharmacol* **54**(5), 844-856
369.   Ibrado, A. M., Kim, C. N., and Bhalla, K. (1998) *Leukemia* **12**(12), 1930-1936
370.   Kottke, T. J., Blajeski, A. L., Martins, L. M., Mesner, P. W., Jr., Davidson, N. E., Earnshaw, W. C., Armstrong, D. K., and Kaufmann, S. H. (1999) *J Biol Chem* **274**(22), 15927-15936
371.   Ofir, R., Seidman, R., Rabinski, T., Krup, M., Yavelsky, V., Weinstein, Y., and Wolfson, M. (2002) *Cell Death Differ* **9**(6), 636-642
372.   Lowe, S. W., Ruley, H. E., Jacks, T., and Housman, D. E. (1993) *Cell* **74**(6), 957-967
373.   Sherr, C. J. (1998) *Genes Dev* **12**(19), 2984-2991
374.   Harper, J. W., Adami, G. R., Wei, N., Keyomarsi, K., and Elledge, S. J. (1993) *Cell* **75**(4), 805-816
375.   el-Deiry, W. S., Tokino, T., Velculescu, V. E., Levy, D. B., Parsons, R., Trent, J. M., Lin, D., Mercer, W. E., Kinzler, K. W., and Vogelstein, B. (1993) *Cell* **75**(4), 817-825
376.   Moos, P. J., and Fitzpatrick, F. A. (1998) *Cell Growth Differ* **9**(8), 687-697
377.   Makhija, S., Taylor, D. D., Gibb, R. K., and Gercel-Taylor, C. (1999) *Int J Oncol* **14**(3), 515-521
378.   Lamendola, D. E., Duan, Z., Yusuf, R. Z., and Seiden, M. V. (2003) *Cancer Res* **63**(9), 2200-2205
379.   Okano, J., and Rustgi, A. K. (2001) *J Biol Chem* **276**(22), 19555-19564
380.   Kim, M. S., So, H. S., Lee, K. M., Park, J. S., Lee, J. H., Moon, S. K., Ryu, D. G., Chung, S. Y., Jung, B. H., Kim, Y. K., Moon, G., and Park, R. (2000) *Gen Pharmacol* **34**(5), 349-355
381.   Bantel, H., Engels, I. H., Voelter, W., Schulze-Osthoff, K., and Wesselborg, S. (1999) *Cancer Res* **59**(9), 2083-2090

10 ACKNOWLEDGMENTS

11 LIST OF ACADEMIC TEACHERS

Philipps-University, Marburg, Germany:

Prof. Dr. F. Czubayko

PD Dr. A. Aigner

Prof. Dr. G. Seitz

Prof. Dr. M. Petersen

Prof. Dr. T. Kissel

Prof. Dr. U. Matern

Prof. Dr. G. Klebe

Prof. Dr. K. Kuschinsky

Prof. Dr. J. Kriegelstein

Alazhar-University, Gaza, Palestine:

Dr. A. Massoud

Dr. S. Sousi

Dr. N. Khodeir

Dr. A. Hamed

Dr. M. Alsaga

Dr. M. Khatab

Dr. S. Alejbour

12 DECLARATION

I hereby declare that I have worked on my thesis „The Fibroblast Growth Factor-binding Protein (FGF-BP) and the Human Epidermal Growth Factor Receptor-2 (HER-2): Functional Studies on Two Gene Products Relevant in Ovarian Cancer" independently and without assistance, and the work presented here is original.

The thesis has not been submitted in the current or a similar form to any other university.

Parts of the work were published (Chapter 14).

Marburg, August 2005

(Shaker Abuharbeid)

12 Ehrenwörtliche Erklärung

Ich erkläre ehrenwörtlich, dass ich die dem Fachbereich Medizin Marburg zur Promotionsprüfung eingereichte Arbeit mit dem Titel „The Fibroblast Growth Factor-binding Protein (FGF-BP) and the Human Epidermal Growth Factor Receptor-2 (HER-2): Functional Studies on Two Gene Products Relevant in Ovarian Cancer" im Institut für Pharmakologie und Toxikologie der Philipps-Universität Marburg unter Leitung von Prof. Dr. Frank Czubayko ohne sonstige Hilfe selbst durchgeführt und bei der Abfassung der Arbeit keine anderen als die in der Dissertation angeführten Hilfsmittel benutzt habe. Ich habe bisher an keinem in- oder ausländischen Medizinischen Fachbereich ein Gesuch um Zulassung zur Promotion eingereicht, noch die vorliegende oder eine andere Arbeit als Dissertation vorgelegt.

Teile der vorliegenden Arbeit wurden veröffentlicht (Kapitel 14).

Marburg, den ....

(Shaker Abuharbeid)

13 CURRICULUM VITAE

Personal Data:

Name: Abuharbeid

First name: Shaker M H

Date of birth: 23.01.1974

Place of birth: Gaza / Palestine

Marital status: Married, 3 children

Education:

1982-1987   Primary school, Gaza

1987-1989   Secondary school, Gaza

1989-1992   Grammar school, Gaza

1992-1997   Study of Pharmacy, Alazhar-University, Gaza

03.08.1997   Exam; B.Sc. in Pharmacy

09/1997-03/1998   Practical training, Al-Schifa Pharmacy, Gaza

04/1998-01/1999   Employment as a pharmacist, Al-Rimal Clinic, Gaza

03/1999-09/1999   Language course (Speak and Write School), Marburg

10/1999-10/2001   Study of Pharmacy, Philipps-University, Marburg

31.10.2001   Final exam (2. Staatsexamen)

11/2001-08/2005   Ph.D. thesis (Human Biology)

                         Department of Pharmacology and Toxicology, School of Medicine,

                         Philipps-University, Marburg

                         Title: The Fibroblast Growth Factor-binding Protein (FGF-BP) and

                         the Human Epidermal Growth Factor Receptor-2 (HER-2):

                         Functional Studies on Two Gene Products Relevant in Ovarian

                         Cancer

                         (Supervisor Prof. Dr. F. Czubayko)

14 PUBLICATIONS

14.1 List of own publications

1. **Abuharbeid, S.,** Apel, J., Sander, M., Fiedler, B., Langer, M., Zuzarte, M. L., Czubayko, F., and Aigner, A. Cytotoxicity of the novel anti-cancer drug rViscumin depends on HER-2 levels in SKOV-3 Cells (2004) *Biochem Biophys Res Commun* 321(2), 403-412

2. **Abuharbeid, S.,** Apel, J., Zugmaier, G., Knabbe, C., Sander, M., Gilbert, S., Czubayko, F., and Aigner, A. Inhibition of HER-2 by various targeting strategies increases paclitaxel resistance of SKOV-3 ovarian carcinoma cell (2005) *Naunyn Schmiedebergs Arch Pharmacol* 371(2), 141-151

3. Urban-Klein, B., Werth, S., **Abuharbeid, S.,** Czubayko, F., and Aigner, A. RNAi-mediated gene-targeting through systemic application of polyethylenimine (PEI)-complexed siRNA in vivo (2005) *Gene Ther* 12(5), 461-466

4. **Abuharbeid, S.,** Hagenbusch, J., Czubayko, F., and Aigner, A. Evidence for an intracellular inhibitory function of FGF-BP based on its interaction with nuclear FGF-2 (Manuscript is in preparation)

14.2 Contributions to congress

1. Urban-Klein, B., Sander, M., **Abuharbeid, S.,** Grzelinski, M., Czubayko, F. and Aigner, A.
Comparison of ribozym-targeting and RNA interference (RNAi) shows the high potential of both methods for specific and efficient reduction of gene expression
94. Annual Meeting of American Association for Cancer Research, Juli 2003, Washington DC, USA

2.   Urban-Klein, B., Sander, M., **Abuharbeid, S.,** Grzelinski, M., Czubayko, F. und
        Aigner, A.
        RNA interference (RNAi) and ribozyme-targeting: two efficient ways to down-
        regulate gene expression
        *44. Spring conference of the German Association for Pharmacology and Toxicology
        (DGPT), March 2003, Mainz, Germany*

3.   Urban-Klein, B., Werth, S., Grzelinski, M., **Abuharbeid, S.,** Martens, T., Lamszus,
        K., Czubayko, F. and Aigner, A.
        Anovel tool for RNAi in vivo: Direct application of PEI-complexed siRNAs
        *96. Annual Meeting of American Association for Cancer Research, April 2005,
        Anaheim, USA*

4.   **Abuharbeid, S.,** Apel, J., Zugmaier, G., Langer, M., Fiedler, B., Czubayko, F. and
        Aigner, A.
        HER-2 (c-erbB2) receptor expression levels determine the resistance of SKOV-3
        ovarian carcinoma cells towards Paclitaxel and rViscumin
        *96. Annual Meeting of American Association for Cancer Research, April 2005,
        Anaheim, USA*

5.   Urban-Klein, B., Werth, S., Grezelinski, M., **Abuharbeid, S.,** Martens, T., Lamszus,
        K., Czubayko, F. and Aigner, A.
        RNAi in vivo through direct application of PEI-complexed siRNAS
        DECHEMA Annual Meeting 2005, Wiesbaden, Germany (lecture)

6.   **Abuharbeid, S.,** Apel, J., Zugmaier, G., Langer, M., Fiedler, B., Czubayko, F. and
        Aigner, A.
        Resistance of SKOV-3 ovarian carcinoma cells towards Paclitaxel and rViscumin is
        dependent on HER-2 (c-erbB2) receptor expression levels
        *46. Spring conference of the German Association for Pharmacology and Toxicology
        (DGPT), March 2005, Mainz, Germany*

7.   Urban-Klein, B., Werth, S., Grezelinski, M., **Abuharbeid, S.,** Martens, T., Lamszus, K., Czubayko, F. and Aigner, A.
     Direct application of PEI-complexed siRNAs - a novel tool for RNAi in vivo
     46. Spring conference of the German Association for Pharmacology and Toxicology (DGPT), March 2005, Mainz, Germany